Analysis of Single and Group Micropile Behavior

MSc Thesis Report

Geo-Engineering

By:

Marziyeh Sadat Feiz

03-12-2018

Analysis of Single and Group Micropile Behavior

The Bearing Capacity of Single Pile and Pile Groups under Axial Tensile Loading using FEM

By:

M. S. Feiz

A thesis submitted in partial fulfillment of the requirements for the degree of Master of Science in Civil Engineering, Geo-Engineering track at Delft University of Technology

03-12-2018

Author:

Marziyeh Sadat Feiz
4093852
Email: mfeiz1371@gmail.com

Assessment Committee:

Dr. Ir. W. Broere	Department of Geo-Engineering Delft University of Technology
Dr. Ir. R. B. J. Brinkgreve	Department of Geo-Engineering Delft University of Technology
Prof. Dr. K. G. Gavin	Department of Geo-Engineering Delft University of Technology
Dr. Ir. M. A. N. Hendriks	Department of Structural Engineering Delft University of Technology
Ir. J. K. Haasnoot	Department of Geo-Technical and Foundation Engineering, Crux Engineering B.V.

PREFACE

This thesis has been written in collaboration with CRUX Engineering Company and is the result of one year research and work at Delft University of Technology to obtain the degree of Master of Science in Civil Engineering, track Geo-engineering at Delft University of Technology.

Without support and help of many people I would not be able to finish and complete my work as it is now. Therefore I would like to express my gratitude and sincere thanks to a number of people who helped me throughout this research.

First of all I would like to thank Ir. J. K. Haasnoot from CRUX Engineering Company who introduced me to the topic and provided me with valuable information.

Furthermore I want to thank Dr. Ir. W. Broere and Dr. Ir. R. B. J. Brinkgreve for the support and guidance during the committee meetings. Special thanks to other assessment committee members, Prof. Dr. K. G. Gavin and Dr. Ir. M. A. N. Hendriks.

I would also like to thank my friend Ir. M. Agah-Nav for the feedback and advice during my study.

Finally I would like to thank my fiancé M. Nadi for his love and support throughout the toughest part of my study and many thanks to my parents, brother and sister for their support in different kind of ways during my hard times of study life.

M. S. Feiz
Delft, December 2018

ABSTRACT

This thesis investigates the behavior of single and group micro piles under axial tensile loading. Micro piles are small diameter piles consist of grout and steel rebar and they are capable of absorbing tensile loads. By constructing a group of piles the bearing capacity of each pile within a group is less compared to the single pile. The reason is due to the existence of group effect in the pile group which influences the bearing capacity.

During the production of the piles for Amsterdam car parking project, load tests are performed to check whether the piles behave according as expected which can be considered as acceptance tests. However in this test, only individual piles are tested and not a pile group. CUR 236 design procedure states that the bearing capacity of a pile in a pile group is less than the bearing capacity of that pile when it is loaded not in a group. To take this effect into account for the acceptance test, an additional load is added to the test load. It turned out at the Amsterdam car parking project that piles failed the acceptance tests due to this additional load which is required to apply according to CUR 236 design guide. However this procedure is questionable because the pile is loaded into a much higher level than it will actually experience during its lifetime. Therefore an evaluation of the standards and the influence of group effects on micro pile behavior is needed.

The initial plan of approach was to investigate the standards of other countries and compare them to Dutch standards to find the eventual existing gap and propose an improvement method which did not succeed. The reason was that the standards of other countries were all written in their national language and therefore it was not possible to study them. Seeking for the research on tension pile group behavior did not help so much because many researchers believe that including a realistic group effect in the design is not an easy task and there was no clear conclusion on micro pile group influence.

The direction of approach is then changed towards the numerical modelling and based on it the influence of group effects on micro pile behavior is presented.

First a single micro pile is modelled with Finite Element Method in Plaxis. The single pile is finally modelled in plane strain by using Embedded Beam Row element. Model parameters and properties are defined based on Amsterdam case study. The load-displacement behavior of the single pile model was comparable with the one from Amsterdam field failure test and is therefore validated based on field failure test data.

After development of single pile model, the model for pile groups is made. This group model is made to represent the practical situation in a building pit for Amsterdam case study. Three models for the pile group have been made which differ in pile spacing and the impact of this parameter on the capacity per micro pile is investigated. The different used pile spacings are 5D, 10D and 15D which are equal to 1 meter, 2 meters and 3 meters. Also for each pile spacing, the dominant failure mechanism is determined. According to the results it was concluded that for 5D and 10D pile spacing, the failure mechanism is based on soil plug pull-out while for 15D, it is according to slip failure. By validation of the pile group model, an improvement for the space between the piles within a pile group can be proposed as 10D where the soil plug pull-out is dominant failure mechanism.

It is recommended to validate the pile group model based on full-scale failure test on pile groups or by small-scale test using Geo-centrifuge models. Also by monitoring, a real data base of the group behavior can be obtained. Comparing the monitoring data to the design values based on CUR 236 could give an idea how well the design guide is formulated.

CONTENTS

LIST OF FIGURES AND TABLES

CHAPTER 1: GENERAL INTRODUCTION

1.1 INTRODUCTION

Micro-piles are long and slender piles used as foundation elements and are applied in various situations. They regularly use as a foundation element in the form of tension piles. Micro-piles cast in place and have a diameter of maximum 300 mm. The piles consist of a grout column with a steel bar in the center. Micro-piles are used worldwide and different anchor pile systems are developed. GEWI anchor system is commonly used in the Netherlands. Figure 1 shows a visualization of this anchor pile system.

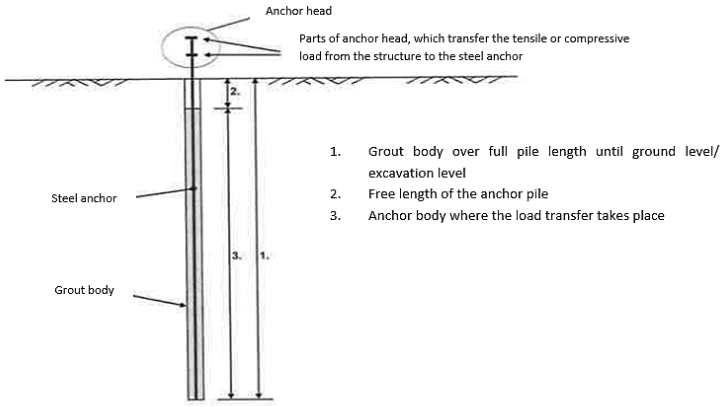

FIGURE 1: VISUALIZATION OF ANCHOR PILE

Micro piles or tension piles are commonly used in the Netherlands to stabilize the excavation floor of the basements. The main function of these piles is to balance the uplift forces. Two failure criteria are of importance in the bearing capacity design which are;

1. Friction capacity between the grout and soil
2. The cone of soil that can be mobilized around the pile

Based on recent experience the soil cone can become the governing factor in testing the production piles. An important aspect for this is the group effect, the reduction in bearing capacity of closely spaced tension piles, as this determines the testing load for the production piles.

1.2 PROBLEM DESCRIPTION

The pile design parameters of tension piles are based on pile tests that are performed on site, in which the piles are loaded up to failure. Quality control is done by testing a number of production piles to a certain loading level, as is described in the Euro-codes.

The design of the production piles is based on the failure tests that are conducted just before the design is done. The failure tests are performed and interpreted according to CUR236.

During the production of the piles for Amsterdam car parking project, load tests are performed to check whether the piles behave according as expected which can be considered as acceptance tests. However in this test, only individual piles are tested and not a pile group.

CUR 236 design procedures states that the bearing capacity of a pile in a pile group is less than the bearing capacity of that pile when it is loaded not in a group (as is done during the acceptance test). To take this effect into account for the acceptance test, an additional load is added to the test load.

The maximum gross test load for acceptance test is calculated based on the following formula in CUR 236;

$$F_P = n.F_d + R_{s;wr} \quad (1)$$

Which:

F_p is the maximum gross test load for the acceptance test [kN];

F_d is design value of the tested tension pile [kN];

$R_{s;wr}$ is the contribution of pile shaft friction that should be excavated at a later stage [kN];

n is the factor in which the design value of test load should be multiplied to compensate for:

- Influence group effect (f_2)
- Influence of load variation
- Influence of soil layers or de-watering during excavation

This procedure is questionable because the pile is loaded to a much higher level than it will actually experience during its lifetime.

It turned out at the Amsterdam car parking project that piles failed the acceptance tests due to this additional load which is needed to apply according to CUR 236 guide line.

To have a solution for the explained problem, an evaluation of the standards and project execution is needed. This research focuses on the improvement of design standards for a group of tension piles based on advanced numerical analyses and validates the results by evaluating to Boerenwetering (Albert Cuyp) car parking project in Amsterdam as a case study.

1.3 SUB RESEARCH TASKS

The main research question is to evaluate the Dutch design standards for group of tension piles based on the international methods used in other countries and advanced numerical methods.

In order to reach the main goal of this thesis, some steps need to be taken towards the main research question and therefore the following sub tasks should be included which are;

- Comparison of international design standards to the Dutch design standards for tension piles
- Evaluating Dutch design standards about design bearing capacity of single and group tension piles
- Finding an appropriate model for single and group tension piles by using Finite Element Method
- The importance of pile spacing within a group
- The effect of different pile spacing on failure mechanism in the pile group

1.4 GOALS AND OBJECTIVES

Objective of this thesis is to focus on both failure criteria from a design and testing perspectives and comparing the results to field test observations. The research tools will include analytical and FEM (Plaxis) analysis. The test results from previous projects are provided for the further analyses.

In this research the following points will be also considered and included:

- The effect of applied stress to the soil during installation of the piles
- Shaft resistance between pile and the surrounding soil
- Effect of different soil types

The results of the thesis should give insight in the relation between friction capacity, group effect and the mobilized soil cone as well as recommendations for a trial to verify the results.

1.5 METHODOLOGY AND APPROACH

The plan of approach to this research is as indicated below;

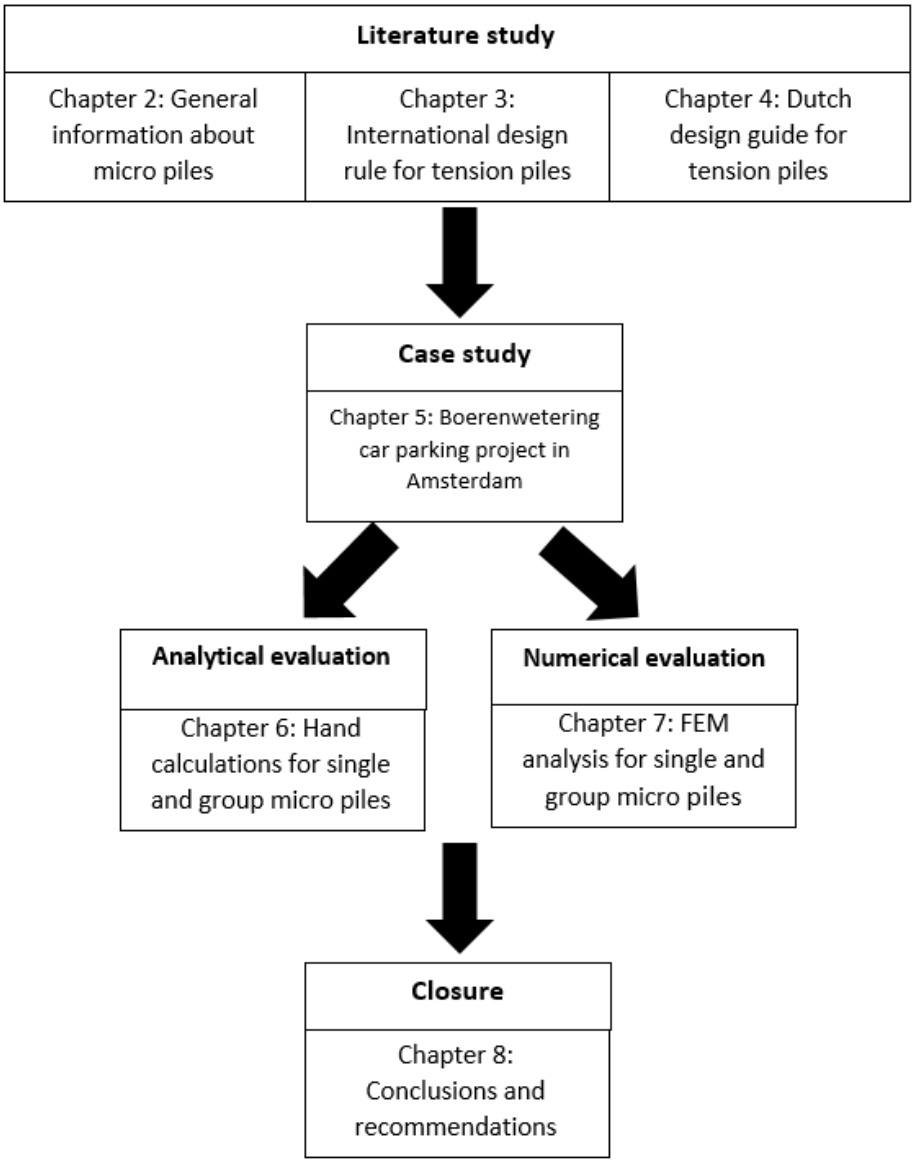

FIGURE 2: PLAN OF APPROACH

CHAPTER 2: MICRO PILES

2.1 INTRODUCTION

Over the past 15 to 20 years, the usage of slender anchor piles (also called micro-piles) as vertical foundation elements which are formed in the ground has increased significantly. They can offer a constructive and economically attractive solution for a large number of geotechnical issues. Examples include temporary anchoring of underwater concrete floors or permanent anchoring of structural floors of tunnels. In addition, long anchor piles are used for foundation reinforcement and in special situations with limited work space.

FIGURE 3: GEWI PILES IN DE-WATERED CONSTRUCTION PIT

Anchor piles have a grout-shaped anchor body which is capable of absorbing high axial loads and are economically attractive. Pile shafts have a relatively small diameter of approximately 150 mm to 300 mm, but larger diameters are possible depending on the specific system. In order to transfer the forces from the construction to the anchor pile, they have a single central solid steel rod over the entire length.

The installation takes place from existing ground level, or a (partially) excavated construction pit. Depending on the anchor pile system and local soil conditions, pile tip levels of 40 m to 50 m below ground level or even deeper can be realized.

However such anchor piles are usually used to transfer tensile loads of up to 1 MN or more to the deeper subsurface, but they are also increasingly used as compression piles. These anchor piles, despite their slenderness, are very capable of absorbing high compression loads.

In this chapter the following aspects will be taken into account and described in more details to have a complete understanding of micro piles;

- The pile type and the associated method of installation of the pile
- The structure and the properties of the soil
- The load characteristics
- The arrangement of the piles in a pile group

Also further in this chapter a parametric study is done to check how the tensile load influences the pile bearing capacity and stresses in the soil.

2.2 MICRO PILE TYPES

It is important to take in to account that all types of anchor pile systems are highly sensitive to the execution method and therefore are classified from A to E different types based on their mechanisms.

Since for Boerenwetering car parking, type A micro pile is used, in this research only this type of micro piles is considered and in detail explained. Other types of micro piles will be briefly introduced.

Hereby regarding CUR 236, a distinction is made to the following micro pile types;

Type A: Micro pile bored with a double casing and an inside spoil

Micro pile with double casing avoids excessive ground excavation and is the most traditional method of installation in the Netherlands. The installation process is in the way that at the same time, an outer tube and inner tube are drilled at depth. The drill head of the rotating inner tube cuts off the ground by the drilling fluid that is injected vertically downwards from the tip of the inner tube. Water is used as drilling fluid during drilling, but sometimes a thin grout mixture with w/c factor ≥ 1.0 is also used.

The drilled soil is discharged upwards between the inner tube and the outer tube. The outer tube acts as casing and thus ensures a stable borehole during the drilling. The tip of the outer tube then runs on the tip of the inner tube. This is to prevent too much disturbance of the soil layers around the borehole due to the drilling fluid coming out of the tip of the inner tube.

FIGURE 4: DRILL BIT OF OUTER TUBE (LEFT) AND DRILL HEAD OF INNER TUBE (RIGHT)

After reaching the desired depth, the inner tube is pulled, the GEWI rod is placed and the bore fluid is replaced with a w/c factor of 0.45 to 0.5 grout mixture. In order to form a better attachment to the soil layers, an over-pressure is applied to the grout mixture and the outer tube is pulled about 0.5 meters. Due to applied pressure water that is present in the grout is then squeezed out and the mixture hardens.

As soon as the pressure on the grout has increased, the outer tube can be pulled another 0.5 meter and the same procedure is continued until about 4 meter below ground level or excavation level. The overpressure is changed to hydrostatic pressure to prevent from blow-out and at the end the outer tube is pulled completely.

Type B: Micro-piles bored with a single casing and an outside spoil

It is similar to type A micro piles. However it includes a single casing micro pile with an outside spoil. The grout body is also pressurized for this type of micro piles.

FIGURE 5: DRILLING WITH SINGLE CASING

Type C: Self-drilling micro piles

It consists of self-drilling micro piles in which no casing is used. The grout is injected through the steel bar which keeps the bore hole stable and cuts the soil. Brittle failure is expected for this type of piles.

FIGURE 6: SELF-DRILLING MICRO PILES WITH INJECTION OF GROUT

Type D: Screw injection micro piles

It is rotary micro piles. A continuous flight auger cuts the soil while a bore fluid is injected at the blades resulting a mixture of soil and grout which keeps the bore hole stable.

FIGURE 7: ROTARY MICRO PILES WITH SCREW BLADES

Type E: Vibro-fluidization micro piles

This type is a high frequency vibration and fluidization micro pile. Vibration method is used in the way that the casing is installed through the desired depth. Then a GEWI- bar is placed and the casing is filled with water and is pulled while at the bottom of the casing grout is applied under high pressure.

FIGURE 8: INSTALLATION OF VIBRO-FLUIDIZATION MICRO PILES

2.3 STRUCTURE AND PROPERTIES OF THE SOIL

Large parts of the Netherlands are characterized by a soil structure consisting of young Holocene layers (clay / sand / peat), which are deposited on a moderate to densely packed Pleistocene sand formation. Tensional capacity can be derived from the Pleistocene sand package by mobilizing the shear strength of this sand. The shaft friction depends, among other things, on the packing density and the horizontal and vertical effective stresses present in this formation. In some areas, tensional capacity is also derived from sand layers in the Holocene formations.

The cohesive layers in the Holocene package, due to their low stiffness and shear strength, often provide a very limited contribution to the tensional capacity.

In the Dutch situation the shaft friction in the sand layers is usually significant for the tensional capacity. The specific properties of the sand such as grain distribution, grain shape, grain material (in the Netherlands usually quartz) and the relative density play an important role.

The Cone penetration test (CPT) is the main source of information for the layer structure and the bearing capacity of the soil layers contributing to the tensile strength. The measured cone resistance is used to estimate the shear strength and relative density of the soil. In addition to this, laboratory research on soil samples can be carried out with a view to the following properties because these aspects play an important role in the bearing capacity of the piles and must be taken into account;

- Volume weight
- Minimum and maximum density
- Grain distribution and grain shape
- The angle of internal friction of the sand, the stiffness properties and possibly the dilation properties at different densities

The bearing capacity of the piles in compression is based on the base resistance and shaft friction of the pile while for the tension piles, it is only based on the shaft friction. It is accepted by many researchers that the area of the shaft and the shear stress acting on the shaft define the maximum bearing capacity. The shear stress depends on the stresses in the soil and will vary by increasing depth. The end bearing in compression is about 10 to 15% of total bearing capacity of the pile due to its small cross section.

2.4 TYPE OF THE LOAD AND FUNCTION

Based on the soil structure and condition, micro piles can be made in lengths up to 30 meters and can be used as tension or compression piles. They can resist forces up to 1 MN as well in tension as in compression.

Micro piles can be used for different functions. Their regular use is a foundation element in the form of tension piles. Tensional loads on foundation piles are present in tunnels beneath ground water level, dry docks, deep basements and in quay walls and power pylons. Figure 9 gives number of examples. They are also useful in cases that the working space is limited due to their high bearing capacity and minimum disturbances of the soil and adjacent structures.

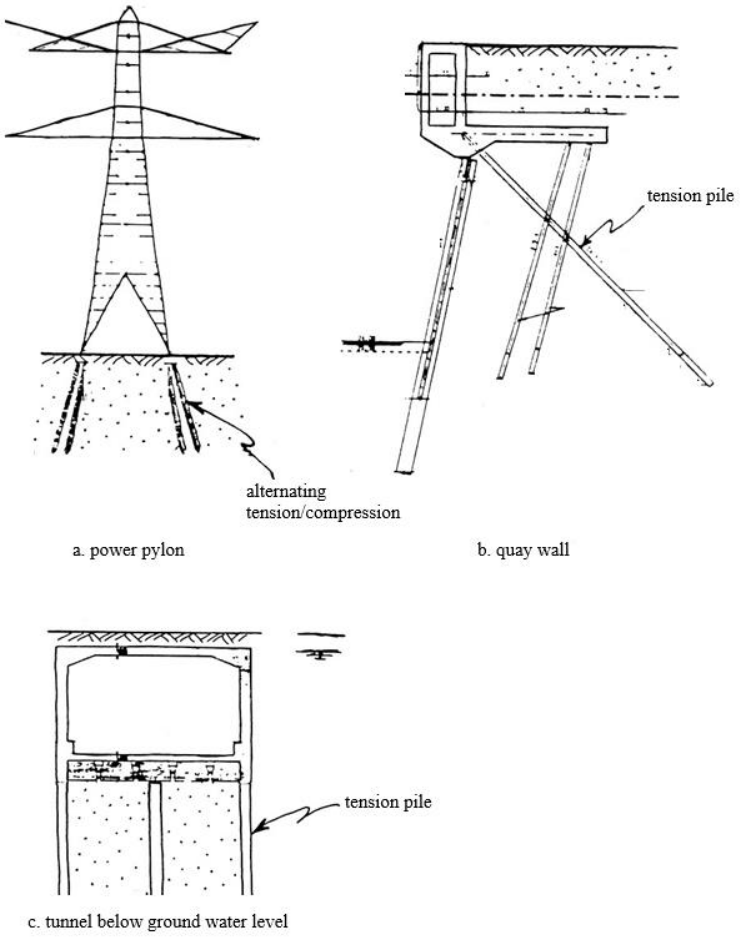

FIGURE 9: EXAMPLES OF TENSION PILES (CUR 2001-4 REPORT)

2.5 BEHAVIOUR OF A PILE GROUP

If a pile is part of a pile group with center to center distances that are so small, the piles influence each other during installation stage and after that. One of the effect that occur in the group of piles in the installation stage is densification. As result an average higher densification can be achieved and also the applied stresses will be increased in the soil. Densification happens within a pile spacing of approximately 6 times the equivalent diameter of the pile.

In the operational stage when loading a pile group in tension, the following effects occur:

- Due to applied tensile load on the foundation, a so called relaxation happens and therefore the vertical stress reduces in the ground which leads to a lower bearing capacity of the piles.

- If all piles are loaded in tension simultaneously in an extended pile field, this upward load can maximum be redistributed as an average ground surface area per pile. The influence of the vertical effective stress depends on the pile distance, the length and the wall roughness of the piles. The upper limit for the tensile capacity is found in the geometry in which the entire cone of soil between the piles is mobilized upwards (mobilized soil cone of pile groups).

According to CUR 2001-4 report, it is also very important to check the following two boundary conditions for tension piles:

- The total tension force may not cause the piles to rise along with the soil between the piles, especially for pile groups; this is called check on the weight of soil mass between the piles

- In all cases, the tension force may not lead to a single pile being pulled out; this is called check on slip or tensional capacity

2.6 PARAMETRIC STUDY

If a tensional load is applied on the pile, this load will be transferred to the soil by means of shear resistance. There are several aspects that are important to consider in this respect;

Dilation:

Dilatancy is an increase in soil volume due to shearing of the soil. Since dense sand are packed together by particle interlocking, if tensional load is applied they will remove from this densely packed configuration and dilatancy occurs. Many authors like Lehane (1994), Houlsby (1991) and Jardine (1994) believe that dilatancy has effect on shaft friction capacity of the pile.

The area around the pile shaft during the pull-out force is called dilation zone. Based on the studies by Houlsby (1991), the thickness of this zone is 10 to 15 multiplied by grain diameter of the soil (D_{50}). The thickness of this zone depends on the pile roughness. If the roughness is the same along the total length of the pile, then maximum friction is dependent on the ratio between thickness of the dilatancy zone and pile diameter. Therefore a pile with larger diameter in dense sand creates a smaller friction comparing with a pile with smaller diameter. Other authors like Lehane (1994) and Jardine (1994) illustrate that the increase of radial stress due to dilatancy is inversely proportional with the radius of the pile.

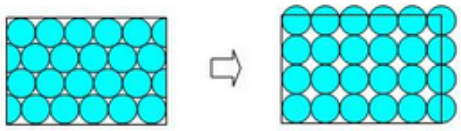

FIGURE 10: DILATION CAUSES VOLUME INCREASE FOR DENSELY PACKED SOILS

Poisson effect:

It is the phenomenon in which the pile tends to contract in in case of pull-out force and expand if compression is applied. According to De Nicola (1994) and Randolph (1994), due to change of diameter, the radial stresses of the pile by tensional load decreases and as result the maximum shaft friction resistance becomes smaller. The changes of the pile are highly dependent on the pile stiffness, dimension of the pile and the amount of the load.

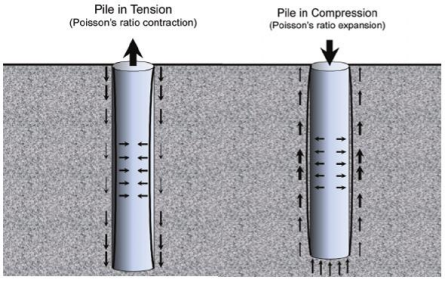

FIGURE 11: POISSON EFFECT BY TENSION AND COMPRESSION LOADING

Rotation of principal stresses:

Due to tensional loading of the pile, rotation of the principal stresses in the surrounding soil occurs. This phenomenon could be explained by circle of Mohr and studies done by Lehane (1993) (see figure 12).

If no force is applied to the pile, the orientation of the principal stresses show no shear stress (left picture). As long as a tensional force is applied, shear stresses occur and as result a rotation of the principal stresses too (right picture). The rotation direction of the principal stresses show whether a tension or compression load is applied. If the direction of principal stresses is towards to surface, then it is tensional load and if they point deeper underlying layers, then it is compression.

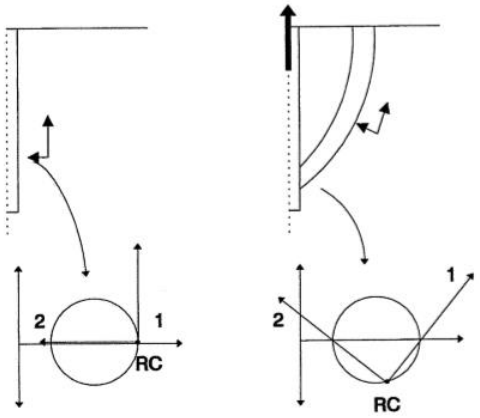

FIGURE 12: SCHEMATIZATION OF THE ROTATION OF PRINCIPAL STRESSES

CHAPTER 3: INTERNATIONAL DESIGN RULES FOR TENSION PILES

3.1 INTRODUCTION

There are different types of research done by many people for the calculation of pile bearing capacity due to the fact that the axial capacity of piles is in the area of greatest uncertainty in foundation design. Therefore there are different methods and formulas implemented for predicting the pile capacity. However the accuracy of the design methods are often questioned by Randolph (1994) and Olson (2002). In practice it is common to use conservative factors of safety since measured pile capacities have been found to differ from the calculated capacities by more than three times Olson (2002).

In this chapter the methods for calculating pile axial load capacity employed in practice is discussed.

3.2 THE BASIC APPROACH OF PILE BEARING RESISTANCE

If the pile is in compression, the capacity of the pile is equal to base friction (Q_b) + the skin friction of the shaft (Q_s), while in tension, only the resistance of the pile shaft (Q_s) is considered, see figure 13.

The skin friction of vertical piles under tensile loads is exactly calculated in the same way as skin friction under compression. However, for cyclic loading the skin friction is subjected to the rate of load and degree of degradation of the soil particles at the interface with pile wall.

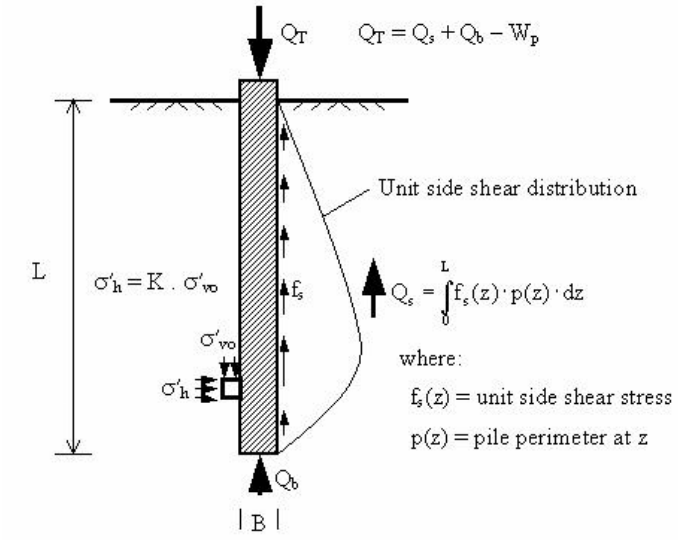

FIGURE 13: ILLUSTRATION OF LOAD TRANSFER OF A PILE LOADED IN COMPRESSION

The concept of the separate evaluation of shaft friction and base resistance forms the basis of all 'static' calculations of pile carrying capacity. The basic equation (according to Tomlinson) is as follow for compression and tension piles;

Compression: $Q_c = Q_s + Q_b - W_P$ (2)

Tension: $Q_t = Q_s + W_P$ (3)

Which:

Q_c and Q_t = Ultimate resistance of the pile,

Q_s = Ultimate resistance of the shaft ($=\int_0^L f_s(z).p(z)\,dz$)

Q_b = Ultimate resistance of the base which is null for tension piles, ($=q_b.A_b$)

W_p = Weight of the pile

3.3 API 2010 METHOD

The American Petroleum Institute (API) provides practical recommendations based on laboratory data for pile bearing capacity in tension. The bearing capacity is fully based on shaft capacity of the pile and there is no difference between shaft capacity of the pile in tension and compression.

According to API 2010, the unit shaft capacity f is determined using following formulas for cohesive and non-cohesive soils.

Cohesive soils:

$$f = \alpha \cdot c_u \quad (4)$$

$$\alpha = \frac{1}{2} \cdot \left(\frac{c_u}{p'_o}\right)^{1/2} \quad \text{for } c_u \le p'_o \quad (5)$$

$$\alpha = \frac{1}{2} \cdot \left(\frac{c_u}{p'_o}\right)^{1/4} \quad \text{for } c_u > p'_o \quad (6)$$

In these equations, c_u and p'_o are respectively the undrained shear strength and effective overburden pressure at the depth.

Non-cohesive soils:

$$f = \beta \cdot p'_o \le f_{max} \quad (7)$$

Values for ß (shaft friction) and f_{max} can be determined based on the next table;

TABLE 1: DESIGN PARAMETERS FOR COHESIONLESS SILICEOUS SOIL (API, 2010, P.64)

Relative density	Soil description	β [-]	f_{max} [kPa]
Very loose 0-15% Loose 15-35% Loose 15-35% Medium dense 35-65% Dense 65-85%	Sand Sand Sand-Silt Silt Silt	*	*
Medium dense 35-65%	Sand-Silt	0.29	67
Medium dense 35-65% *Dense 65-85%*	Sand *Sand-Silt*	*0.37*	*81*
Dense 65-85% Very dense 85-100%	*Sand* Sand-Silt	*0.46*	*96*
Very dense 85-100%	Sand	0.56	115

Total shaft capacity is then can be calculated with the following formula;

$$Q_t = f.A_s \tag{8}$$

Which:

f = Unit shaft capacity [kPa]

A_s = Shaft area [m^2]

3.4 SKIN FRICTION CPT BASED METHODS

There are two CPT based methods evaluated in this section which are ICP (05) and UWA (05). Both of them were stablished by testing driven steel piles (close or open ended) in offshore practice.

3.4.1 ICP (05)

This method was developed at the Imperial College Pile (ICP) in London based on a series of investigations using instrumented field test piles. The instrument used in Imperial College method was a tubular closed and open-ended steel pile which has been driven into sand in order to provide support for offshore structures in oil industry.

The unit shaft capacity for piles based on this method in sand is determined with the following equation:

$$q_s = a \cdot \left[0.029 \cdot b \cdot q_c \cdot \left(\frac{\sigma'_{v0}}{p_{ref}}\right)^{0.13} \cdot \left(\max\left\{\frac{h}{R^*}, 8\right\}\right)^{-0.38} + \Delta\sigma'_{rd}\right] \cdot \tan(\delta_f) \tag{9}$$

Which:

a = 0.9 for open ended piles in tension and 1.0 for all other cases

b = 0.8 for piles in tension and 1.0 for piles in compression

σ'_{v0} = Vertical effective stress

p_{ref} = Reference stress (= 100 kPa)

h = Height above pile base

R* = Equivalent radius = $(R_o^2 - R_i^2)^{0.5}$, with R_i is internal radius

$\Delta\sigma'_{rd}$ = Change in radial stress during pile loading according to equation 10.

δ_f = Interface friction angle (≈2/3*ϕ)

$$\Delta\sigma'_{rd} \approx \frac{4G}{D} \cdot \Delta y \qquad (10)$$

G = Shear modulus

$$\frac{G}{q_c} = 185 * q_{c,IN}^{-0.75} \qquad with\ q_{c,IN} = \frac{\frac{q_c}{p_a}}{(\frac{\sigma'_{v0}}{p_a})^{0.5}} \qquad (11) \text{ and } (12)$$

Δy ≈ 0.02 mm (radial displacement during pile loading)

3.4.2 UWA (05)

UWA method is developed at University of Western Australia and it is mainly for siliceous sands. This method is similar to ICP (05) and is based on offshore practice for driven steel piles.

The unit shaft capacity of UWA (05) method is determined using the following formula:

$$q_s = \frac{f_t}{f_c} \cdot \left[0.03 \cdot q_c \cdot A_{r;eff}{}^{0.3} \cdot \left(\max\left\{\frac{h}{D}, 2\right\}\right)^{-0.5} + \Delta\sigma'_{rd}\right] \cdot \tan(\delta_f) \qquad (13)$$

For closed ended piles, $A_{r;eff}$ is 1. f_t/f_c is the ratio of tension to compression capacity and is equal to 1.0 for compression and 0.75 for tension. h is the distance above pile base level and D is the pile outer diameter. The term $(h/D)^{-0.5}$ has a similar effect to the shaft resistance as $(h/R^*)^{-0.38}$ in the ICP-method. Finally, $\Delta\sigma'_{rd}$ and δ_f are equal to the ICP-method.

3.5 FHWA Design rule

3.5.1 Geotechnical capacity of micro pile

The Federal Highway Administration (FHWA) of U.S. sponsored a project about micro pile design and construction guide lines. The document is intended to contain sufficient information on micro pile design, construction specifications, inspection, testing procedures and information on safety and cost-effective use of micro piles on transportation projects. The manual is updated in December 2005. The following information and design guide lines are based on this updated version of FHWA report.

Establish stratum for bond zone:

The maximum tension load resisted through grout to ground bond over a specific length of micro pile. This length called bond zone or bond length. This length can be formed in most soil and rock layers and the only difference is the grout to ground bond strength. Therefore the main objective in the design process is to evaluate the required length of this bond zone to carry compression and tension loads.

An important step in the design is to review all borings to find an appropriate value for the micro pile bond zone. Assuming soil deposits such as organic soils, cohesive soils with an average liquidity index greater than 0.2 or an average liquid limit greater than 50 or an average plastic index greater than 20; if the micro piles installed in these layers, they are susceptible to excessive creep deformations at testing and working loads. If used, higher factor of safety e.g. 2.5 should be applied.

Select ultimate bond stress and calculate bond length:

The allowable geo-technical bond capacity, $P_{G\text{-allowable}}$ is calculated as follow:

$$P_{G-allowable} = \frac{\alpha_{bond}}{FS} \times \pi \times D_b \times L_b \tag{14}$$

Which:

α_{bond} = Grout to ground ultimate bond strength; (depends on ground condition and methods of grouting)

FS = Factor of safety applied to the ultimate bond strength;

D_b = Diameter of the drill hole;

L_b = Bond length

By rearranging the above formula the bond length to resist compression or tension loads (uplift capacity) is therefore:

$$L_b = \frac{P_{G-allowable} \times FS}{\alpha_{bond} \times \pi \times D_b} \tag{15}$$

In FHWA report the micro piles are classified in to 4 types from A to D. Figure 14 shows the differences between the installation techniques of these types.

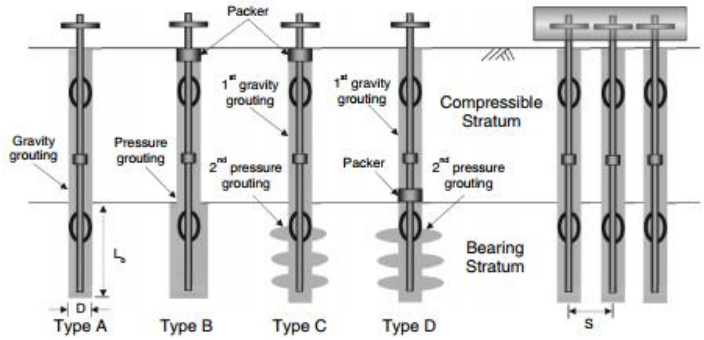

FIGURE 14: TYPE OF MICRO PILES WITH DIFFERENT INSTALLATION METHODS

It should be noted here that however the naming of pile types is similar to what has been already described according to CUR 236 but the characteristics are different. The explanations of different methods are as follow (FHWA reference manual, 2005);

Type A: Gravity grouting method. For this type of micropiles, grout is placed under gravity head only. Sand-cement mortars or neat cement grouts can be used. The micropile excavation may be under reamed to increase tensile capacity, although this technique is not common or used with any other micropile type. This type of micro pile is constructed for bond zones in rock. There are also 3 sorts of drill casing available for this type which are temporary or unlined (open hole or auger), permanent (full length) and permanent (upper shaft only).

Type B: Pressure through casing. This type indicates that neat cement grout is placed into the hole under pressure as the temporary drill casing is withdrawn. Injection pressures typically range from 0.5 to 1 MPa to avoid hydro fracturing the surrounding ground or causing excessive grout takes, and to maintain a seal around the casing during its withdrawal. This type is assumed for bond zones in soil. Different sorts of drill casing are available for type B which are temporary or unlined (open hole or auger), permanent (partial length) and permanent (upper shaft only).

Type C: Single global post grout. Type C indicates a two-step process of grouting including: (1) neat cement grout is placed under gravity head as with Type A; and (2) prior to hardening of the primary grout (after approximately 15 to 25 minutes), similar grout is injected one time via a sleeved grout pipe without the use of a packer (at the bond zone interface) at a pressure of at least 1 MPa. For this type of micro pile only temporary or unlined (open hole or auger) drill casing method is used.

Type D: Multiple repeatable post grout. Type D indicates a two-step process of grouting similar to Type C. With this method, neat cement grout is placed under gravity head (as with Types A and C) and may be pressurized (as for Type B). After hardening of the initially placed grout, additional grout is injected via a sleeved grout pipe at a pressure of 2 to 8 MPa. A packer may be used inside the sleeved pipe so that specific horizons can be treated several times. Types of drill casing are temporary or unlined (open hole or auger) and permanent (upper shaft only).

Next table 2 gives information to estimate the values for grout to ground ultimate bond strength for these different types of micro piles.

TABLE 2: TYPICAL A_{BOND} (GROUT-TO-GROUND BOND) VALUES FOR MICRO PILE DESIGN

Soil / Rock Description	Grout-to-Ground Bond Ultimate Strengths, kPa (psi)			
	Type A	Type B	Type C	Type D
Silt & Clay (some sand) (soft, medium plastic)	35-70 (5-10)	35-95 (5-14)	50-120 (5-17.5)	50-145 (5-21)
Silt & Clay (some sand) (stiff, dense to very dense)	50-120 (5-17.5)	70-190 (10-27.5)	95-190 (14-27.5)	95-190 (14-27.5)
Sand (some silt) (fine, loose-medium dense)	70-145 (10-21)	70-190 (10-27.5)	95-190 (14-27.5)	95- 240 (14-35)
Sand (some silt, gravel) (fine-coarse, med.-very dense)	95-215 (14-31)	120-360 (17.5-52)	145-360 (21-52)	145-385 (21-56)
Gravel (some sand) (medium-very dense)	95-265 (14-38.5)	120-360 (17.5-52)	145-360 (21-52)	145-385 (21-56)
Glacial Till (silt, sand, gravel) (medium-very dense, cemented)	95-190 (14-27.5)	95-310 (14-45)	120-310 (17.5-45)	120-335 (17.5-48.5)
Soft Shales (fresh-moderate fracturing, little to no weathering)	205-550 (30-80)	N/A	N/A	N/A
Slates and Hard Shales (fresh-moderate fracturing, little to no weathering)	515-1,380 (75-200)	N/A	N/A	N/A
Limestone (fresh-moderate fracturing, little to no weathering)	1,035-2,070 (150-300)	N/A	N/A	N/A
Sandstone (fresh-moderate fracturing, little to no weathering)	520-1,725 (75.5-250)	N/A	N/A	N/A
Granite and Basalt (fresh-moderate fracturing, little to no weathering)	1,380-4,200 (200-609)	N/A	N/A	N/A

Type A: Gravity grout only
Type B: Pressure grouted through the casing during casing withdrawal
Type C: Primary grout placed under gravity head, then one phase of secondary "global" pressure grouting
Type D: Primary grout placed under gravity head, then one or more phases of secondary "global" pressure grouting

The minimum bond length is usually used in most projects. The design engineer may use lower values if ground consists of loose granular materials or for cohesive material with medium to high plasticity. Type of micro piles is also has influence on the value of α.

Also proof testing must be conducted on the total installed piles. In general proof tests should be done on 5 percent of production micro piles.

3.5.2 MICRO PILE GROUP UPLIFT CAPACITY

Micro pile group in cohesive soils:

The group uplift capacity in cohesive soil can be calculated by using the following formula:

$$Q_{ug} = 2Z \times (X + Y) \times \overline{s_u} + W_g \qquad (16)$$

Which:
s_u is the average undrained soil shear strength over the depth of micro pile embedment along the group perimeter and W_g is the effective weight of the pile/soil block including the pile cap.

A factor of safety of 2.0 should be used to estimate the allowable group uplift capacity. For long term loading a safety factor of 2.5 to 3 would be sufficient.

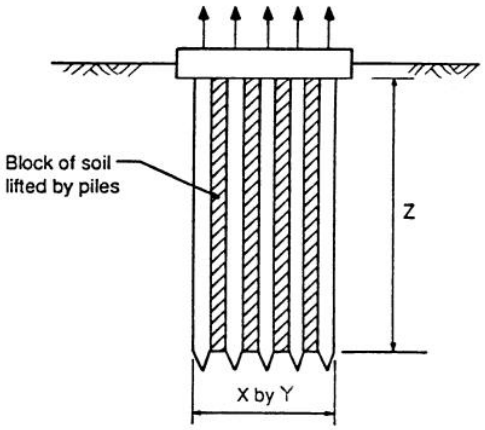

FIGURE 15: MODEL TO CALCULATE MICRO PILE GROUP UPLIFT CAPACITY IN COHESIVE SOILS

Micro pile group in cohesion-less soils:

The uplift capacity of group of micro piles in cohesion less soils can be calculated according to the following expression;

$$Q_{ug} = \left[\frac{1}{3} \times \left(A_{base} + A_{top} + \sqrt{A_{base} \times A_{top}}\right) \times D\right] \times \gamma \qquad (17)$$

Which:

$A_{base} = B_g \times L_g$

$A_{top} = (B_g + D/2) \times (L_g + D/2)$

D= Diameter of the pile

γ = Effective unit weight of the soil

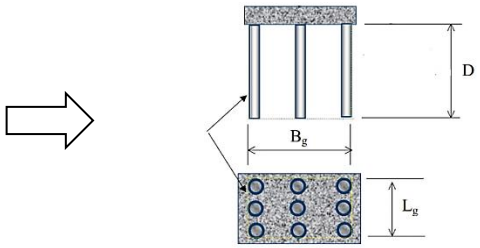

The term in the bracket is therefore the total volume of the enclosed soil. The uplift capacity is considered as effective weight of a block of soil extending upward from the base of micro pile at a slope of 1H: 4V (see figure 16). The weight of micro piles within the block is conservatively considered equal to weight of soil.

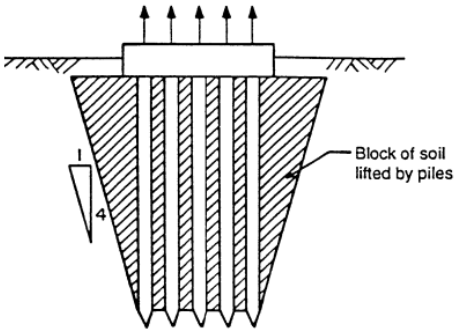

FIGURE 16: MODEL TO CALCULATE MICRO PILE GROUP UPLIFT CAPACITY IN COHESION-LESS SOILS

In this evaluation it is assumed that the allowable micro pile group capacity would be equal to calculated value based on above formula.

After all, the allowable uplift capacity according to formula for cohesive or cohesion-less soils should be compared to the allowable uplift capacity of a single micro pile multiplied by the number of micro piles in the group and the design should have lower group capacity.

When calculating the uplift of a single pile or group of piles using the Euro-code 7 recommendations it should be noted that where the uplift load is derived. From live loading, such as wind, the live load should be increased 30% by a partial factor of γ_F=1.3 to 1.5. Where the dead load of the structure is favorable in resisting uplift and critical it is reduced 5% by a partial factor γ_F=0.95.

Skin friction to resist uplift load can be increased by ten times or more by skin grouting. It is a process of injecting grout under pressure into the interface between shaft and the surrounding soil after completion of driving a tubular steel pile.

The following points could be also considered or included in Dutch design code;

- Considering different α values according to FHWA method for cast in place micro piles.
- There is no information about the inclined micro piles.
- Geometry is not considered.
- Using new method to calculate uplift capacity which is considering effective weight of a block of soil extending upward from the base of micro pile at a slope of 1H: 4V for cohesion less soils while in Dutch code, the soil enclosed by the micro pile has combination of cylinder and cone shape.
- Adding the frequency pattern in the code could be another interesting thing. Since $\gamma_{m,var,qc}$ is only dependent on F_{min} and F_{max} and two different frequency pattern with the same F_{min} and F_{max} will have the same value for $\gamma_{m,var,qc}$ which is not correct.

3.6 STUDIES DONE BY D. KYUNG AND J. LEE FOR INCLINED MICRO PILES

In this study the uplift capacity of inclined micro piles is investigated. For this purpose an experimental testing program was established. In order to check the validity a full scale up lift load tests were conducted. The uplift load capacity of micro piles was obtained by considering different conditions such as installation angle (θ), spacing (S) and group configuration. For this purpose a series of model uplift load tests was conducted for both single and group micro piles with θ of 0 to 45° and S of 3D to 7D.

The uplift load capacity of inclined micro piles is based on decomposed axial and lateral loads and resistance components.

3.6.1 METHOD OF DESIGN

In this method various installation conditions of single and group configurations, different installation angles and micro pile spacing were considered in the test.

Micro piles are small size cast in place pile foundations with diameter of normally 150 to 300 mm. The uplift capacity should be always considered because it controls the design and usually is smaller than compressive resistance.

For uplift and compressive cases the end bearing capacity is not taken into account because of smaller diameter characteristics of micro piles.

The uplift load capacity of micro piles is calculated based on mobilized pull out strength along the bond length which varies with different soil conditions and grouting methods (FHWA 2005). It is for cast in place micro piles and does not work for prefabricated micro piles.

The difference between single and group micro piles is expressed by using group effect factor, i.e., ratio of group to single micro pile load capacities. Another method is by using the assumed mass of soil block enclosed by group micro piles (FHWA 2005).

If the micro piles installed in an inclined condition, the installation angle θ affects the load carrying behavior. The uplift load capacity of inclined micro piles in group would be affected by installation factors such as type of micro piles and geometry in addition to group effect.

Design of micro piles:

Micro piles are classified into 4 types (A to D) according to grouting method, see figure 14 (FHWA 2005).

It is important to consider which type of installation is going to be applied as the grouting method affects borehole conditions and therefore has influence on load carrying capacity.

The uplift load capacity of micro piles is obtained base on the mobilized shear strength along the bond length within the uncased bearing stratum.

The uplift load capacity is given by the following formula:

$$P_{\text{up,SMP}} = \alpha_{\text{bond}} \pi D L_b \tag{18}$$

Which:

$P_{up;SMP}$ = Uplift load capacity of a single micro pile;

α_{bond} = Grout-to-soil bond strength;

D = Diameter of borehole;

L_b = Bond length

The factor of safety for single micro pile can be included in the above formula in a range of 2 to 2.5 but a lower value can be also considered if sufficient field tests are performed and material is not creep susceptible.

For the uplift load capacity, this article refers to FHWA method which is using the soil block approach. For granular soils the uplift load capacity is taken as the effective weight of the soil block enclosed by a sloped lateral boundary extending upward from the base to the top. This procedure is only for vertical piles and there is no detail explained for inclined micro piles.

Group effect of micro piles:

The group efficiency for uplift load capacity when installed in group given as follows:

$$P_{\text{up,GMP}} = \eta_{\text{GMP}} \sum P_{\text{up,SMP}} \tag{19}$$

Which:

$P_{up;GMP}$ and $P_{up;SMP}$ = Uplift load capacities of group and single micro piles, respectively;

η_{GMP} = Group-effect factor

The group effect factor is generally smaller than unity since interaction among neighboring piles reduce the overall load carrying capacity. Das et al. (1976) reported that the efficiency of uplift load capacity for pile groups increases with pile spacing, but decreases with an increasing number of piles in a pile group. Shanker et al. (2006) reported similar results that, however, indicated lower group efficiency with increasing pile length-to-diameter ratio. For vertically installed micro piles, Sharma and Buragohain (2014) reported that changes in group efficiency are not significant with micro pile spacing (S) and length-to-diameter ratio (L/D). It was found that the range of group effect factor is from 0.65 to 0.76, insensitive to spacing. However there is no information about the inclined micro piles.

3.6.2 TEST DESCRIPTION FOR INCLINED MICRO PILES

To investigate the effect of micro pile configuration 4 installation angles θ of 0, 15, 30 and 45 and 3 micro pile spacing of 3D, 5D and 7D (D= micro pile diameter) were adopted in the tests. The diameter of the micro pile for all cases was 5mm. The bond length of both SMP and GMP was 310 mm, corresponding to a length-to-diameter ratio equal to 62. The micro piles were coated with fines to increase surface roughness as boring and grouting procedures usually result in rough surface conditions.

Figure 17 shows the detailed configuration of the test.

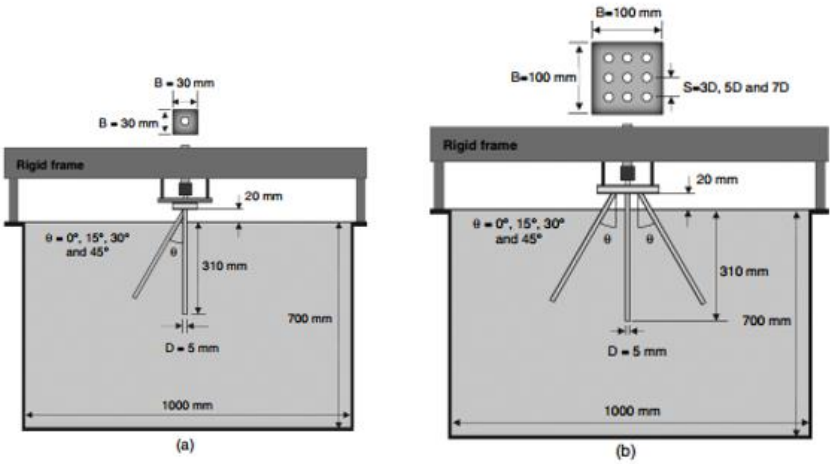

FIGURE 17: UPLIFT LOAD TESTS A) SMP B) GMP

For installing micro piles, the authors placed guide frames on the top of the test chamber and used to push micro piles into soil sample. The guide frames were then removed and the micro pile cap was positioned on the top of micro piles, 20 mm above the soil surface. The authors then installed a load cell at the center of the model foundations and two LVDTs were installed at the edges of the micro pile cap. Loads were applied using a hydraulic jack with an increment of 0.02–0.05 kN.

Finally, It was concluded that the uplift load capacity of both single and group micro piles are increased with θ up to 30° but decreased for a higher installation angle of θ=45° . Micro pile spacing had less effect on the uplift load capacity for group micro piles. The uplift displacement ($s_{up;max}$) at the ultimate state increased with increasing θ and S, indicating improved ductility

in the load response. The values of $s_{up;max}$ for GMPs became close to those of SMP as micro pile spacing increased. The uplift load-carrying mechanism of micro piles in an inclined condition was proposed based on the decomposed axial and lateral load and resistance components. Both vertical and inclined micro piles were installed and tested. The uplift load capacities estimated using the proposed inclined method were in close agreement with measured field capacities.

CHAPTER 4: DUTCH DESIGN GUIDE FOR TENSION PILES

4.1 INTRODUCTION

The design methods that are used in the Netherlands can be subdivided into methods for calculating single piles and methods for calculating pile groups.

Since in the Netherlands CPT and determining cone resistance is very popular and also the results are better comparable with the reality, the q_c method is used for the determination of maximum bearing capacity of a single tension pile or a pile within a group.

In this chapter a distinction is made between the calculation of design bearing capacity of single and group micro piles. It is important to determine the value of shaft friction coefficient to be able to calculate the bearing capacity of the pile and will be further described. Also in this chapter about the applied limit values according to CUR 236 and how they affect the total bearing capacity of the pile are discussed.

4.2 SINGLE PILE

The calculation rule is valid for piles that obtain a great part of their bearing capacity for tensional loads from sandy layers. The calculation rule is set up based on the test loads. According to the design guide, the minimum value of the length/diameter ratio for the test loads is 13.5 with a minimum pile length of 7 m and a maximum pile length of 50 m.

A pile is often part of a pile group. If the spacing between the piles in the pile plan is very large it is not possible to say beforehand if the pile should be regarded as a single pile or as part of a pile group. Therefore the bearing capacity must be determined for a pile in a pile group.

The calculated value of the bearing capacity of a single pile loaded in tension is determined using the following formula:

$$F_{r;tension;d} = \int_0^L O_{p;av} \cdot p_{r;z;d}\, dz \tag{20}$$

In which:

$F_{r;tension;d}$	Design value of the tensional bearing capacity of the pile in [kN];
$O_{p;av}$	Average perimeter of the pile in [m];
L	Length of the pile over which shaft friction is calculated in [m];
$p_{r;z;d}$	Design value of the shaft friction at a depth z in [kPa];
z	Depth in [m]

The design value of the shaft friction follows from:

$$p_{r;z;d} = \alpha_t \cdot q_{c;z;d} \tag{21}$$

In which:

α_t Factor which takes the influence of the installation process into account

$q_{c;z;d}$ Design value of the cone resistance at a depth z in [kPa], In case of natural over-consolidation or of an excavation, a reduction should be taken into account

TABLE 3: VALUES FOR α_t IN SAND AND GRAVELY SAND

Pile type	Installation method	$\alpha_{t,limit}$	$\alpha_{t,expected}$	$\alpha_{t,lower\ bound}$
A	Double casing with pressurized grout	0.025	0.017 (0.012)	0.011 (0.008)
B	Single casing with pressurized grout	0.025	0.017 (0.012)	0.011 (0.008)
C	No casing with grout injection through steel bar	0.025	0.012	0.008
D	Continuous flight auger	0.025	0.012	0.008
E	Vibration	0.025	-	0.006

*Values in brackets have to be applied when the grout body is not pressurized over the whole length

The values for α_t is based on test loads in sand layers and are not given for every pile type. For different pile types the value for α_t must be determined.

For piles which are only located in clay layers, the factors given above are not relevant. In these cases the values in table 4 are used.

TABLE 4: VALUES OF α_t FOR CLAY AND SILT

soil type	relative depth z/D_{eq}	α_t
clay/silt $q_c \leq 1$ MPa	$0 < z/D_{eq} < 20$	0.02
clay/silt $q_c \leq 1$ MPa	$z/D_{eq} > 20$	0.025
clay/silt $q_c > 1$ MPa	–	0.025

* The values for α_t are not based on test loads but are based on literature;

4.3 PILE IN PILE GROUP

For a pile in a pile group, it is necessary to use a different calculation rule than for a single pile due to two aspects:

- The effect of densification due to the installation of the pile group;
- The relaxation due to the tensional load on the pile group.

These two effects are taken into account using the factors f_1 and f_2. The design value of the shaft friction of a pile in a pile group follows from:

$$p_{r;z;d} = f_1 \cdot f_2 \cdot \alpha_t \cdot q_{c;z;d} \tag{22}$$

In which:

$p_{r;z;d}$ Design value of the shaft friction at depth z in [kN/m²];

*α_t Factor which takes into account the installation method [-];

$q_{c;z;d}$ Design value of the cone resistance at depth z in [kPa];

f_1 and f_2 Factors for the effect of the densification and the stress release respectively, due to the tensional load of the pile group.

*Note that α_t is derived based on failure test which is done on a single pile. However this α_t value is also used for the piles in the group.

4.3.1 LIMIT VALUES

CUR 236 states limit values for cone resistance q_c, maximum mobilized shear stress $\tau_{mob,max}$ and the calculated tensional shaft friction coefficient α_t. They are mainly used to prevent unrealistic designing of the pile capacity. Table 5 shows these proposed limit values according to CUR 236 for each pile type.

TABLE 5: PROPOSED LIMIT VALUES ACCORDING TO CUR 236 FOR EACH PILE TYPE

Pile type	$q_{c,limit}$ [MPa]	τ limit [kN/m²]	$\alpha_{t,\ limit}$ [-]
A	20	500	0.025
B	20	500	0.025
C	20	500	0.025
D	15	375	0.025
E	15	375	0.025

These above mentioned three parameters are related to each other according to the next formula;

$$\alpha_t = \frac{\tau_{mob,max}}{q_c} \tag{23}$$

When these parameters are above their limit values, they should be limited. Values below the limit value do not need to be adopted and stay the same.

Figure 18 shows a visualization of the relation between these three parameters and the effect of applying limit values. Note that α_t is the slope of q_c and $\tau_{mob,max}$ in the figure.

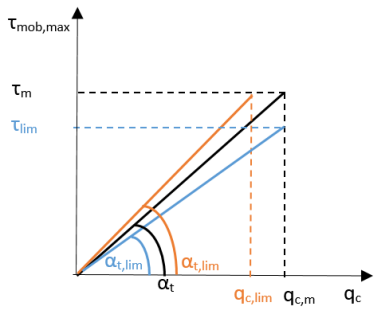

FIGURE 18: RELATION BETWEEN LIMIT VALUES

The reason and the way how the limit values affect a possible design will be further explained;

- The first limit value is for the cone resistance. It is necessary to limit the cone resistance due to over consolidation effect on sand which carries a high over burden pressure. Over consolidation packs the particles of sand together more tightly and creates more vertical effective stress. If the overburden is removed due to excavation, particles return to their initial state and therefore vertical stress decreases to its normal values. Therefore a limited cone resistance should be used in the design to take care of this explained phenomenon in the soil. By limiting the cone resistance, the value for α_t will be increased if the maximum mobilized shear stress stays the same (see orange line). However the final design capacity of the pile remains the same but it can mislead to an overestimation of the actual capacity of the pile.

- Next limit value is for $\tau_{mob,max}$. According to CUR 236 it should be defined as 2.5% of $q_{c,lim}$ which is 500 MPa for micro piles type A, B and C and 375 MPa for micro piles D and E. This is done to have some safety in the design and to prevent un-realistic high values and overestimation of the actual capacity of the pile. By applying the limit value for maximum mobilized shear stress, the value for tensional friction coefficient will become smaller if cone resistance remains the same which again acts as a safety in the design (see blue line). It should be noted that very small values of $\tau_{mob,max}$ will also lead to a conservative design which is not desirable.

- Finally the calculated tensional friction coefficient should be limited itself which is the slope of cone resistance and maximum mobilized shear stress. It should be maximized on 0.025. This limit value acts again as safety margin in the design. Again small values of α_t will lead to a conservative design and could underestimate the actual capacity of the pile.

It is therefore useful to use limit values to prevent unrealistic designing (conservative or over-estimation) of the actual capacity of the pile.

4.3.2 SHAFT FRICTION COEFFICIENT α_t

There are two ways for determining tensional shaft friction coefficient α_t based on CUR 236.

1. Using the lower bound values from table 6.1 in CUR 236 (see table 3) .This option is good for small projects with small amount of piles (≤ 100 piles). In this case failure test is not advised due to testing costs which is not cost effective for small projects.

2. Performing failure test before hand and derive an appropriate α_t based on the data. This option is therefore for big projects which large amount of piles (more than 100 piles) need to be installed. Also a validation test and check need to be done on at least 3% (with minimum of 3 piles) of the installed piles. Some rules and details about the failure test will be explained in the next paragraph.

Procedure of pile failure testing:

Testing of the piles should be done according to CUR 236. Test piles have to be installed and tested. The purpose of failure tests is to be able to determine the maximum bearing capacity of the pile and later on finding the relation between pile shaft and the bearing soil layers. However this value and the relation is only valid for this specific field and should not be used for other locations. The procedure of failure testing based on CUR 236 is as follow;

Step 1: Before installation of the piles, number of CPT's should be performed close to where the piles are going to be installed in order to have information about the soil structure and cone resistance value q_c.

Step 2: Calculate the expected failure load by using the following equation;

$$F_{test;max;gross} = R_{s;max} + R_{s;fr} + R_{s,head} \quad (24)$$

Which $F_{test;max;gross}$ is the expected failure load in [kN], $R_{s;max}$ is the net bearing capacity at soil mechanical failure in [kN], $R_{s;fr}$ is friction losses along the free length of the pile in [kN] and $R_{s,head}$ is pile head resistance in [kN].

Applying load procedure should be done step wise according to the next figure;

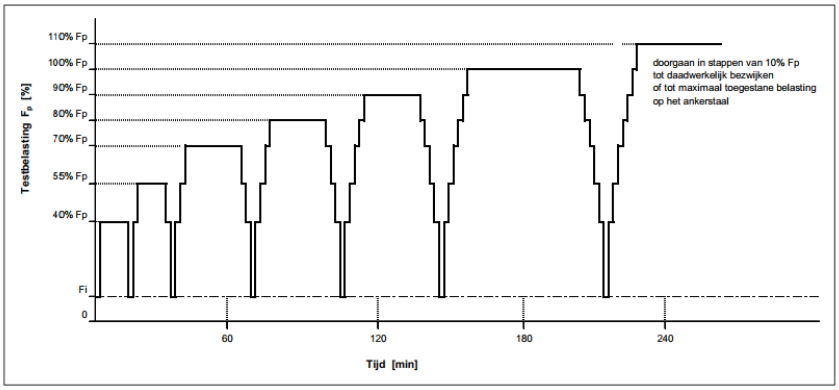

FIGURE 19: LOADING PROCEDURE ACCORDING TO CUR 236

The test load is increased from pre-loading F_i in 6 steps with unloading and re-loading steps, to value F on which soil mechanical failure of the test pile is expected. If no soil-mechanical failure has occurred, then these steps continue with an increase of 10% each time until failure occurs.

During the loading, the pile head movements will be measured and recorded. From the unloading part the plastic deformations after each loading step can be determined. Table 6 shows the load steps with corresponding time duration in each step.

TABLE 6: LOAD STEPS WITH CORRESPONDING TIME DURATION IN EACH STEP

Loading step	Load Duration [min]
Pre-loading	5
Step 1 (40% F)	15
Step 2 (55% F)	15
Step 3 (70% F)	30
Step 4 (80% F)	30
Step 5 (90% F)	30
Step 6 (100% F)	60

Step 3: Soil mechanical failure occurs when the creep size (k_s) becomes bigger than 2 mm. The formula for calculating creep size is as follow;

$$k_s = \frac{u_2 - u_1}{\log(t_2/t_1)} \quad (25)$$

Which: k_s is creep size in [mm], t_1 and t_2 are start and end time of a loading step in [mins] and u_1 and u_2 are pile head displacement in [mm] at t_1 and t_2 respectively.

Interpretation of test data:

Based on the above explained failure test, the value for shaft friction coefficient α_t is obtained following the next steps;

Step 1: Finding the maximum allowable load by taking into account that creep size should be equal or smaller than 2 mm.

$$F_{test;max;gross} = F_{test;max} \text{ with } k_s \leq 2.0\ mm \quad (26)$$

Step 2: It is important to find the net load that is actually working on the grout body which connect the pile to the soil. Therefore the next formula should be used;

$$R_{s;max} = F_{test;max;gross} - R_{s;fr} - R_{s;head} \quad (27)$$

Which: $R_{s;max}$ is the net test load working on grout body in [kN], $F_{test;max;gross}$ is the maximum load that has been applied in [kN], $R_{s;fr}$ is loss due to friction along the free length of the pile in [kN] and $R_{s;head}$ is the head resistance in [kN].

Step 3: Determine the maximum mobilized shear stress along the anchor body by using the next formula;

$$\tau_{mob;max} = \frac{R_{s;max}}{\pi \cdot \emptyset \cdot L_a} \quad (28)$$

Which: $\tau_{mob;max}$ is the maximum mobilized shear stress in [kN/m^2], $\emptyset$ is the outer diameter of anchor body in [m] and L_a is the effective length of anchor body in [m] (see figure 20).

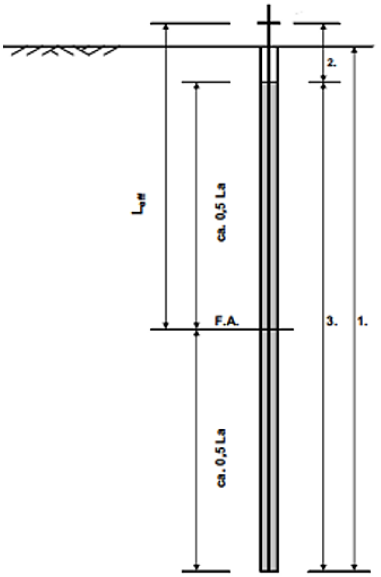

1. Grout body over full pile length until ground level/ excavation level
2. Free length of the anchor pile
3. Anchor body where the load transfer takes place

FIGURE 20: VISUALIZATION OF EFFECTIVE ANCHOR LENGTH

Step 4: Calculate for each test pile, the average cone resistance over the length of anchor body based on corresponding CPT data.

Step 5: Determine the friction coefficient α_t for each test pile by using the next formula; Note that it should be equal or smaller than 2.5%.

$$\alpha_{t;i} = \frac{\tau_{mob;max}}{q_{c;avg}} \leq 2.5\% \tag{29}$$

Which: α_t is the friction coefficient along the anchor body, $\tau_{mob;max}$ is the maximum mobilized shear stress in [kN/m^2] and $q_{c;avg}$ is the average cone resistance along the grout body in [MPa].

**Note that: based on CUR 236, maximum values for $\tau_{mob;max}$ and $q_{c;avg}$ are as follow;

$\tau_{mob;max} = 0.025 * q_{c;avg}$ → **500** kN/m2 (=0.025***20** Mpa) for pile types A,B and C

$\tau_{mob;max} = 0.025 * q_{c;avg}$ → **375** kN/m2 (=0.025***15** Mpa) for pile types D and E

Step 6: Find the average value of friction coefficient with respect to the number of tested piles according to:

$$\alpha_{t;avg} = \frac{\sum \alpha_{t;i}}{N} \tag{30}$$

Which: α_t is friction coefficient along anchor body for the test pile and N is the total number of tested piles.

**Note that: the coefficient of variation (CV) should not exceed 0.12 for all individual values.

$$CV = \frac{\sigma_{test;max;avg}}{\mu_{test;max;avg}} \quad (31)$$

Which:

$$\sigma_{N;test;max} = \sqrt{\frac{\sum_{i=1}^{N}\left(F_{test;max;gross,i} - \mu_{N;test;max}\right)^2}{N}} \quad \text{and} \quad \mu_{N;test;max} = \frac{\sum F_{test;max;gross}}{N} \quad (32) \text{ and } (33)$$

If the CV value is equal or lower than 0.12 go to step 7 and if not go to step 8.

Step 7: determine design value of friction coefficient by using;

$$\alpha_t = \beta_t \cdot \alpha_{t;avg} \quad (34)$$

Which β_t is coefficient which is dependent on the successfully tested piles according to the next table;

TABLE 7: B_T VALUES DEPENDENT ON SUCCESSFULLY TESTED PILES

N	1	2	≥3
β_t	0.8	0.9	1.0

Step 8: In this case the friction coefficient should be equal to the minimum value of friction coefficient test piles.

$$\alpha_t = \alpha_{t;min} \quad (35)$$

4.3.3 DETERMINATION OF $q_{c;z;d}$ AND THE FACTORS f_1 AND f_2

In this paragraph, the determination of $q_{c;z;d}$ and the factors f_1 and f_2 are described. It must be remarked that the factors f_1 and f_2 are valid for sand. They are not valid for clay, and must be set to $f_1 = f_2 = 1.0$.

Step 1: Determine the starting points which consist of the following;

- Soil: cone resistance, volumetric weights and soil layout
- Pile: type and dimensions, the influenced area in a pile group (ex. pile spacing² - A_{pile})

Step 2: Define the value of reduction of the cone resistance by excavation for two cases;

a) Installation after excavation:

$$q_{c;z;exc} = q_{c;z} \cdot \frac{\sigma'_{v;z;exc}}{\sigma'_{v;z;0}} \quad \text{with} \quad q_{c;z;exc} \le 12 \text{ or } 15 \text{ MPa} \quad (36)$$

b) Installation before excavation:

$$q_{c;z;exc} = q_{c;z} \cdot \sqrt{\frac{\sigma'_{v;z;exc}}{\sigma'_{v;z;0}}} \quad \text{with} \quad q_{c;z;exc} \le 12 \text{ or } 15 \text{ MPa} \quad (37)$$

Step 3: Determine the design value of the cone resistance and volumetric weight according to the next formula:

$$q_{c;z;rep} = \xi \cdot q_{c;z;max} \qquad \text{and} \qquad q_{c;d} = \frac{q_{c;z;rep}}{\gamma_{m;b4} \cdot \gamma_{m;var;qc}} \qquad \text{(38) and (39)}$$

In which $q_{c;z;max}$ = cone resistance at depth z (possibly including excavation), ξ = redistribution capacity of the structure (according to NEN 6743), $\gamma_{m;b4}$= material factor for piles loaded in tension according to NEN6740 (=1.4), $\gamma_{m;var;qc}$= factor which shows the influence of the variation of the loads.

Beneath the phreatic water table, the volumetric weight is: $\gamma'_d = \frac{\gamma_{sat}}{\gamma_{m;g}} - \gamma_{water}$ (40)

In which γ'_d = design value for effective volumetric weight and $\gamma_{m;g}$ = material factor for the self-weight of the soil. This is 1.0 if a high value of the unit weight is unfavorable, and 1.1 if a low value is unfavorable.

Step 4: determine the effect of the installation (factor f_1) in sand by using the next formulas. According to CUR 236, this value is equal to 1.0 for micro piles.

$$f_1 = e^{3 \cdot \Delta R_e} \text{ with } \Delta R_e = \frac{\sum_1^n \Delta e}{(e_{max} - e_{min})} \text{ and } \sum_1^n \Delta e = -\frac{(r-6)}{5.5} \cdot \frac{(1+e_0)}{50} \qquad \text{(41), (42) and (43)}$$

In which r = the distance c.t.c. expressed in D_{eq} of a pile to the pile with a maximum of $r = 6$. If $r > 6$ the densification effect is neglected.

Step 5: Determine the effect of applying the tensional load (factor f_2) based on:

$$f_2 = \frac{q_{c;z;2}}{q_{c;z;1}} \qquad (44)$$

In which : $q_{c;z;1}$ is the design value of the cone resistance at a depth z after the installation of the pile and before the tensional load has been applied in [MPa] and $q_{c;z;2}$ is the design value of the cone resistance at a depth z after the tensional load has been applied in [MPa].

$$f_{2;i} = \frac{-M_i + \sqrt{M_i^2 + \left(2\sigma'_{v;d;j;0} + \gamma'_{d;i} \cdot d_i\right)\left(2\sigma'_{v;d;j;0} + \gamma'_{d;i} \cdot d_i - 2\sum_{n=0}^{i-1} T_{d;n}\right)}}{\left(2\sigma'_{v;d;j;0} + \gamma'_{d;i} \cdot d_i\right)} \qquad (45)$$

with: $M_i = \frac{f_{1;i} \cdot O_{p;i} \cdot \alpha_t \cdot q_{c;d;i} \cdot 1000 \cdot d_i}{A}$ and $T_{d;i} = M_i \cdot f_{2;i}$ (46) and (47)

Step 6: Finally calculate the bearing capacity of the pile by applying the next formula:

$$F_{r;tension;d} = \int_0^L q_{c;z;d} \cdot \ f_1 \cdot f_2 \cdot O_{p;z} \cdot \alpha_t \, dz = A \cdot \sum_{i=1}^{m} (M_i \cdot f_{2;i}) \tag{48}$$

Because of possible disturbances, the upper meter of soil around the pile is regarded as disturbed. The shaft friction in this layer must be set to 0.

Step 7: Control the weight of the soil between the piles; shape of the volume of the soil around the pile that is to be mobilized.

It may be assumed that it is not possible to mobilize the entire weight of the sand between the piles of a pile group in order to develop the bearing capacity of the pile. It may be assumed that a conical shaped slip surface can originate, starting from the pile tip. This effect is taken into account by comparing the weight of the soil in the cone and cylinder shape with the calculated bearing capacity of the pile in the pile group using:

$$F_{r;tension;max;d} = \left(V_{cone} + V_{cylinder}\right) \cdot \gamma'_d \tag{49}$$

Step 8: For the final pull-out capacity of the pile, the calculation value of the effective weight of the pile may be added by using:

$$\left(F_{r;tension;d} \le F_{r;tension;max;d}\right) + G'_{pile;d} \tag{50}$$

$$G_{pile;d} = V_{pile} \cdot \gamma'_{pile;d} \tag{51}$$

For the detailed explanations and derivations of the mentioned steps and formulas, the reader is referred to appendix B.

CHAPTER 5: CASE STUDY

5.1 INTRODUCTION

Due to existence of heterogeneity and diversity in subsoil behavior and availability of different methods of installation, it is very necessary to test the piles in-situ or use model piles and compare the results with national standards and design guide line calculations. In this chapter a detailed description of the used case study including the important information of the location of field failure test and corresponding loading procedure is demonstrated.

Based on this case study, further in chapter 6 and 7, analytical and numerical modeling of the pile will be done.

5.2 DESCRIPTION OF BOERENWETERING CAR PARKING PROJECT

Boerenwetering or Albert Cuyp car parking which opened on 22 May 2018 is an underground car parking in the Boerenwetering between the Ruysdaelkade and the Hobbemakade in Amsterdam. It provides space for approximately 600 cars and 60 bicycles.

For the construction of this car parking, GEWI piles with grout body are made to prevent the upward forces of "under water concrete floor and basement" during the construction and use phase. The tension element used for the piles consists of a GEWI Ø 63.5 mm, with a steel quality GEWI steel S555/700.

For the grout that comes into direct contact with the bar, blast furnace cement which is special type of cement is used. The grout is made with a water/ binding agent factor of approx. 0.4 to 0.45.

Figures 21 and 22 show a top view and cross section of this car parking project respectively.

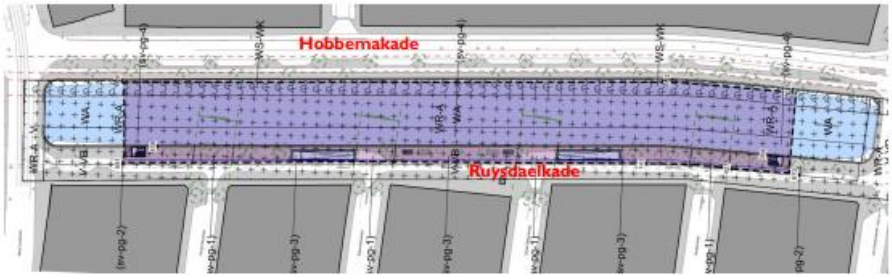

FIGURE 21: TOP VIEW OF BOERENWETERING CAR PARKING

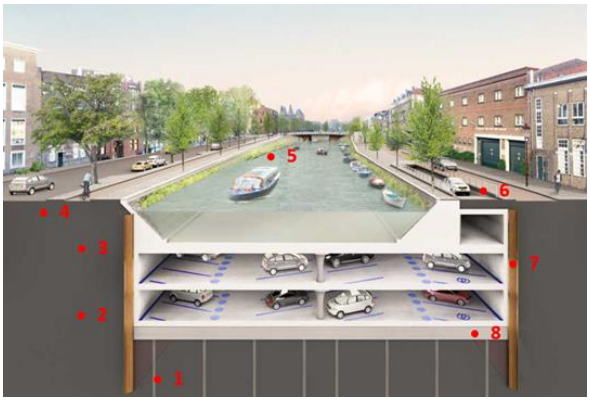

FIGURE 22: CROSS SECTION OF BOERENWETERING CAR PARKING

The explanation of the red dots in figure 22 is as follow;

1→ There are more than 1000 Micro-piles installed. A pile has a length of approximately 14 meters and is applied between NAP-9m and NAP-23m.

2→The car parking consists of two parking floors and provides parking space for of 600 cars and 60 bicycles.

3→ In total, about 80,000 cubic meters soil is excavated.

4→The ground level is at NAP + 0.5 m and the sheet piles reach to NAP-14m.

5→ The car parking has a length of approximately 260 meters and is approx. 30 meters wide.

6→ The entrance and exit of the car parking are situated on the Ruysdaelkade.

7→ The sheet piles are used to construct the construction pit and they are left behind permanently in the ground.

8→ The bottom of the underwater concrete comes at NAP-10.6 m.

Construction Phases of the Boerenwetering car parking:

The following descriptions show the construction phases for the car parking project;

1. Place the sheet piles in the construction pit;

2. Wet excavation to NAP-3.0m;

3. Apply struts to NAP-2,5m and pre-stress;

4. Wet excavation until bottom of underwater concrete floor (= NAP-10.8m);

5. Installing anchor piles;

6. Deposit under water concrete floor and dry construction pit;

7. Deposit deck / floor -3;

8. Remove the strut after completion of floor -1 and floor -2.

5.3 IN-SITU PULL-OUT TEST ON MODEL PILES

There are 6 single piles divided in two series of A and B tested until they have reached the failure value. In the following sections site characteristics, the work plan description and the procedure of pile load failure test are presented.

Friction between the soil and the grout is the determining factor in the tensile capacity that the pile can handle. It is necessary based on the standards for GEWI piles, to define the failure as the force at which the creep size is greater than 2 mm (tensile load).

5.3.1 SITE CHARACTERISTICS AND GEO-TECHNICAL PARAMETERS

The soil structure of the Boerenwetering project is determined based on the in-situ and laboratory tests. The Cone penetration test (CPT) is a well-known and common test to find different layers with corresponding thickness of the ground. This data which is presented in table 8 and 9 is based on 2 CPTs of -30 m NAP which can be found in appendix A. The height reference of CPT data is according to NAP which refers to Normaal Amsterdams Peil and is the national Dutch reference level.

Due to the presence of cables and pipes, CPT 1 and 2 are pre-bored to a depth of - 3.5 m. The obtained materials are classified in accordance with NEN 5104. Figure 23 also demonstrates the structure of the soil at location of CPTs.

From the information of CPT's it could be noted that two layers of sand are available which are important for the analytical and numerical modeling of this research. The first sand layer is considered starting from -12.5 m NAP to -17.5 m NAP and the second one from -17.5 m NAP to -27.5 m NAP.

TABLE 8: SOIL STRUCTURE AT SITE

Layer Number	Soil type	Top Level Layer [m NAP]
L1	Sandy fill	+0.6
L2	Dutch Peat	-2.9
L3	Clay deposits	-4.5
L4	Base Peat	-10.0
L5	First Sand Layer	-12.5
L6	Clayey/Silty Sand	-15.0
L7	Second Sand Layer	-17.5

TABLE 9: WATER LEVEL AT SITE

Ground water	Top level [m NAP]
Phreatic groundwater	-0.4
Water head in the first sand layers and under laying layers	-2.5

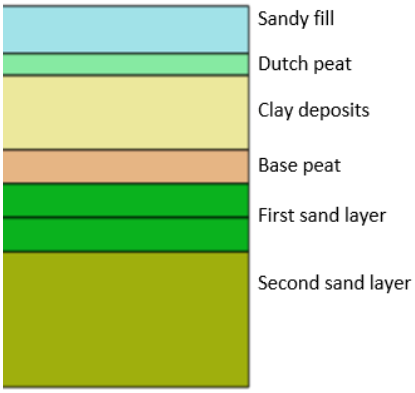

FIGURE 23: STRUCTURE OF SOIL AT CPT LOCATION

5.3.2 WORK PLAN

A total of six piles were tested in two different series of A and B. Series A (pile 1, 2 and 3) consist of three piles which has a total length of 23.5 meters and reached until the second sand layer and series B (pile 4, 5 and 6) includes another three piles with a total length of 18.5 and reached until the first sand layer.

Series A: GEWI piles Ø63.5 mm grout plug in 2nd layer of sand (failure test)

- Drill casing to the desired depth;
- Installing the anchor element;
- Apply grout and pressurize simultaneously with pulling the casing;
- Perform the load failure test after at least 10 calendar days; After completion of the failure test, remove the extension rod from the anchor to NAP -17.5m (anchor remains behind of approx. NAP -17.5 m = top of grout body);
- Fill up the free space with cement bentonite.

Series B: GEWI piles Ø63.5 mm grout plug in 1st layer of sand (failure test)

- Drill casing to the desired depth;
- Installing the anchor element;
- Apply grout and pressurize simultaneously with pulling the casing;
- Perform the load failure test after at least 10 calendar days; After completion of the failure test, remove the extension rod from the anchor to NAP -12.5m (anchor remains behind of approx. NAP -12.5 m = top of grout body);
- Fill up the free space with cement bentonite.

Figure 24 shows a cross section of the failure test site.

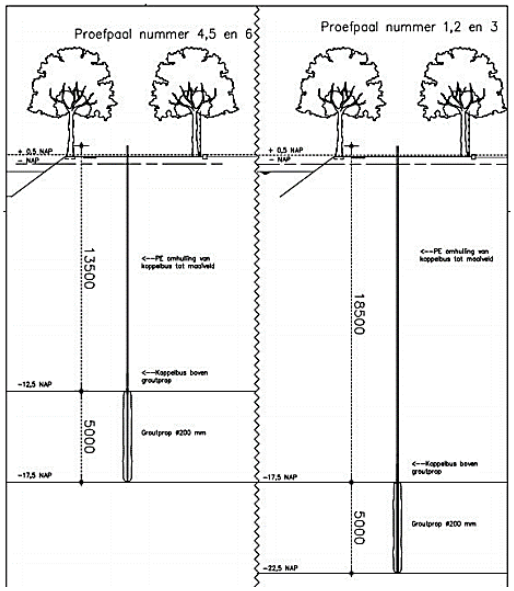

FIGURE 24: CROSS SECTION OF THE FAILURE TEST AT SITE

The physical description of the used test piles are provided in table 10 below;

TABLE 10: PHYSICAL DESCRIPTION OF THE USED TEST PILES

Pile number	GEWI bar diameter [mm]	Steel quality	Pile shaft diameter [mm]	Grout body from/to [NAP m]	Grout body length [m]	Free anchor length [m]	Drilling method
1	63.5	S555/700	200	-17.5/-22.5	5	18	Double casing
2	63.5	S555/700	200	-17.5/-22.5	5	18	Double casing
3	63.5	S555/700	200	-17.5/-22.5	5	18	Double casing
4	63.5	S555/700	200	-12.5/-17.5	5	13	Double casing
5	63.5	S555/700	200	-12.5/-17.5	5	13	Double casing
6	63.5	S555/700	200	-12.5/-17.5	5	13	Double casing

5.3.3 PILE LOAD TEST PROCEDURE

CUR 236 has been used as a guideline for carrying out the failure test. A total of six piles were tested in two different series of A and B. At the start a pre-loading of 100 kN was applied. Subsequently, the strength was increased in steps of 40%, 55%, 70%, 80%, 90% and 100% of the expected bearing capacity of the pile. After each step, it is unloaded to the initial force of 100 kN. During the loading, the pile head movements were measured and recorded. From this unloading part the plastic deformations after each loading step can be determined.

Table 11 and 12 illustrate the load steps and the final tensile load for series A and B pile load test.

TABLE 11: SERIES A PILE LOAD TEST

Loading step	Load [kN]	Load Duration [min]
Pre-loading	100	5
Step 1 (40% F)	566	15
Step 2 (55% F)	778	15
Step 3 (70% F)	990	30
Step 4 (80% F)	1131	30
Step 5 (90% F)	1273	30
Step 6 (100% F)	**1414**	**60**

The pre-calculated capacity of these piles was reached at step 6 (100% F) with a load of 1414 kN and creep value smaller than 2 mm.

Below the load-displacement diagrams for series A of piles for piles 1,2 and 3 which are in second sand layer are plotted. The x-axis shows the increasing load and the y-axis is the plastic displacement on the pile head. Also it shows the elastic unloading-reloading based on the point measurements.

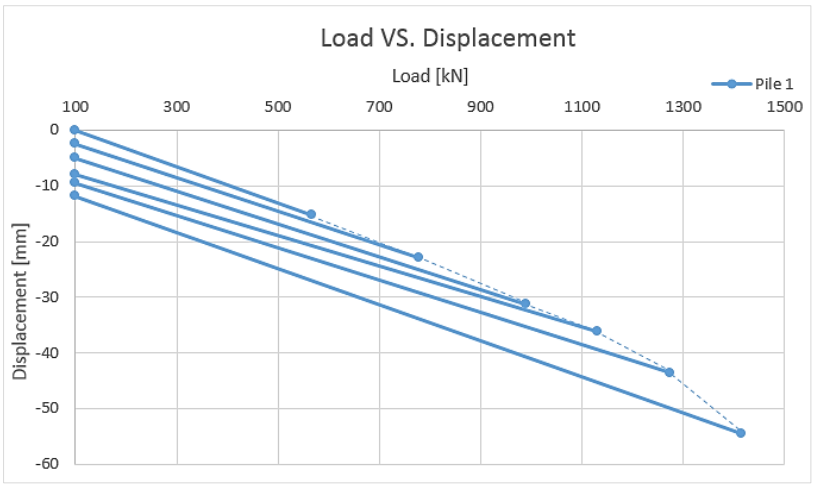

FIGURE 25: LOAD VS. DISPLACEMENT, PILE 1

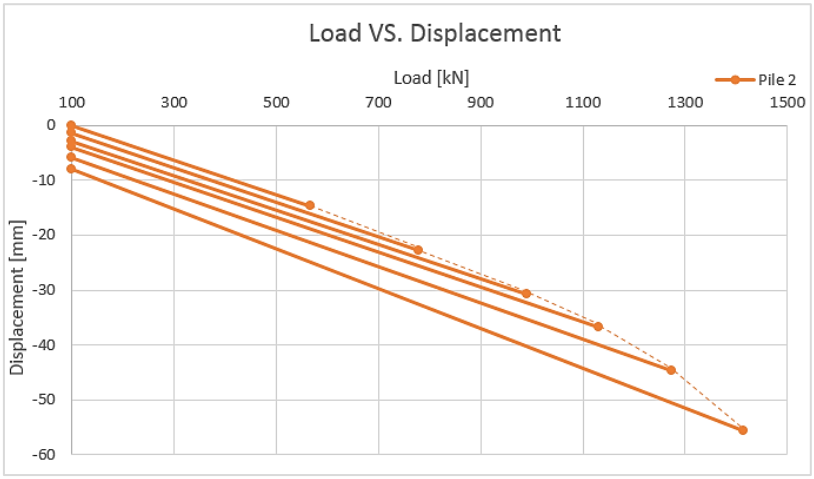

FIGURE 26: LOAD VS. DISPLACEMENT, PILE 2

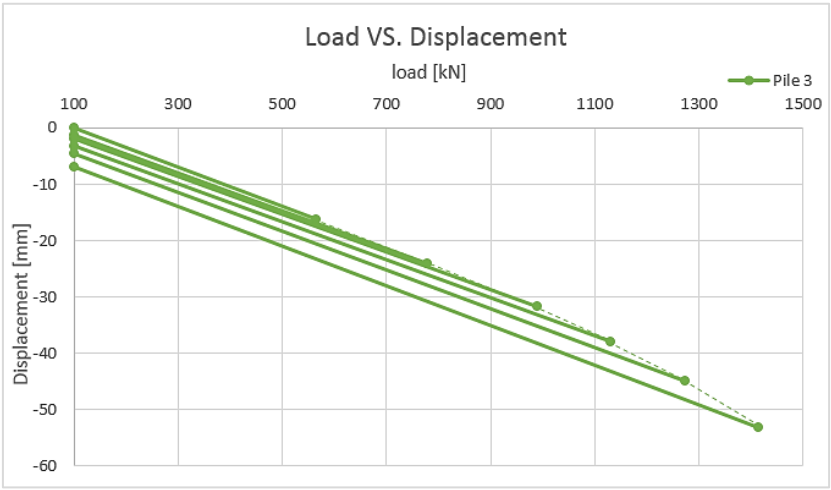

FIGURE 27: LOAD VS. DISPLACEMENT, PILE 3

TABLE 12: SERIES B PILE LOAD TEST

Loading step	Load [kN]	Load Duration [min]
Pre-loading	100	5
Step 1 (40% F)	151	15
Step 2 (55% F)	208	15
Step 3 (70% F)	264	30
Step 4 (80% F)	302	30
Step 5 (90% F)	340	30
Step 6 (100% F)	**377**	**60**
Step 7 (120% F)	**453**	**60**
Step 8 (150% F)	566	60

A total capacity of 377 kN was determined for these piles. An additional loading step was performed for this series. Pile 5 was failed at loading step 143% F (=540 kN) and pile 6 tested until failure with load 139% F (=525 kN). At this level the anchor remain stable and the creep value is smaller than 2 mm.

Here is again the load-displacement diagrams for series B of piles in the first sand layer is plotted.

The difference in pull-out capacity could be due to the fact the behavior is highly influenced by the installation effects even if they have the same length and material characteristics and installed in the same ground condition.

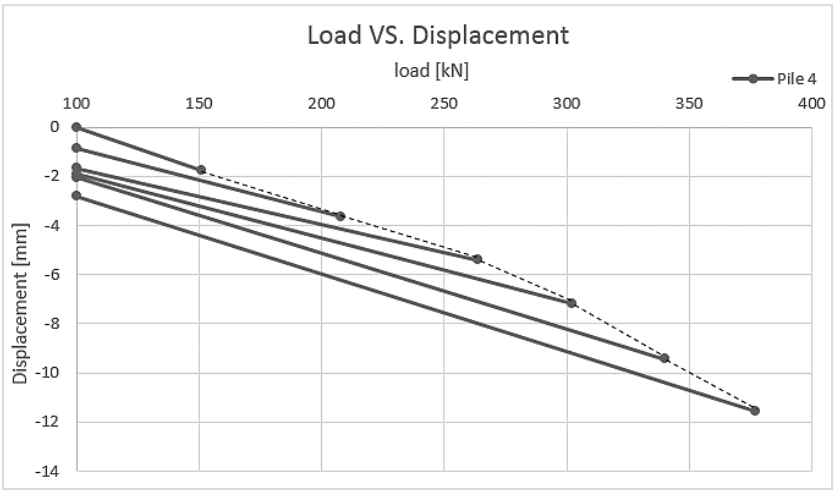

FIGURE 28: LOAD VS. DISPLACEMENT, PILE 4

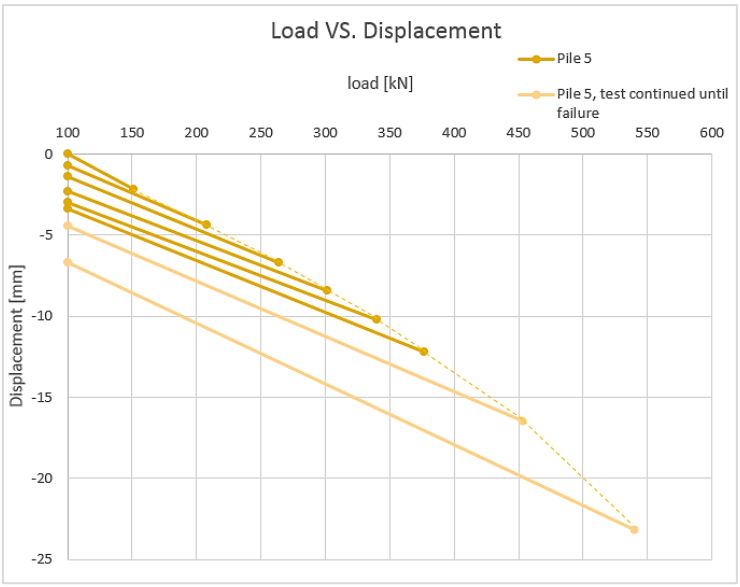

FIGURE 29: LOAD VS. DISPLACEMENT, PILE 5

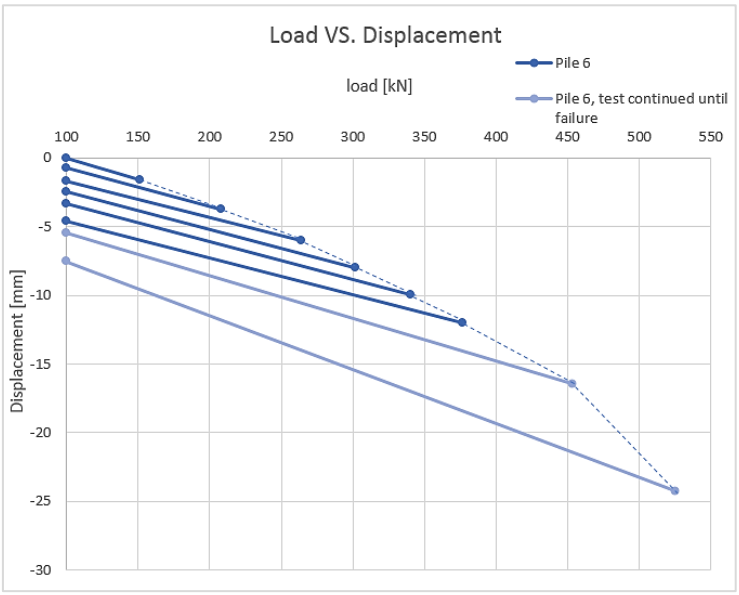

FIGURE 30: LOAD VS. DISPALCEMENT, PILE 6

The summary of test results are as follow can be found in table 13. The creep value of all 6 tested piles in the last stage was smaller than 2 mm.

TABLE 13: SUMMARY OF 6 PILE TESTS RESULT

Pile number	Maximum test load [kN]	Maximum test displacement [mm]
1	1414	54.5
2	1414	55.6
3	1414	53.3
4	377	11.5
5	453	16.4
6	453	16.4

5.3.4 LIMITATIONS REGARDING TO FAILURE TEST DATA

There are some limitations and uncertainties in the data study of failure test which are as follow;

Diameter, length and shape of grout body

The diameter of the pile is one of the uncertainties. Since the installation is performed in situ at site, the diameter of the installed pile is unsure and there is no test done to verify the diameter of the pile. Diameter is important to know since it will affect the frictional area of the pile and as result maximum mobilized shear stress. Depending on smaller or bigger actual diameter of the installed pile, maximum mobilized shear stress can be under- or overestimated.

The length of the grout body is another uncertainty. Since the pile is created in the soil, it is difficult to control the length of grout body and make an exact length of it. Shorter or longer grout body influences the frictional area of the pile and as thus again we would have under- or overestimation of the mobilized shear stress of the pile.

Shape of grout body also has similar effect as diameter and length of grout body which affects maximum mobilized shear stress and can lead to an under- or overestimation of it.

Gross failure load

Failure test is done according to the steps and procedure of CUR 236. When a certain loading step is successfully achieved, the next loading step will be increased with 10% of the previous step. The limitation of this method is that when for example a loading step of 110% is not achieved and the pile fails within a loading stage of 107% of the expected load, the loading step 100% is taken as final failure loading stage. Therefore an underestimation of the actual load is made by this testing procedure.

Soil conditions

Before failure test, the Cone Penetration Tests (CPT) are done to define the structure of the soil. However the CPT is done close to the failure test location. Due to highly variable characteristic and heterogeneity of the soil, there is not a guarantee if the soil structure at CPT location is exactly the same as one at failure test.

Pile installation

Installation of the piles are important aspect to consider and should follow the planning. If a pile is planned to have the grout body only in sand layer but due to poor installation the grout body continues until the clay layer above it, it would not behave as expectations and should be installed correctly.

α_t for specific location

The derived value for α_t based on failure test is specific for the soil at Boerenwetering site in Amsterdam. It is possible that in another site or location different values is found.

CHAPTER 6: ANALYTICAL MODEL

6.1 INTRODUCTION

In this part it has been tried to do a calculation of axial strength of single and group tension pile(s) used for Amsterdam case study as introduced in NEN 9997-1, CUR 236 and CUR 2001-4. To do so, it is initially needed to define a proper shaft friction coefficient which is further in this chapter determined. Also the design bearing capacity of single pile is calculated based on the international design methods explained in chapter 3 and the outcome is compared to reference single pile from field failure test. For the detailed calculation the reader is referred to appendices C and D.

6.2 DETERMINATION OF α_t

6.2.1 DESIGN BASED ON FAILURE TEST (RAW DATA)

In previous chapter, the performed failure test for Boerenwetering car parking is described. In this part α_t is derived based on raw data obtained from failure test. With failure test the maximum capacity of the pile is measured. Based on the results the value for maximum mobilized shear stress and shaft friction coefficient can be derived for raw data. These values are then compared to the values derived based on CUR 236 guide line.

There are 6 piles all based on type A micro piles planned to be tested in total. Before installation of test piles, two CPTs (A and B) are performed close to the location of the test piles. Next figure 31 shows the location of the test piles and the corresponding location of the CPTs.

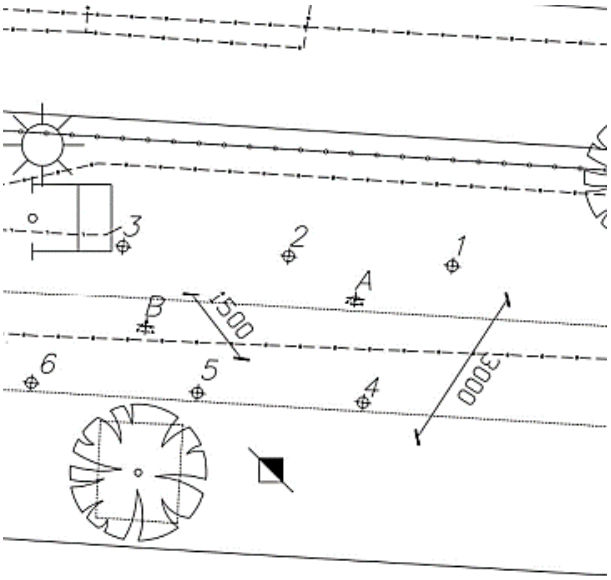

FIGURE 31: LOCATION OF THE TEST PILES AND THE CORRESPONDING LOCATION OF THE CPTS

The structure of the soil is already explained in section 5.3.1. The CPTs A and B can be found in appendix A. The average of these two CPTs are used to determine the cone resistance q_c at pile test location.

The average values for q_c per pile can be found in table 14. These values are based on the measured average cone resistance along the anchor length of the pile.

TABLE 14: THE AVERAGE VALUES FOR QC PER PILE

Depth	NAP -12.5m to NAP -17.5m			NAP -17.5m to NAP -22.5m		
Pile number	4	5	6	1	2	3
$q_{c,avg}$ [MPa]	11.66			31.27		

Based on the pile shaft diameter, length of the grout body and the maximum test load, the maximum mobilized shear stress can be calculated with the next relationship and the results can be found in table 15.

$$\tau_{mob;max} = \frac{R_{s;max}}{\pi \cdot \emptyset \cdot L_a} \quad (52)$$

Which $R_{s;max}$ is the maximum test load in [kN], ø is diameter of the pile shaft in [m] and L_a is grout body length in [m].

TABLE 15: MAXIMUM MOBILIZED SHEAR STRESS PER TESTED PILE

Pile number	Pile shaft diameter [mm]	Grout body length [m]	Total pile length [m]	Maximum test load [kN]	$\tau_{mob,\ max}$ [kN/m²]
1	200	5	23	1414	450
2	200	5	23	1414	450
3	200	5	23	1414	450
4	200	5	18	377	120
5	200	5	18	453	144
6	200	5	18	453	144

According to the average cone resistance from table 14 and maximum mobilized shear stress from table 15, the value for α_t can be determined by using the next formula;

$$\alpha_{t;i} = \frac{\tau_{mob;max}}{q_{c;avg}} \quad (53)$$

The values of α_t for each test pile and the average α_t for each sand layer are shown in table 16.

TABLE 16: VALUES OF A_T FOR EACH TEST PILE AND THE AVERAGE A_T FOR EACH SAND LAYER

Pile number	First sand layer			Second sand layer		
	4	5	6	1	2	3
$\tau_{mob,\ max}$ [kN/m²]	120	144	144	450	450	450
q_c [MPa]	11.66			31.27		
α_t [-]	0.0103	0.0123	0.0123	0.0144	0.0144	0.0144
Average α_t [-]	0.0117			0.0144		

6.2.2 DESIGN BASED ON CUR 236

In this part α_t values are calculated based on CUR 236. This is done according to the design scheme which can be found in section 4.3.2. Basically CUR 236 considers some maximum values for cone resistance and mobilized shear stresses. Next table shows a comparison between values obtained based on raw data and based on CUR 236 design scheme.

TABLE 17: COMPARISON OF A_T VALUES BASED ON RAW DATA AND CUR 236 DESIGN SCHEME

	Raw data				CUR 236			
Pile number	$\tau_{mob,max}$ [kN/m²]	q_c [MPa]	α_t [-]	$\alpha_{,t\ average}$ [-]	$\tau_{mob,max}$ [kN/m²]	q_c [MPa]	α_t [-]	$\alpha_{t,average}$ [-]
1	450	31.27	0.0144	0.0144	450	19.54	0.023	0.0230
2	450	31.27	0.0144		450	19.54	0.023	
3	450	31.27	0.0144		450	19.54	0.023	
4	120	11.66	0.0103	0.0117	120	11.07	0.0108	0.0122
5	144	11.66	0.0123		144	11.07	0.013	
6	144	11.66	0.0123		144	11.07	0.013	

The main difference that can be seen is that the values based on CUR 236 are higher than raw values. The reason is that the cone resistance is maximized on 20 MPa.

6.2.3 BEARING CAPACITY BASED ON RAW DATA AND CUR 236

To check the differences of design bearing capacity based on raw data and CUR 236, the next equation is used;

$$R_{t,d}=\int_0^{L_g} \frac{(f_1 . f_2 . \alpha_t . q_{c,z} . \pi . D)}{\gamma_{m,var} \cdot \gamma_{s,t} \cdot \xi_{m,n}}\, dz \tag{54}$$

According to the equation, the only variables are q_c and α_t and the other parameters are constant for the same considered pile. Therefore equation 54 can be simplified to the following equation to do a rough comparison of the bearing capacity;

$B = \alpha_t . q_{c,z}$ in which B is the comparable bearing capacity in [MPa] (55)

The comparable bearing capacity of the piles based on raw data and CUR 236 is displayed in the next table 18.

TABLE 18: COMPARISON OF FINAL DESIGN BEARING CAPACITY BASED ON RAW DATA AND CUR 236

	Raw data			CUR 236		
Pile number	q_c [MPa]	α_t [-]	B [MPa]	q_c [MPa]	α_t [-]	B [MPa]
1	31.27	0.0144	0.45	19.54	0.023	0.45
2	31.27	0.0144	0.45	19.54	0.023	0.45
3	31.27	0.0144	0.45	19.54	0.023	0.45
4	11.66	0.0103	0.12	11.07	0.0108	0.12
5	11.66	0.0123	0.14	11.07	0.013	0.14
6	11.66	0.0123	0.14	11.07	0.013	0.14

It can be seen that the bearing capacity is the same for both raw data and CUR 236. The difference in α_t values does not make any change to the final bearing capacity value. However the values of α_t based on CUR 236 are higher and therefore give a misrepresentative view on the final capacity of the pile.

6.2.4 OVERALL COMPARISON OF CALCULATED VALUES WITH CUR 236

As it has been already explained, CUR 236 presents some design values for α_t to come to micro pile design capacity. There are two types of values stated in the CUR 236 for α_t, lower bound values and expected values. The lower bound values is used when there is no failure test

performed beforehand and the expected values is used when the failure test is executed. Next table 19 shows the overall values of α_t from raw data, following CUR 236 design guide and values stated in CUR 236.

TABLE 19: COMPARISON OF DIFFERENT A_T VALUES

				Raw data	CUR 236 design	Sated values in CUR236	
	Pile number			αt, avg[-]	αt, avg [-]	αt lower bound [-]	αt expected [-]
2nd sand layer	1	2	3	0.0144	0.0230	0.011	0.017
1st sand layer	4	5	6	0.0117	0.0122	0.011	0.017

From the results it can be concluded that the value of α_t based on CUR 236 design for second sand layer is higher compared to the expected value stated in CUR 236. It is due to the fact that the cone resistance is maximized on 20 MPa and therefore for the calculation it is used from a lower average cone resistance which caused to heighten α_t.

For the first sand layer the α_t value based on raw data, CUR 236 design guide and the lower bound value are all close to each other and about 50% lower than the expected value stated in CUR 236. The reason could be because the values of cone resistances are not limited since they were below limit.

In general, the values of raw data for both first and second sand layer are close to the values stated in CUR 236. This rises the idea that CUR 236 has used from raw data to determine α_t. However still higher values of α_t based on CUR 236 design and the expected values stated in CUR 236 could mislead to an image of the pile with high bearing capacity than it actually is.

6.3 AXIAL STRENGTH IN TENSION

Single pile

In this part the calculation of design bearing capacity of type A single tension pile in Ultimate Limit State (ULS) is done based on CUR 236 design guide and according to the international design methods described in chapter 3. For the detailed calculation, the reader is referred to the appendices C and D.

The following formula (equation 54) is used for the calculation of design bearing capacity of the pile based on CUR 236.

$$R_{t,d}=\int_0^{L_g} \frac{(f_1 \cdot f_2 \cdot \alpha_t \cdot q_{c,z;exc} \cdot \pi \cdot D)}{\gamma_{m,var} \cdot \gamma_{s,t} \cdot \xi_{m,n}}\, dz$$

Which:

$R_{t,d}$= Design value for tensional resistance [kN]

L_g= Length of grout body in which shaft friction can develop [m]

f_1= Factor which determines densification only used for sand =1.0 for micro piles [-]

f_2= Factor which determines the effective stress reduction due to tensile load on a pile group ≤ 1.0 [-]

α_t = Shaft friction coefficient which takes into account the influence of pile installation [-]

$q_{c,z,exc}$ = Cone resistance at depth z which takes into account the excavation or over-consolidation [MPa]

$$q_{c;z;exc} = q_{c;z} * \frac{\sigma_{v;z;exc}}{\sigma_{v;z;0}} \text{ for pile type E}$$

$$q_{c;z;exc} = q_{c;z} * \sqrt{\frac{\sigma_{v;z;exc}}{\sigma_{v;z;0}}} \text{ for pile types A to D}$$

$$q_{c;z;NC} = q_{c;z;OC} * \sqrt{\frac{1}{OCR}} \text{ for pile type E in geologically over-consolidated situation}$$

OCR= Over-consolidation ratio [-]

D= Diameter of the grout body [m]

$\gamma_{m,var}$= Load variation factor = 1.0 [-]

$\gamma_{s,t}$ = Partial resistance factor of piles in tension= 1.25 [-]

$\xi_{m,n}$= correlation factor with respect to number of CPT's and the redistributive capacity of a construction = 1.39 (flexible) [-]

Factors f_1 and f_2 are equal to 1.0 for the design bearing capacity of the single pile. Also since there is no excavation prior to the failure test, $q_{c,z;exc}$ is equal to $q_{c,z}$.

Table 20 and 21 show the outcome of all calculations based on international methods, raw data of CPT and CUR design method for first and second sand layer. The calculations are compared to the reference value from field failure test and the ratios to it are determined in percentage.

TABLE 20: COMPARISON OF DESIGN BEARING CAPACITY OF THE SINGLE PILE IN FIRST SAND LAYER

Method name	First sand layer	
	$R_{t;d}$ [kN]	Ratio to failure test [%]
Reference: Failure test value	377	100
Method 1: API (2010)	137	36
Method 2: ICP (05)	191	51
Method 3: UWA (05)	205	54
Method 4: FHWA	283	75
$q_{c,avg}$ as is, $\alpha_{t,raw}$=0.0117	271	72
*$q_{c,CUR}$, $\alpha_{t,\ design}$=0.0122	274	73
$q_{c,CUR}$, $\alpha_{t,lower\ bound}$=0.011	247	66
$q_{c,CUR}$, $\alpha_{t,expected}$=0.017	382	101
$q_{c,avg}$, $\alpha_{t,fit}$=0.0162	**377**	**100**
$q_{c,CUR}$, $\alpha_{t,fit}$=0.0167	**377**	**100**

*Based on CUR: peaks of q_c cuts off on 20 Mpa

TABLE 21: COMPARISON OF DESIGN BEARING CAPACITY OF THE SINGLE PILE IN SECOND SAND LAYER

Method name	Second sand layer	
	$R_{t;d}$ [kN]	Ratio to failure test [%]
Reference: Failure test value	1414	100
Method 1: API (2010)	243	17
Method 2: ICP (05)	402	28
Method 3: UWA (05)	394	28
Method 4: FHWA	1068	76
$q_{c,avg}$ as is, $\alpha_{t,raw}$=0.0144	895	63
*$q_{c,CUR}$, $\alpha_{t,\ design}$=0.0230	914	64
$q_{c,CUR}$, $\alpha_{t,lower\ bound}$=0.011	437	31
$q_{c,CUR}$, $\alpha_{t,expected}$=0.017	676	48
$q_{c,avg}$, $\alpha_{t,fit}$=0.0227	**1414**	**100**
$q_{c,CUR}$, $\alpha_{t,fit}$=0.0356	**1414**	**100**

*Based on CUR: peaks of q_c cuts off on 20 Mpa

According to the results, the following conclusions are made for design bearing capacity of the first sand layer and second sand layer;

First of all, it can be concluded that the design bearing capacity of the pile based on first three mentioned international methods are not comparable to the reference value from field failure test. The reason could be because these methods are designed for driven steel piles (open and close ended) in offshore practice and they differ with the tensile micro piles. Therefore the applicability of these methods is limited in general.

The value of $R_{t;d}$ according to FHWA gives a better match to the field failure test value. In fact FHWA method makes a distinction between different pile types similar to CUR 236 and the design bearing capacity is based on the defined values of grout-to-ground ultimate bond strength. However the pile types in FHWA differ from the ones in CUR 236. To be able to estimate $R_{t;d}$, it has been assumed that pile type B in FHWA is similar to the constructed tension pile at Amsterdam case study. Therefore the applicability of this method is also limited.

Next the design bearing capacity of the pile is calculated according to raw values from CPT data and based on CUR 236 by applying limit values. It can be seen from table 20, that the obtained values of $R_{t;d}$ for first sand layer are comparable to reference pile, while for the second sand layer (table 21), the values are less comparable.

At the end the fitted value of α_t is determined for two cases of cone resistance. For the first case, an average cone resistance is used and for the second case, q_c is limited based on CUR 236. It is aimed to have a bearing capacity which is 100% comparable to the reference single pile value for both cases. The derived $\alpha_{t,fit}$ for the first sand layer based on $q_{c,avg}$ and $q_{c,lim}$ is 0.0162 and 0.0167 respectively and for the second sand layer is 0.0227 and 0.0356 respectively. It can be seen that the fitted α_t values for the first sand layer either by taking an average q_c or using the limit value of q_c are close to each other and also close to the expected α_t value stated in CUR 236 due to the fact that q_c values are below the limit in general. However for the second sand layer it is not the case and the derived values differ. By using $q_{c,avg}$ more reasonable value is found (0.0227) but by applying $q_{c,limit}$ the derived value for α_t is found to be even higher than maximum allowable α_t of 0.025. The reason is that cone resistance values in second sand layer are strongly limited which caused to heighten α_t. Therefore for the second sand layer α_t value could lead to an over-estimation of the pile capacity and eventually give a wrong image of it.

Pile Groups

For the calculation of bearing capacity of the pile in group, the same formula as what has been mentioned for single pile will be used. The only difference is including factor f_1 and f_2 in the formula due to three aspects:

- The effect of densification due to the installation of the pile group; the closely spaced piles cause an increase friction between the pile and the surrounding soil which therefore increases the total bearing capacity. This effect is controlled by increasing the cone resistance value with a factor f_1. However according to CUR 236 it is considered to be 1.0 for micro piles.
- The relaxation due to the tensional load on the pile group. This effect will decrease the vertical effective stress in the subsoil and therefore will also decrease the bearing capacity. This effect is taken into account by adjusting the cone resistance with a factor f_2.
- There is another stress reduction in the soil due to an excavation which caused less friction between the pile and soil and therefore result in a lower bearing capacity. By decreasing the cone resistance based on the excavation value, this effect is also controlled.

These effects are taken into account when calculating a pile in pile group. The calculation is done considering an excavation of 10.5 m and for a total pile length of 12 meter starting from NAP -10.5 m until NAP -22.5 m and the grout body is 10 m located in first and second sand layer. Also the value of $\alpha_{t,\ design}$ is used which is 0.023 for the second sand layer.

For the calculation it has been used from a representative CPT profile after excavation (see appendix A.2) and the values of cone resistance are maximized on 20 MPa based on the CUR 236 design guide. The calculation is done for 3 different pile groups spacing of 5D, 10D and 15D with diameter of 0.2 m which are 1 meter, 2 meters and 3 meters. The detailed calculation can be found in appendix D.2.

Table 22 illustrates a summary of the final values for design bearing capacity calculated for the different pile spacing.

TABLE 22: FINAL VALUES FOR DESIGN BEARING CAPACITY CALCULATED BASED ON PILE SPACING

Pile spacing [m]	$F_{r,t,d}$ [kN]
1	159
2	646
3	1198

The bearing capacity of the pile is compared to the reference single pile from failure test in second sand layer which was 1414 kN. The ratio of bearing capacity of the pile in group to the single pile is defined for different pile spacing which is plotted in the next figure 32.

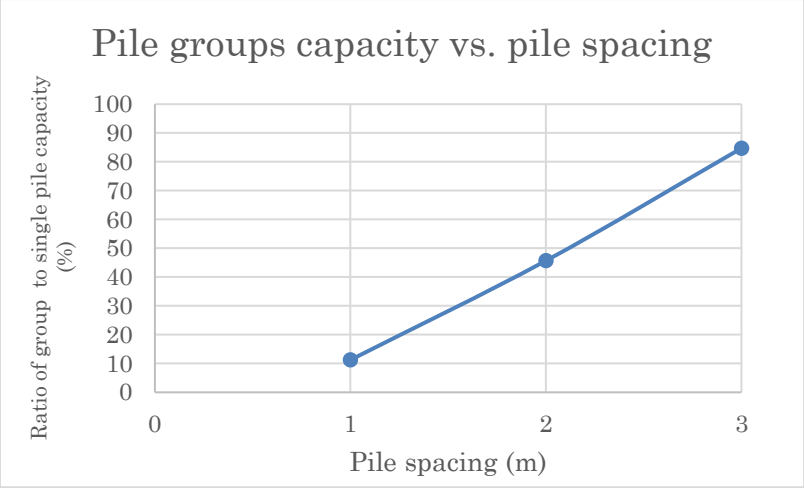

FIGURE 32: PILE GROUPS CAPACITY RATIO PER PILE FOR DIFFERENT PILE SPACING

From the results it can be seen that by increasing the space between piles in the group, the bearing capacity of the piles increases due to the decrease of group effects.

It may be assumed that it is not possible to mobilize the entire weight of the sand between the piles of a pile group in order to develop the bearing capacity of the pile. Therefore it is assumed that a conical shape surface can originate starting from the pile tip. This effect is taken into account by comparing the weight of the soil in the cone and cylinder shape with the calculated bearing capacity of the pile in the pile group. The calculated bearing capacity should be smaller than the weight of the soil in the cone and cylinder shape. According to CUR 2001-4 report, the lower angle of the cone is 45° or 2/3ϕ for soil displacing and non-displacing piles respectively. Since it is not clear if tension piles are soil displacing or non-displacing piles, the weight of the soil between the piles is calculated for both cases. Note that angle of internal friction ϕ is considered to be 32° for sand at Boerenwetering location.

The layout of the piles with different pile spacing and different lower angle cases is shown in the next figure.

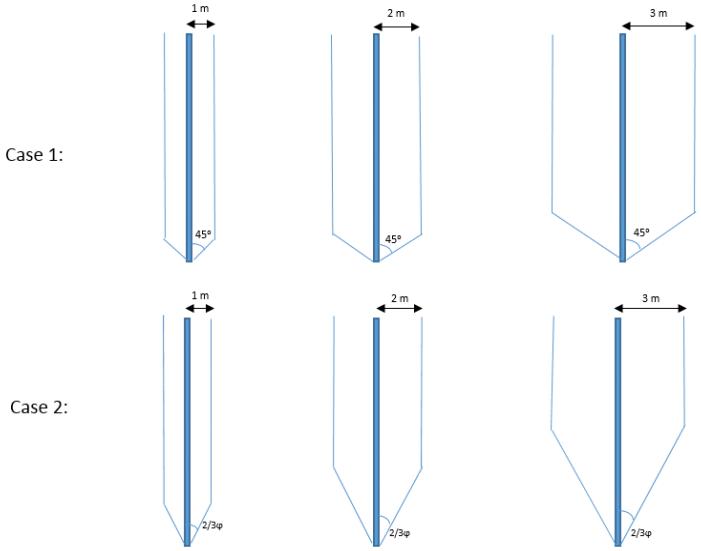

FIGURE 33: LAY-OUT OF THE PILES WITH DIFFERENT PILE SPACING FOR TWO CASES

The result of the calculation is presented in the next table 23. For detailed calculation the reader is referred to appendix D.2.

TABLE 23: COMPARISON OF DESIGN AND MAXIMUM BEARING CAPACITY OF PILE WITHIN PILE GROUP

	Pile spacing (m)		
	1	2	3
$F_{r;t;d}$ (kN)	**159**	**646**	**1198**
$F_{r;t;max;d}$ for case 1 (kN)	291	1099	2318
$F_{r;t;max;d}$ for case 2 (kN)	265	884	1593

It can be seen that all the calculated design values for bearing capacity of the pile for different pile spacing are smaller compared to the maximum design bearing capacity value for case 1 and case 2 (soil plug pull-out mechanism). Therefore the calculated design values are acceptable.

CHAPTER 7: FINITE ELEMENT MODELLING IN 2D (PLAXIS)

7.1 INTRODUCTION

The goal of pile modelling is finding an appropriate single micro pile model that can be validated based on the full-scale field failure test on single micro piles and later on the group effect for micro piles under tensile loading will be evaluated. Further in this part the used material parameters and constitutive soil model are explained. The model is analyzed in axisymmetric as well as plane strain condition.

Axisymmetric analysis allows for a 3D problem analysis by rotating the model about the y- axis and assuming x=0 .In fact the input is 2-dimensional, but because of the rotational symmetry, a symmetric 3-dimensional problem could be analyzed. Since the pile group is finally modelled in plane strain condition, the single pile model in axisymmetric condition can be found in appendix E and further the single and pile group model based on plane strain are elaborated.

Plane Strain assumes the problem is of infinite length normal to the plane section of the analysis. By definition, the out-of-plane displacement (strain) is zero in a Plane strain analysis. Figure 34 shows a visualization of these two conditions.

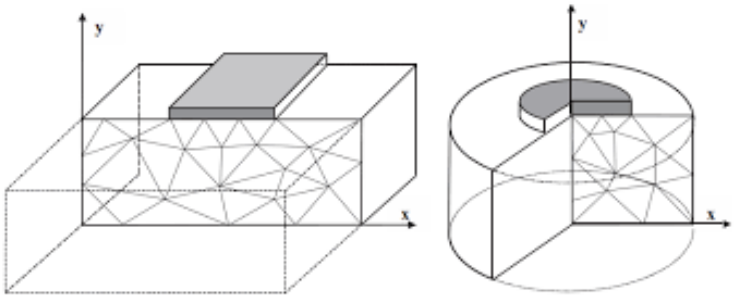

FIGURE 34: LEFT: PLANE STRAIN MODEL, RIGHT: AXISYMMETRIC MODEL, BRINKGREVE ET AL., 2014

7.2 FINITE ELEMENT MODELING

Soil behavior is non-linear and depends at least on stress state of soil. Stress state of soil consist of stress level, stress path that soil has passed and strains which have occurred in this loading path. Conventional soil models will not able to consider these factors due to missing a non-linear stress dependent elastic modulus and disability to distinguish between loading and unloading modulus. To overcome these issues new constitutive models are introduced which will be further explained. Also about different structural elements which are available in Plaxis will be discussed in this section.

7.2.1 CONSTITUTIVE MODELS

Several constitutive models exist in Plaxis. Considering scope of this study, grout pressure will affect stress state in soil. Important point is ability of constitutive model to consider effect of change in stress state on stiffness modulus of soil. Mohr-Coulomb model (MC) is linear elastic perfectly-plastic model and is used as a first order approximation. In spite of great capabilities of MC for numerical modellings, it has also some limitations. One of them is that it only

considers a single stiffness modulus in all states of stress and does not distinguish between loading and unloading stiffnesses.

Hardening Soil (HS) model is introduced to consider different modulus for different stress states of soil. This model is applicable for both 2D and 3D modelling. In the HS model, soil stiffness is calculated much more accurately by using three different stiffnesses namely; secant stiffness in standard drained triaxial testE_{50}^{ref}, tangent stiffness for oedometer loading $E_{oed}^{ref}$and unloading-reloading stiffness E_{ur}^{ref} (Schanz et al. 1999).

Also MC model represents Young's modulus of soil in in-situ stress state while HS model accounts for stress-dependency of stiffness moduli. The input stiffnesses relate to a reference stiffness (usually 1 bar) are visualized in the next figure.

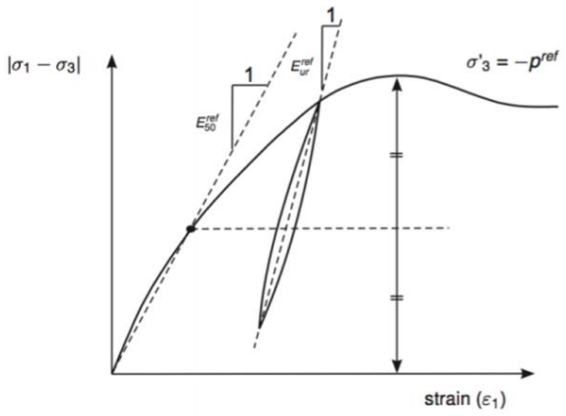

FIGURE 35: PARAMETER DEFINITION FOR HARDENING SOIL MODEL

Hardening Soil with small strain stiffness (HSs) model is a modification of HS model that accounts for non-linearly increasing of stiffness of soil at small strains. It involves two additional parameters compared to HS model which are G_0^{ref} and $\Upsilon_{0.7}$. G_0^{ref} is small-strain shear modulus and $\Upsilon_{0.7}$ is the strain level at which the shear modulus has reduced to about 70% of the small-strain shear modulus (Benz 2007).

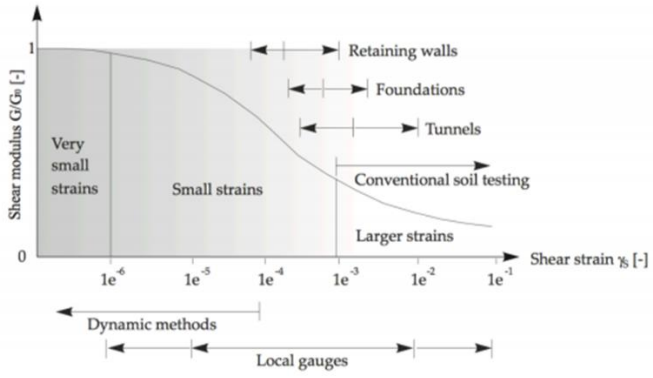

FIGURE 36: MODULUS REDUCTION ACCORDING TO SHEAR STRAIN WITH PRACTICAL EXAMPLES INVOLVED

HS model has great capabilities in modelling mechanical behavior of sand including some parameters which are difficult to be determined. For determination of m exponent which takes into account the dependency of stiffness to stress, in case of dense sand, m will be taken 0.5 and for loose sand it will be 1.

Due to the fact that stiffness parameters are difficult to determine and they need extensive laboratory tests to be performed, and only CPT results exist in this study, values are taken according to the studied literatures for numerical modelling. It is stated that value of unloading reloading stiffness E_{ur}^{ref} is three times of secant stiffness in standard drained triaxial test E_{50}^{ref}. E_{50}^{ref} is taken equal to E_{oed}^{ref} when no extensive data are available.

7.2.2 STRUCTURAL ELEMENTS FOR MICRO PILE MODELLING

Different options for modeling of the micro piles are available in Plaxis but careful understanding of the mechanism regarding each option should be done to be able to use them correctly. List of available choices are as follows (Plaxis 2D manual 2018 and Sluis 2012);

1. Plate
2. Node to Node Anchor
3. Embedded beam row
4. Interface

1. Plate:

Plate elements are used when no interaction is needed to be modelled and heat transfer option is of concern because of ability of thermal properties definition. By introducing interfaces, interaction could be modelled but then un-realistic shear planes may be developed. Also axial and flexural stiffness properties are required to define this type of structure. Sheet piles and tunnel linings are main structures which plate elements are used for their modelling.

2. Node to node anchor:

This type of anchor connects two ends of defined element using elastic spring. No interaction with soil is presented in this model, in other words soil can only flow through node to node anchors. There is no possibility to enter a bending stiffness and to calculate structural forces in the pile.

3. Embedded beam row (EBR):

One of the recent improvements in structural elements, is the availability of embedded beam row. The “embedded beam row” element can be used to simulate a row of piles with a certain spacing perpendicular to the model area. Three different types of usage for this structural element could be defined namely; behavior of piles, Rock bolts and grout body.

Three options are available for considering shaft skin resistance which are linear, multi-linear and layer dependent. In linear form, start and end skin friction is determined and capacity is calculated but when multi-line approach is considered, a table of skin friction is introduced to calculate capacity over height of micro pile. Mostly used method is the last one which is layer dependent. It uses parameters of adjacent soil by taking into account reduction factor determined in interface tab. The advantages of using this element compared to other methods are: possibility to model interaction with soil due to line to line interfaces, soil can flow through the embedded pile row, possibility to enter bending stiffness and calculating structural forces in the pile and obtaining realistic shear planes.

4. Interface:

Interface elements are used to model soil structure interaction. Consider a rough sheet pile or regular concrete pile embedded in soil. There must be a transition zone between stiff structure and soil which is weaker than soil or with same strength of soil which transfers the displacements or forces from structure to soil. Two different options are available for interface definition. First is to use adjacent soil by introducing strength reduction factor for soil and second method is by defining another material and setting interface strength reduction factor for this material to 1 and assigning it only to interface.

7.3 PLANE STRAIN APPROXIMATION FOR SINGLE PILE

7.3.1 SOIL MODEL AND STRUCTURE

Based on the above information and the studies done about different constitutive models, Hardening Soil with small strain stiffness (HSs) model is used for determination of the soil behavior at Amsterdam site which is consisted of 7 different layers.

The structure of soil including soil type, top level layer, dry volumetric weight, saturated volumetric weight and angle of internal friction for each layer can be found in table 24. Figure 37 also shows the structure of the soil and model pile in first sand layer in Plaxis. The boundary conditions is assumed to be 30 m, far enough from model at each side. This is validated to be sufficient since it does not influence the stress diagram of the model. Also it should be noted that second sand layer starts from NAP -17.5 m and ends in NAP -27.5 m, so it has a thickness of 10 m.

TABLE 24: SOIL STRUCTURE AT SITE, AMSTERDAM

Layer Number	Soil type	Top level (m NAP)	γ_{dry} $(\frac{kN}{m^3})$	γ_{sat} $(\frac{kN}{m^3})$	φ (degree)
L1	Sandy fill	+0.6	17	19	28
L2	Dutch Peat	-2.9	10.5	10.5	17
L3	Clay deposits	-4.5	16.5	16.5	25
L4	Base Peat	-10.0	12	12	18
L5	1st Sand Layer	-12.5	18	20	32
L6	Clayey/Silty Sand	-15.0	18.5	18.5	28
L7	2nd Sand Layer	-17.5	18	20	32

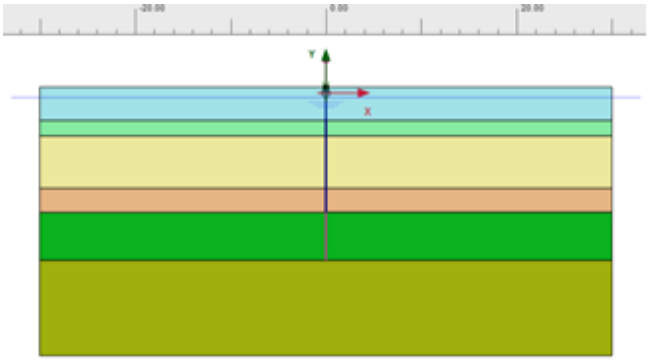

FIGURE 37: STRUCTURE OF SOIL AND MODEL PILE IN FIRST SAND LAYER

*Based on the field test data, first sand layer is assumed to be 5 meters thick starting from NAP-12.5 m until NAP -17.5 m.

Next table shows the used parameters and values for modeling of the first and second sand layer based on HSs modeling behavior.

TABLE 25: HARDENING SOIL WITH SMALL STRAIN STIFFNESS PARAMETERS

HSs Parameters for 1st and 2nd Sand Layers		
Material	Value	Unit
Υ_{unsat}	17.00	kN/m^3
Υ_{sat}	19.00	kN/m^3
Advanced	Default	-
E_{50}^{ref}	30,000	kN/m^2
E_{oed}^{ref}	30,000	kN/m^2
E_{ur}^{ref}	90,000	kN/m^2
m	0.50	-
c'_{ref}	0.10	kN/m^2
φ'	32.0	degree
ψ	2.0	degree
$\Upsilon_{0.7}$	0.0002	-
G_0^{ref}	180,000	kN/m^2
Advanced	Default	-
Strength	Rigid	-
$R_{interface}$	1	-

7.3.2 MODELLING PHASES FOR 1ST AND 2ND SAND LAYER

The pile model is consisted of 13 different phases including unloading and reloading stages. It is important to consider unloading and reloading stages since pile field failure test and final maximum tensional capacity is obtained based on several unloading and reloading of the pile. Table 26 shows the different phases with their descriptions.

TABLE 26: MODELLING PHASES

Phase Number	**Descriptions**	**Type**	**Start From**
Initial Phase	Initial Conditions	-	-
Phase 1	Active Micropile (Grout Body and Node to Node Anchor)	Plastic	Initial Phase
Phase 2	Pre-loading (5 kN/m)	Plastic	Phase 1
Phase 3	Tensile Load (40%)	Plastic	Phase 2
Phase 4	Unloading	Plastic	Phase 3
Phase 5	Tensile Load (55%)	Plastic	Phase 4
Phase 6	Unloading	Plastic	Phase 5
Phase 7	Tensile Load (70%)	Plastic	Phase 6
Phase 8	Unloading	Plastic	Phase 7
Phase 9	Tensile Load (80%)	Plastic	Phase 8
Phase 10	Unloading	Plastic	Phase 9
Phase 11	Tensile Load (90%)	Plastic	Phase 10
Phase 12	Unloading	Plastic	Phase 11
Phase 13	Tensile Load (100%)	Plastic	Phase 12

7.3.3 PILE STRUCTURE AND PROPERTIES

7.3.3.1 NTN AND EBR WITH GROUT BEHAVIOR MODEL

The pile is modelled in combination of two structural elements. The free length of the pile is modelled by node to node anchor (NTN) element and the 5 meter grout part which interacts with surrounding soil is modelled by embedded beam row (EBR) with grout behavior. There are two types of model pile which differ in length, one has a length of 18 m reaching first sand layer and the other one is 23 m long located in second sand layer.

Linear capacity-first sand layer

In Plaxis there are 3 options for defining axial skin resistance of the pile namely linear, multi-linear and layer dependent. Each has different behavior and therefore based on the situation and calculation the proper option should be chosen. Multi-linear option is out of consideration because the grout body is fully located in one sand layer.

Table 27 shows the properties of node to node anchor which has been used for the free length of micro pile. The value of EA is based on the E modulus of steel and cross section area of GEWI bar. Table 28 indicates the properties of grout body with linear axial skin resistance behavior for first sand layer. The values of E and T_{skin} are defined based on the parametric study in such way that the pile behaves similar to field failure test. Since it is used from linear option, the start and end values are the same for axial resistance of grout body.

TABLE 27: NODE TO NODE ANCHOR PROPERTIES

Node to node element for free length		
Material	Value	Unit
EA	665E3	kN/m
Diameter	0.0635	m
L spacing	20.0	m

TABLE 28: LINEAR APPROACH, USED PARAMETERS IN PLAXIS FOR 1ST SAND LAYER

Grout body-first sand layer (Linear)		
Material	Value	Unit
*1)E	13.0e6	kPa
ϒ	24.0	kN/m^3
Pile Type	Predefined	-
Predefined Pile Type	Mas. Circular Pile	-
Diameter	0.20	m
L spacing	20.0	m
Axial Resistance		
T skin, start, max	75.4	kN/m
T skin, end, max	75.4	kN/m
*2)Interface Stiffness Factor	Default	-

1) The used grout is a mixture of cement, water and limited amount of aggregates. Cement type is blast furnace slag cement III B42.5, indicating that compression strength after 28 days is ≥ 42.5 MPa and less than 62.5 MPa. In the parametric study for determination of E modulus of grout, the maximum range is assumed to be 21e6 kPa and different values below this range is tried to have fit with field test data. It has been concluded that the effect of this parameter is not significant for the analysis. The same method is used for defining E value in the next coming tables in this chapter.

2) Parametric study is done and based on it, an appropriate ISF is used. For the first sand layer it is used from the default value in Plaxis and for the second sand layer by using an ISF value equal to 1.0, a better match to the field test data is achieved. The same method is used for defining ISF value in the next coming tables in this chapter.

Linear capacity-second sand layer

The model pile in second sand layer which starts from NAP -22.5 m is visualized in the next figure 38. Pile has a total length of 23 m in this case.

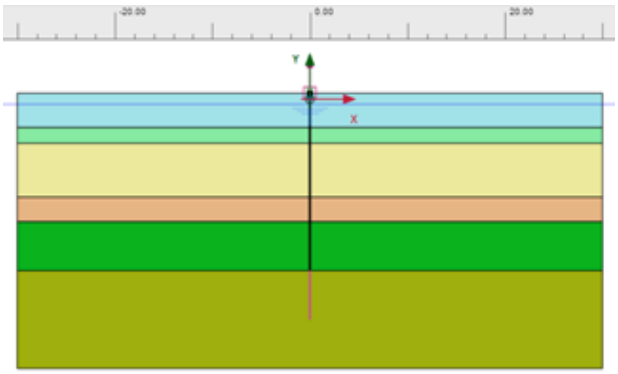

FIGURE 38: STRUCTURE OF SOIL AND MODEL PILE IN SECOND SAND LAYER

Pile in the second sand layer is calculated based on the same approach as first sand layer. The values and parameters for unbounded pile length are always the same as table 27 for all other approaches. Table 29 shows the values for the second sand layer for grout body considering a linear capacity for the pile.

TABLE 29: LINEAR APPROACH, USED PARAMETERS IN PLAXIS FOR 2ND SAND LAYER

Grout body-second sand layer (Linear)		
Material	Value	Unit
E	13.0e6	kN/m^2
ϒ	24.0	kN/m^3
Pile Type	Predefined	-
Predefined Pile Type	Mas. Circular Pile	-
Diameter	0.20	m
L spacing	20.0	m
Axial Resistance		
T skin, start, max	285.0	kN/m
T skin, end, max	285.0	kN/m
Interface Stiffness Factor	1.0	-

Layer dependent-first sand layer

Layer dependent is another option for defining axial skin resistance along the grout body. One of the advantages of using layer dependent behavior is that the installation effect due to grouting could be modelled because Plaxis does not consider this effect and it should be modelled properly to obtain optimal results. As a result of pressurized grouting, effective horizontal stress around the grout body increases which has a positive effect on the anchor capacity of the pile. Effective horizontal stress has a direct relation with lateral earth pressure

coefficient (K_0) since effective vertical stress is constant. By finding an appropriate value for K_0 in the way that the model results fit to the load-displacement diagram of field failure test, the installation effects could be simulated. Initially K_0 could be found according to the following in-equality formula;

$$\frac{1+sin\emptyset}{1-sin\emptyset} \geq K_0 \geq \frac{1-sin\emptyset}{1+sin\emptyset} \tag{56}$$

The same process of what has been done in linear option, is here followed. The values of E and $T_{skin,max}$ are defined based on the parametric study in such way that the pile behaves similar to field failure test and fits to the load-displacement diagram of the field test. Table 30 shows the used parameters and values in case of layer dependent axial resistance of pile.

TABLE 30: LAYER DEPENDENT, USED PARAMETERS IN PLAXIS FOR 1ST SAND LAYER

Grout body-first sand layer (Layer dependent)		
Material	Value	Unit
E	8.0e6	kN/m²
ϒ	24.0	kN/m³
Pile Type	Predefined	-
Predefined Pile Type	Mas .Circular Pile	-
Diameter	0.2	m
L spacing	20.0	m
Axial Resistance		
Axial Skin Resistance	Layer Dependent	-
T max	120.0	kN/m
ISF	Default	-

Layer dependent-second sand layer

The same approach as first sand layer is followed. The only difference is that the model pile is longer and is located in the second sand layer and therefore the value for maximum skin resistance will be different. Table 31 shows a summary of the used parameters and values for grout body in the second sand layer for the layer dependent capacity.

TABLE 31: LAYER DEPENDENT, USED PARAMETERS IN PLAXIS FOR 2ND SAND LAYER

Grout body -second sand layer (Layer dependent)		
Material	Value	Unit
E	20.0e6	kN/m²
ϒ	24.0	kN/m³
Pile Type	Predefined	-
Predefined Pile Type	Mas. Circular Pile	-
Diameter	0.2	m
L spacing	20.0	m
Axial Resistance		
Axial Skin Resistance	Layer Dependent	-
T max	500.0	kN/m
ISF	1.0	-

RESULTS:

First sand layer

The horizontal earth pressure coefficient is calculated 1.9 for layer dependent capacity. The angle of internal friction and dilation are obtained 32 and 2 respectively (see appendix F for calculation procedure of K_0).

The results of maximum tensile failure load for linear and layer dependent capacities are compared with maximum measured tensile failure load at field site which can be found in the next table and plotted in figure 39. Note that the results are for first sand layer.

TABLE 32: COMPARISON OF MAXIMUM LOAD FOR DIFFERENT CASES- 1ST SAND WITH EBR (GROUT)

Displacement (mm)	Field (kN)	Linear (kN)	Layer dependent (kN)
0	100	100	100
2.17	151	150	156
4.38	208	202	210
6.71	264	250	266
8.45	302	292	305
10.221	340	332	342
12.21	**377**	**377**	**377**

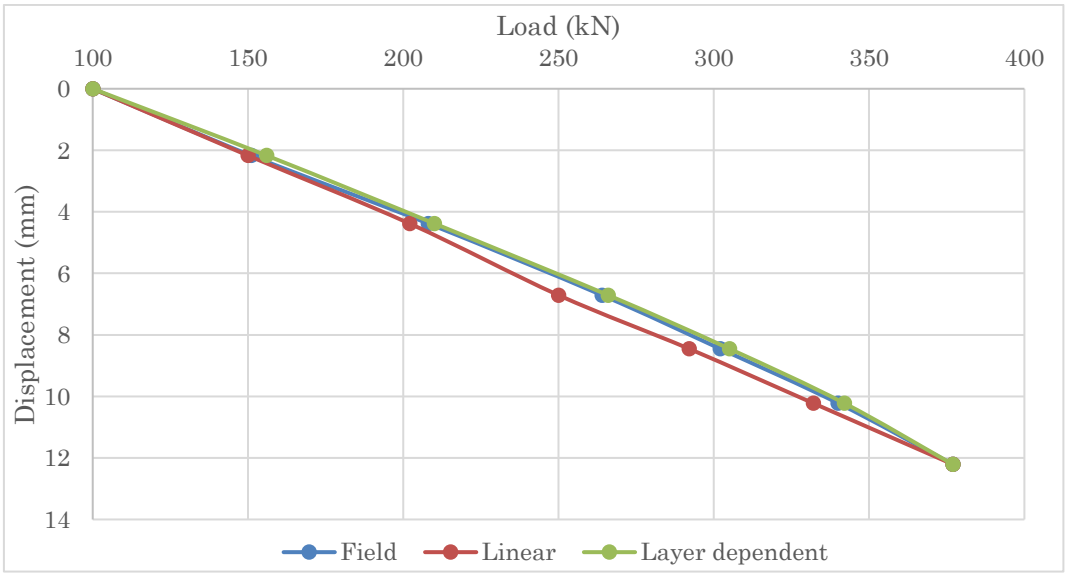

FIGURE 39: MAXIMUM LOAD BASED ON DIFFERENT CASES- FIRST SAND LAYER WITH EBR (GROUT)

Second sand layer

The value for horizontal earth pressure coefficient is calculated 3.85 for second sand layer according to layer dependent capacity. The angle of internal friction and dilation are also calculated which are 38.5 and 8.5 respectively.

The results of maximum tensile failure load for linear and layer dependent capacities are compared with maximum measured tensile failure load at field site which can be found in the next table and also has been plotted in figure 40.

TABLE 33: COMPARISON OF MAXIMUM LOAD FOR DIFFERENT CASES- 2ND SAND WITH EBR (GROUT)

Displacement (mm)	Field (kN)	Linear (kN)	Layer dependent (kN)
0	100	100	100
15.23	566	501	512
22.91	778	737	745
31.31	990	960	975
36.19	1131	1114	1160
43.53	1273	1306	1337
54.5	**1414**	**1441**	**1453**

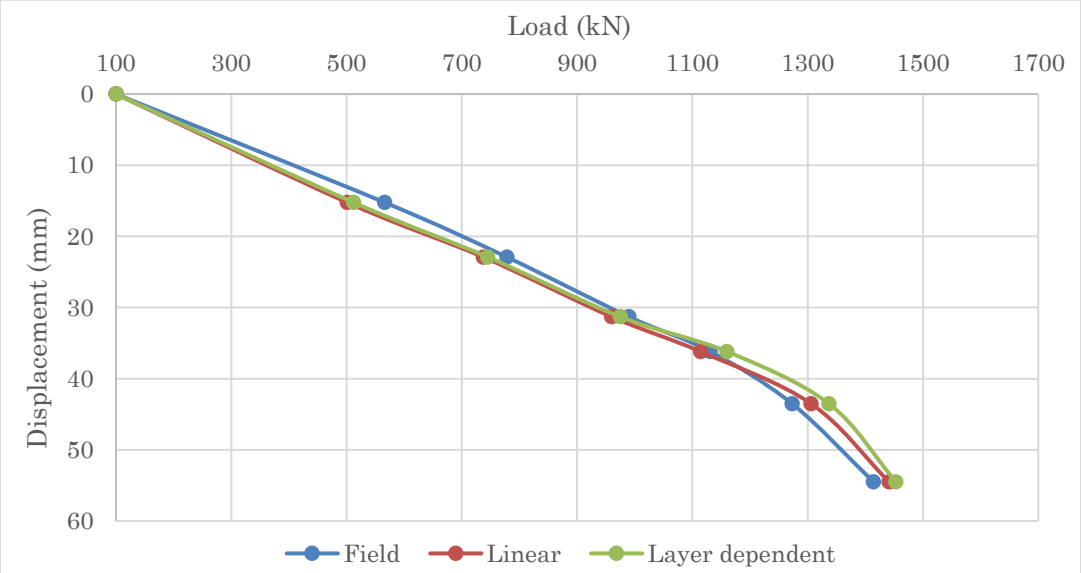

FIGURE 40: MAXIMUM LOAD BASED ON DIFFERENT CASES- SECOND SAND LAYER WITH EBR (GROUT)

7.3.3.2 EBR WITH PILE BEHAVIOR MODEL

Linear capacity-first sand layer

Another way of modelling the micro pile is by only using embedded beam row (EBR) with pile behavior for both free and bounded part of micro pile. When the pile was modelled with the grout body behavior in previous section, there was only one option to use for modelling the free length of micro pile and that was node to node element. If different element than node to node was used for the free length of micro pile, Plaxis gave an error message and could not complete the calculations.

For the unbounded length it has been used from EBR with a diameter of 63.5 mm and E modulus of 210e6 kN/m² (see table 34). Again in this part the micro pile is modelled for both linear and layer dependent capacities and the results are obtained. For the bounded length of the micro pile the used values and properties are based on table 35 for linear capacity.

TABLE 34: PILE PROPERTIES FOR UN-BOUNDED LENGTH OF MICRO PILE

Pile properties for un-bounded length		
Material	Value	Unit
E	210E+06	kPa
ϒ	78.5	kN/m^3
Pile Type	Predefined	-
Predefined Pile Type	Mas. Circular Pile	-
Diameter	0.0635	m
L spacing	20.0	m
Axial Resistance		
T skin, start, max	0.0	kN/m
T skin, end, max	0.0	kN/m
ISF	Default	-

TABLE 35: LINEAR, USED PARAMETERS FOR BOUNDED LENGTH WITH EBR (PILE)- 1ST SAND LAYER

Bounded length with EBR (pile)-first sand layer (Linear)		
Material	Value	Unit
E	13.0e6	kPa
ϒ	24.0	kN/m^3
Pile Type	Predefined	-
Predefined Pile Type	Mas. Circular Pile	-
Diameter	0.20	m
L spacing	20.0	m
Axial Resistance		
T skin, start, max	75.4	kN/m
T skin, end, max	75.4	kN/m
Interface Stiffness Factor	Default	-

It has been tried to model EBR model pile that it behaves similar to the pile at field failure test. Figure 41 left side, shows the model pile located in first sand layer with EBR in Plaxis. The connection points of two defined EBR are rigid.

Other processes of the modeling such as modeling phase and unloading-reloading procedure is the same as before. Figure 41 right side, shows the used mesh size for the model pile. It has been used from very fine mesh as a default mesh and in the place of grout body the mesh is manually more refined to have more detailed results in this part.

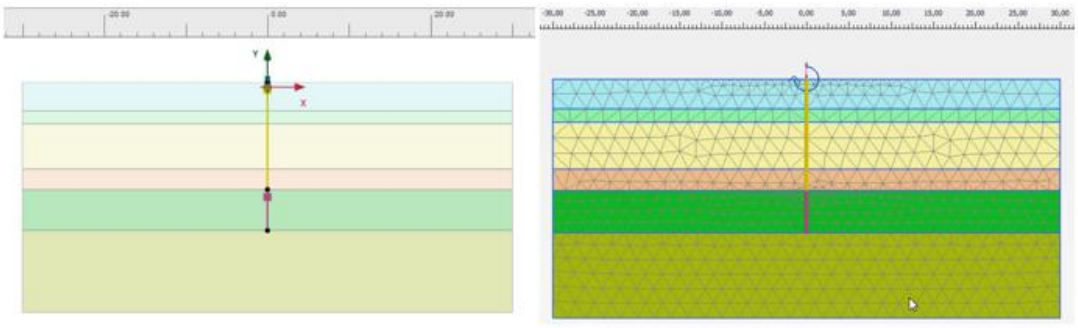

FIGURE 41: MODEL PILE LOCATED IN FIRST SAND LAYER WITH EBR (PILE)

Linear capacity- second sand layer

The model pile in second sand layer and the defined mesh size (very fine) can be found in figure 42 left and right picture respectively.

Pile in the second sand layer is calculated based on the same approach as first sand layer for linear capacity. Table 36 shows the values for the second sand layer for bounded length of the pile when EBR element is used as the pile structure.

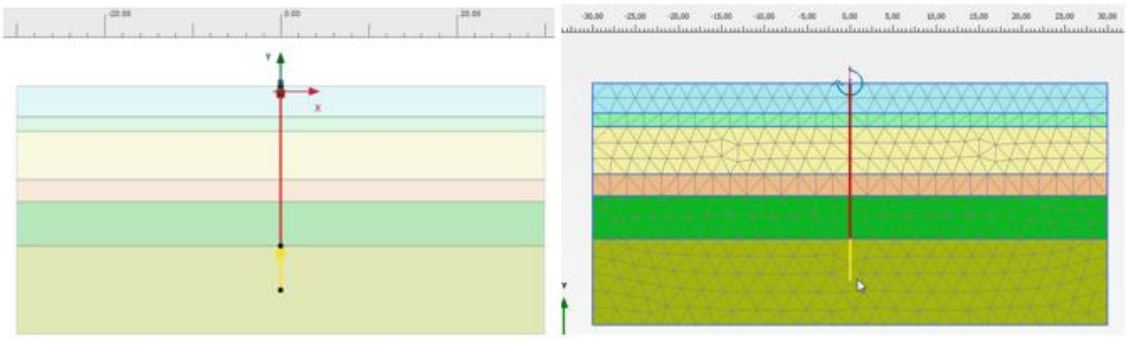

FIGURE 42: MODEL PILE LOCATED IN SECOND SAND LAYER WITH EBR (PILE)

TABLE 36: LINEAR, USED PARAMETERS FOR BOUNDED LENGTH WITH EBR (PILE)- 2ND SAND LAYER

Bounded length with EBR (pile)-second sand layer (Linear)		
Material	Value	Unit
E	13.0e6	kPa
ϒ	24.0	kN/m^3
Pile Type	Predefined	-
Predefined Pile Type	Mas. Circular Pile	-
Diameter	0.20	m
L spacing	20.0	m
Axial Resistance		
T skin, start, max	285	kN/m
T skin, end, max	285	kN/m
Interface Stiffness Factor	1.0	-

Layer dependent- first sand layer

The same process of what has been done in linear option, is here followed. The values of E and $T_{skin,max}$ are defined based on the parametric study in such way that the pile behaves similar to field failure test. For the bounded length of the micro pile the used values and properties are based on table 37 for the layer dependent approach. Also in this part, an appropriate value for K_0 is defined in Plaxis to simulate the installation effects of grouting.

TABLE 37: LAYER DEPENDENT PARAMETERS FOR BOUNDED LENGTH WITH EBR (PILE)- 1ST SAND LAYER

Bounded length with EBR (pile)- first sand layer (Layer dependent)		
Material	Value	Unit
E	8.0e6	kN/m^2
ϒ	24.0	kN/m^3
Pile Type	Predefined	-
Predefined Pile Type	Mas. Circular Pile	-
Diameter	0.2	m
L spacing	20.0	m
Axial Resistance		
Axial Skin Resistance	Layer Dependent	-
T max	120.0	kN/m
ISF	Default	-

Layer dependent- second sand layer

Here again the same method as first sand layer with layer dependent capacity is used. The only difference is that the model pile is longer and is located in the second sand layer. Table 38 shows a summary of the used parameters and values for bounded length of the pile in second sand layer for the layer dependent capacity.

TABLE 38: LAYER DEPENDENT PARAMETERS FOR BOUNDED LENGTH WITH EBR (PILE)- 2ND SAND LAYER

Bounded length with EBR (pile)- second sand layer (Layer dependent)		
Material	Value	Unit
E	10.0e6	kN/m^2
ϒ	24.0	kN/m^3
Pile Type	Predefined	-
Predefined Pile Type	Mas. Circular Pile	-
Diameter	0.2	m
L spacing	20.0	m
Axial Resistance		
Axial Skin Resistance	Layer Dependent	-
T max	500	kN/m
ISF	1.0	-

RESULTS:

First sand layer

The horizontal earth pressure coefficient, angle of internal friction and angle of dilation are calculated 1.75, 33 and 3 respectively for the layer dependent capacity for the model pile (see appendix F for calculation procedure of K_0).

The results of maximum tensile failure load for linear and layer dependent capacities are compared with maximum measured tensile failure load at field site which can be found in the next table and plotted in figure 43. Note that the results are for first sand layer.

TABLE 39: COMPARISON OF MAXIMUM LOAD FOR DIFFERENT CASES- 1ST SAND WITH EBR (PILE)

Displacement (mm)	Field (kN)	Linear (kN)	Layer dependent (kN)
0	100	100	100
2.17	151	150	155
4.38	208	200	210
6.71	264	252	266
8.45	302	292	304
10.221	340	332	339
12.21	**377**	**373**	**369**

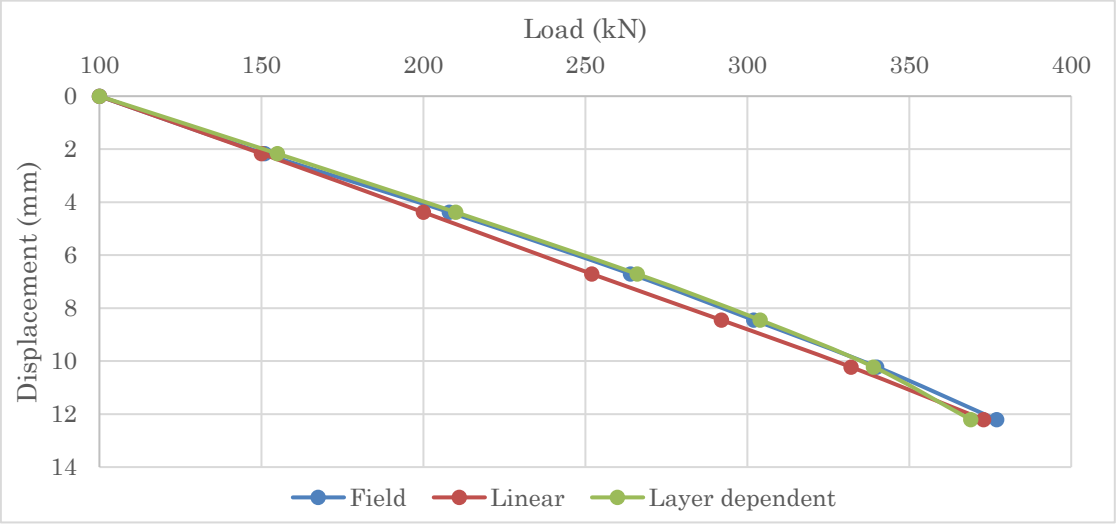

FIGURE 43: MAXIMUM LOAD BASED ON DIFFERENT CASES- FIRST SAND LAYER WITH EBR (PILE)

Second sand layer

The horizontal earth pressure coefficient is obtained 3.85. Angle of internal friction and angle of dilation are calculated 38.5 and 8.5 respectively. Again the results of maximum tensile failure load for linear and layer dependent capacities for second sand layer are compared with maximum measured tensile failure load at field site which can be found in the next table and plotted in figure 44.

TABLE 40: COMPARISON OF MAXIMUM LOAD FOR DIFFERENT CASES- 2ND SAND WITH EBR (PILE)

Displacement (mm)	Field (kN)	Linear (kN)	Layer dependent (kN)
0	100	100	100
15.23	566	477	438
22.91	778	705	706
31.31	990	937	932
36.19	1131	1063	1058
43.53	1273	1292	1285
54.5	**1414**	**1449**	**1448**

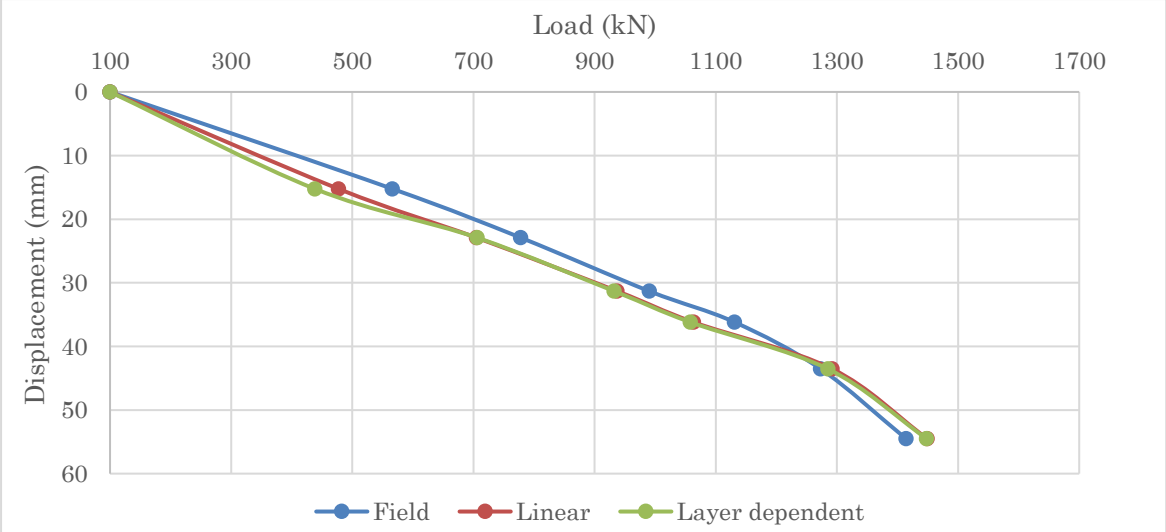

FIGURE 44: MAXIMUM LOAD BASED ON DIFFERENT CASES- SECOND SAND LAYER WITH EBR (PILE)

7.4 PLANE STRAIN APPROXIMATION FOR PILE GROUP

7.4.1 INTRODUCTION

In this part the numerical analysis is performed for the group of micro piles and the influence of group effects on micro pile behavior is studied based on the validated single pile model.

The group effect of micro piles is relevant for construction projects where there are many closed spaced micro piles are available to prevent uplift forces. If the piles are too close to each other, the group effect will increase while it decreases the bearing capacity of each pile. Therefore defining an optimum pile spacing is crucial for designing the bearing capacity of the piles in the group.

In this research the pile spacing is varied to investigate the significance of this parameter in the group effect behavior. There are three different configurations of micro piles evaluated which are 5D, 10D and 15D pile spacing and will be in detail explained in this chapter.

7.4.2 EMBEDDED BEAM ROW

Pile group is modelled for two different options and the results are analyzed. Embedded beam row element has been used for both models since it is a new technique and the calculation time will be faster compared to other methods such as volume element.

The first option is by using node to node element for the free length of the pile and embedded beam row with grout body behavior for the bounded length of the micro pile. The modeling stages and results of it can be found in appendix G. To check and validate the behavior of this model, another option is generated.

In the second model the GEWI bar is modelled with embedded beam row element with friction-less pile behavior. Also the grout body is modelled with embedded beam row element with pile behavior by inputting the grout properties for this section. The grout properties are defined based on the values used in single pile model. Since this model had a better performance compared to first option, this model is further investigated and elaborated in the main part of report and first option can be referred in appendix G.

7.4.3 PILE AND SOIL STRUCTURE

For this research a pile group in soil conditions equal to Amsterdam field data set is made and is modelled based on the final model of single pile in plane strain. The used parameters and properties of the pile group model are same as single pile model which has been already explained in section 7.3.3.2.

In single pile model, the axial resistance of the pile for two different sand layers is defined based on the parametric study. The results of the axial resistance will be used further in this part for modeling the pile as group.

Previously the single pile is modelled for both linear and layer dependent capacities. In this part the pile group is only modelled based on linear capacity and since there are two different types of sand layer (first and second sand layer), multi-linear option should be used. Since the axial resistance of the first sand layer and the second sand layer differs, a distinction should be made. Therefore multi-linear is an appropriate option for this case. Layer dependent is not used due to the fact that defining two different grout body behaviors for first and second sand layer was not possible within this option.

The numerical analysis is divided into 6 main calculation phases which will be later in next section explained. The soil structure and properties are the same as what has been used for single pile model. Figure 45 shows the soil layering and the structure of the pile as group in Plaxis.

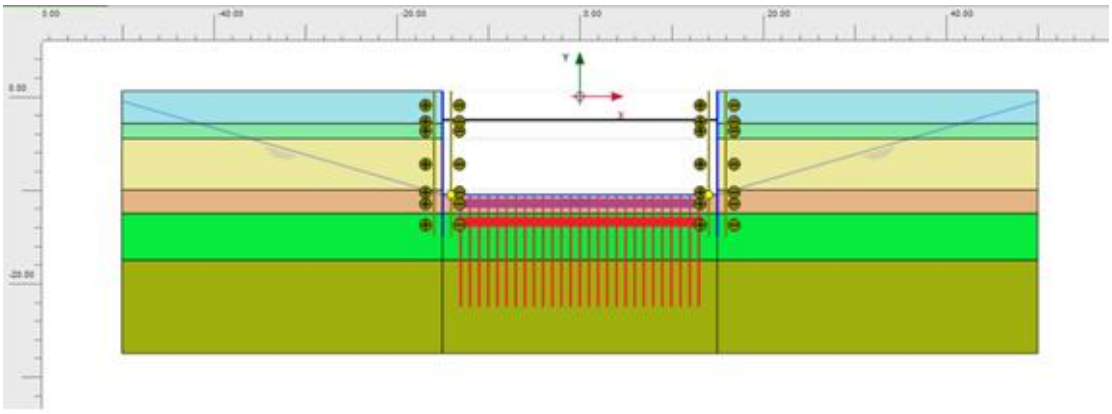

FIGURE 45: SOIL LAYERING AND THE STRUCTURE OF THE PILE AS GROUP IN EBR

For pile group model, there is an excavation of 10.5 m. The total length of the piles are 12 m and the grout body is 10 m long which starts from first sand layer (NAP -12.5 m) and continues until NAP -22.5 m in second sand layer. The width of the excavation is 30 m. The boundary from the center of excavation is assumed to be 50 m, far enough from model at each side to make sure that it does not influence the results. Next figure 46 shows the used mesh size for the model pile group.

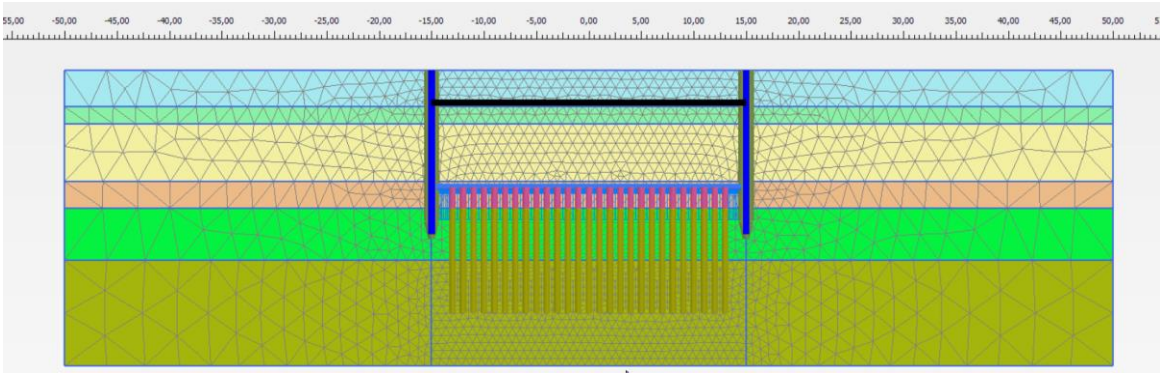

FIGURE 46: USED MESH SIZE FOR THE MODEL PILE GROUP IN EBR

7.4.4 CALCULATION PHASES AND DESCRIPTION

The numerical analysis is divided into 6 main phases. Table 41 describes the identification, type of calculation and loading performed at each phase.

TABLE 41: CALCULATION PHASES AND DESCRIPTION

Phase Number	Identifications	Start From	Type	Loading Type
1	Initial Conditions	-	K_0 Procedure	Staged Construction
2	Activate Sheet Piles and Interfaces	1	Plastic	Staged Construction
3	Excavation and Activate Strut (Node to Node Anchor)	2	Plastic	Staged Construction
4	Activate Ground Anchor and Foundation Floor	3	Plastic	Staged Construction
5	Dewatering	4	Plastic	Staged Construction
6	Tensile Load	5	Plastic	Staged Construction

According to the table, the first phase starts from an initial condition. In this part the generation of the initial stresses is defined. For initial stress it is used from the procedure of K_0. K_0 is the lateral earth pressure coefficient at rest. $\sigma'_{h0} = K_0 . \sigma'_{v0}$ with $K_0 = K_{0;NC} . OCR^{0.5}$.

For NC soils:
$$K_0^{NC} = 1 - Sin\varphi \tag{57}$$

For OC soils:
$$K_0 = K_0^{NC} \times OCR - \frac{vur}{1-vur}(OCR - 1) + \frac{K_0^{NC} \times POP - \frac{vur}{1-vur} \times POP}{\sigma_{yy}^{'0}} \tag{58}$$

Which;

OCR= Over consolidation ratio, POP= pre-overburden ratio, V_{ur} = Poisson ratio for unloading-reloading and $\sigma_{yy}^{'0}$= in-situ vertical effective stress.

In phase 2 the sheet piles with their interface elements will be activated. Interface elements are used because sheet piles have interaction with soil body. Then in phase 3, the excavation will be applied until NAP -11.0 m. To have a stable model, horizontal support such as strut is also modelled and activated in this phase. Activation of the grouted ground anchors and concrete floor will be done in next phase 4. Next phase is de-watering. Because the excavation is done in a saturated soil, it is important to apply de-watering in model by lowering the water table to remove excessive pore water pressure in the construction site. De-watering is usually done prior to excavation to prevent problems that might be causing during excavation. Finally the last phase is applying tensile load on the group of piles model.

All the described phases are illustrated in the next figures from 47 until 53.

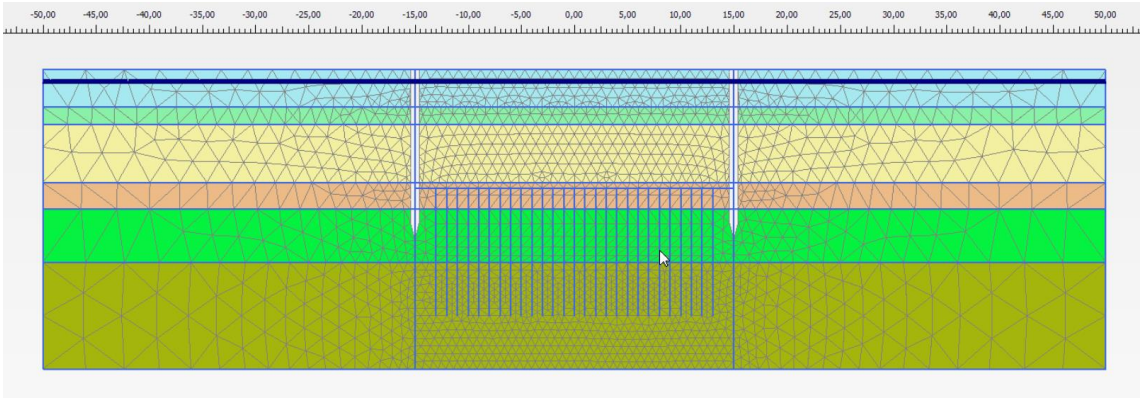

FIGURE 47: INITIAL PHASE

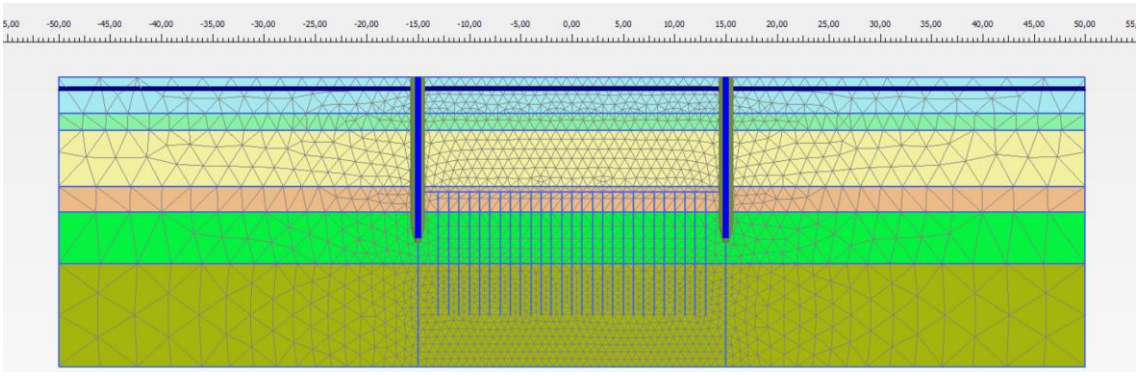

FIGURE 48: ACTIVE SHEET PILES AND INTERFACES

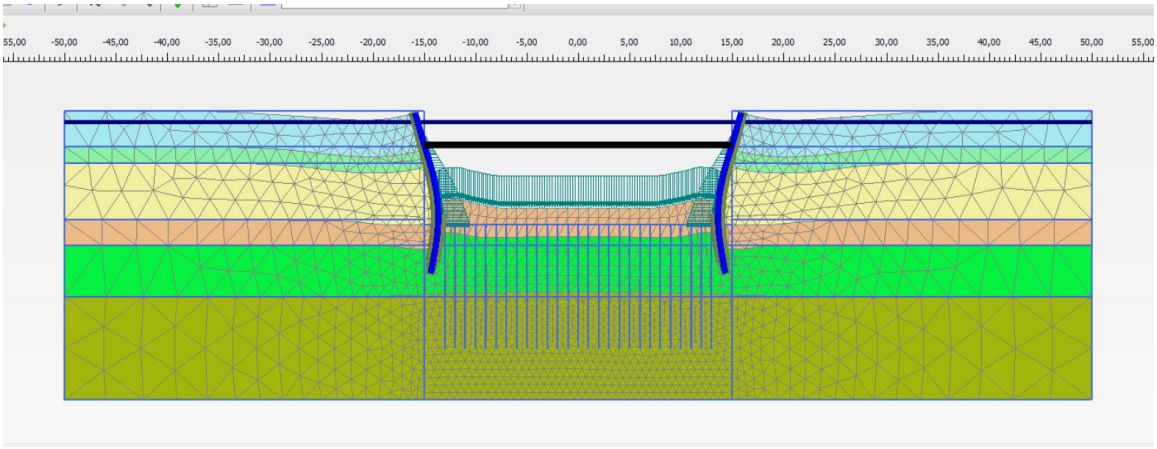

FIGURE 49: EXCAVATION AND ACTIVE STRUT

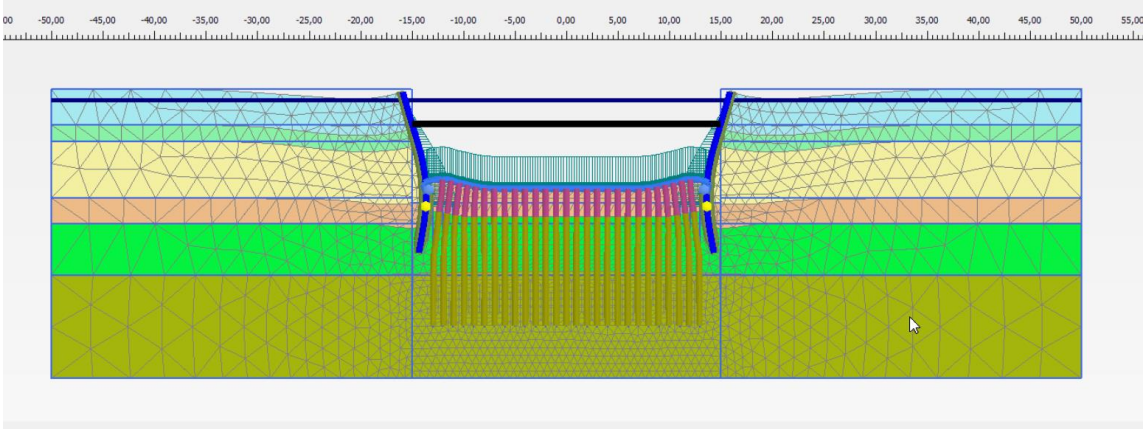

FIGURE 50: ACTIVE GROUND ANCHOR AND FOUNDATION FLOOR

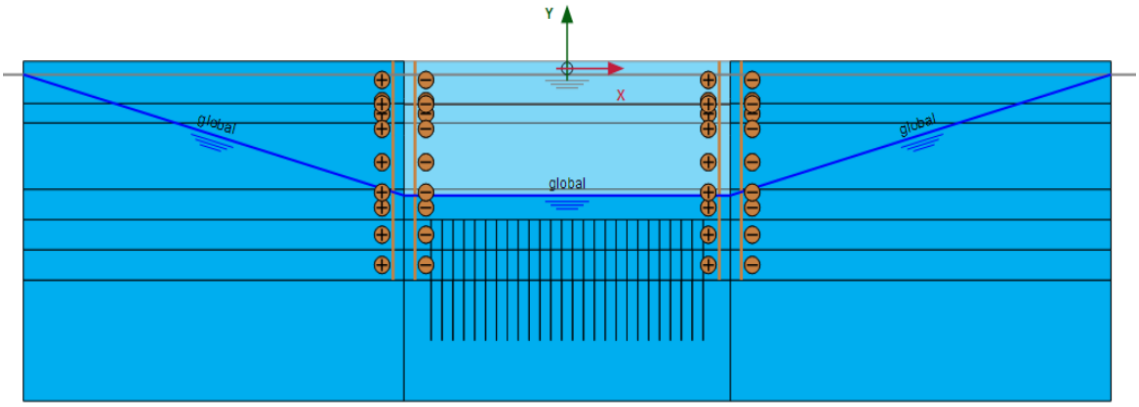

FIGURE 51: DE-WATERING

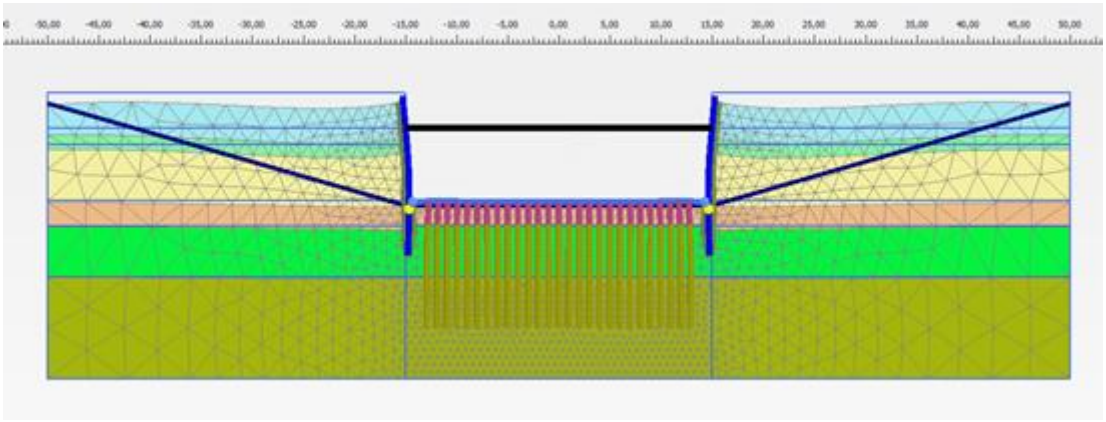

FIGURE 52: PILE GROUP MODEL AFTER DE-WATERING

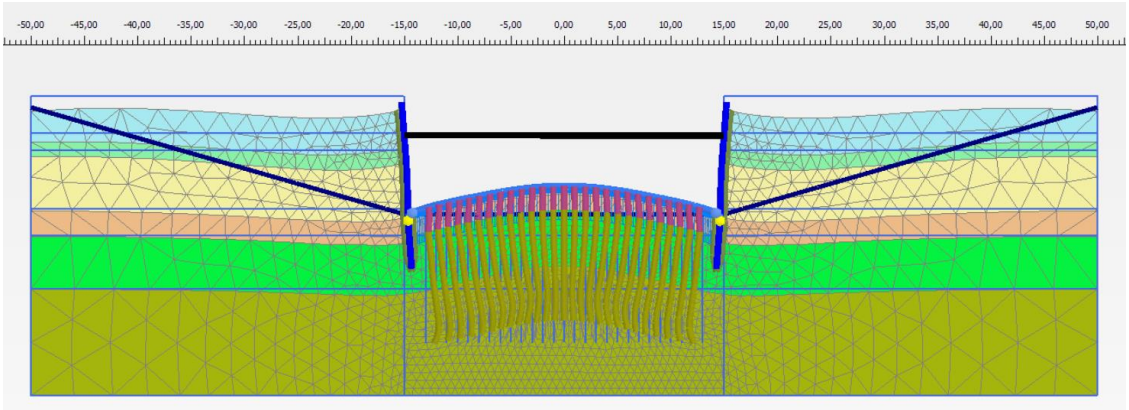

FIGURE 53: APPLYING TENSILE LOAD

In the last phase the pile group is pulled with a tensile load of 150 kN/m². The load is high enough so that the failure occurs.

The piles are modelled for different pile spacing and the significance of this parameter in the group effect is evaluated. There are two failure mechanisms which can happen;

1. Pull-out of soil plug
2. Slip capacity of each individual micro pile is reached

The aim of this evaluation is to determine at what pile spacing, the above mentioned failure mechanisms take place.

7.4.5 ANALYSIS OF THE RESULTS OF PILE GROUP MODEL

In this research the pile spacing is varied to investigate the significance of this parameter in the group effect behavior. The diameter of the bounded section of the micro pile is 0.2 m and the un-bounded part has a diameter of 0.0635 m. There are three different configurations of micro piles evaluated which are 5D, 10D and 15D pile spacing installed in a construction pit with a width of 30 m. The micro piles have a constant $L_{spacing}$ of 3 m in out-of-plane direction and only the pile spacing in x-direction varies.

a) 5D pile spacing

In this model the pile spacing is 5D which is equal to 1 m. The parameters and properties are the same as what has been explained in previous part. The piles are installed and loaded simultaneously in the model. The total vertical displacement is calculated 52.98 mm. Figure 54 shows the result of mesh change for this pile spacing. For a better visualization of the result, the shading contour and line contour of vertical displacement are provided in figure 55 and 56 respectively.

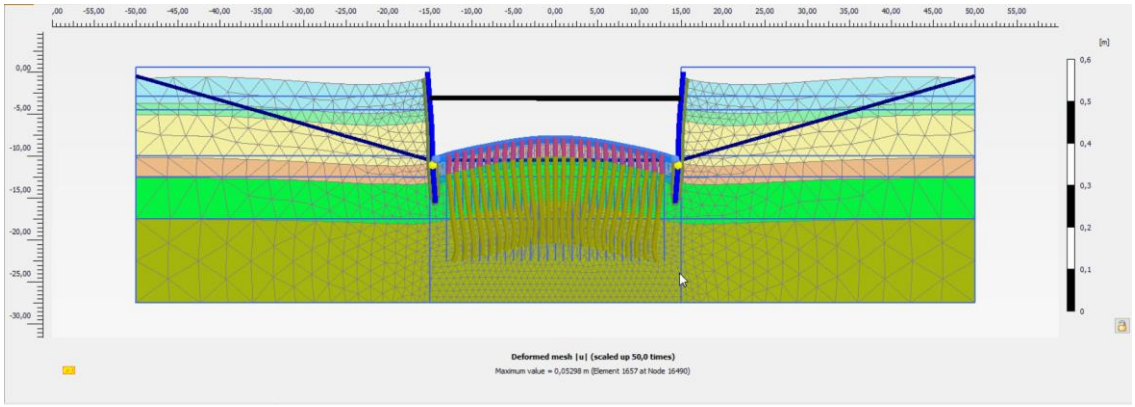

FIGURE 54: MESH CHANGE FOR 5D PILE SPACING

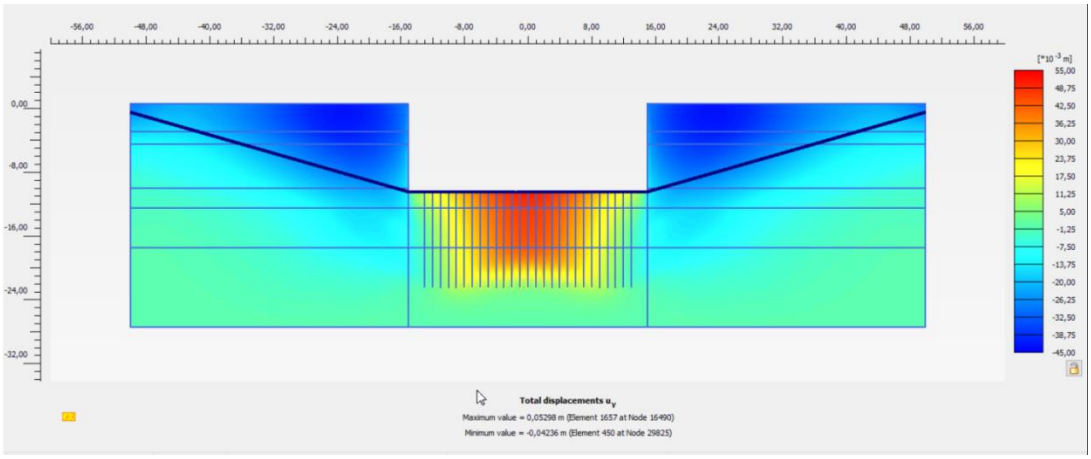

FIGURE 55: RESULT OF SHADING CONTOUR OF VERTICAL DISPLACEMENT FOR 5D PILE SPACING

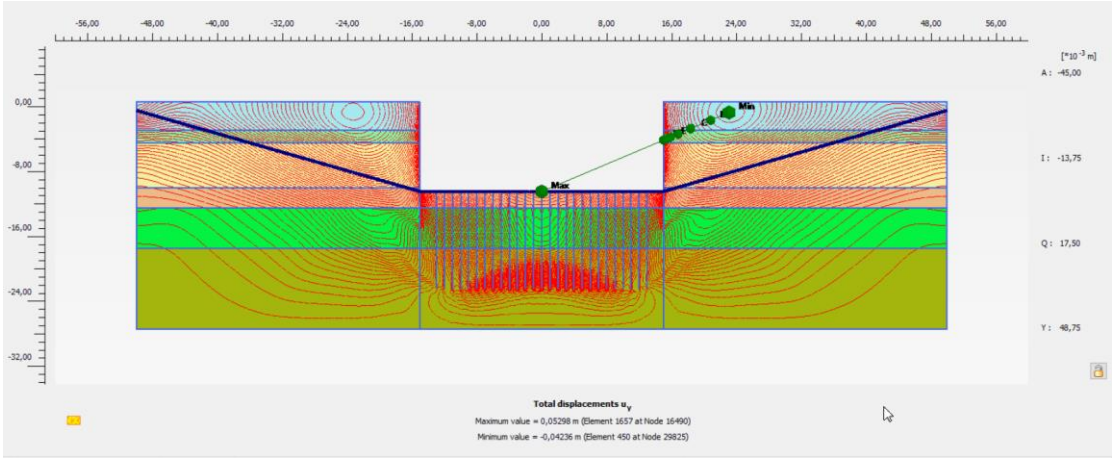

FIGURE 56: RESULT OF LINE CONTOUR OF VERTICAL DISPLACEMENT FOR 5D PILE SPACING

According to the results, it can be concluded that the failure mechanism for 1 m pile spacing is based on the pull-out of soil plug.

In order to make sure that the failure mechanism is based on soil plug pull-out, a cross section of the middle pile in the pile group model and a cross section of soil close to that pile is selected to investigate the pile and soil vertical displacements. Figure 57 shows the result of cross section for middle pile and figure 58 illustrates the cross section result of the soil close to that pile. The maximum calculated vertical displacement for pile and soil is 47.9 mm and 46.9 mm respectively.

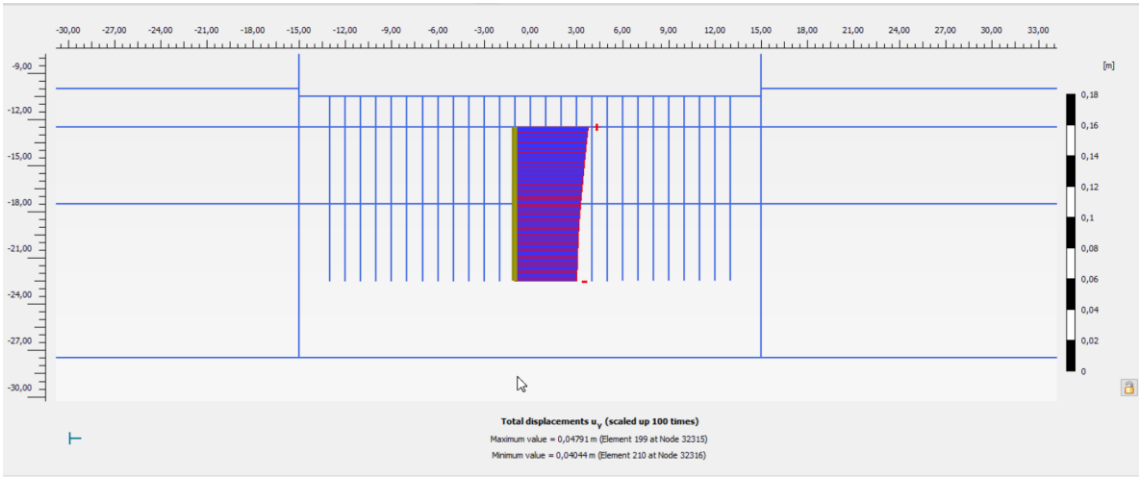

FIGURE 57: VERTICAL DISPLACEMENT OF CROSS SECTION FOR MIDDLE PILE FOR 5D PILE SPACING

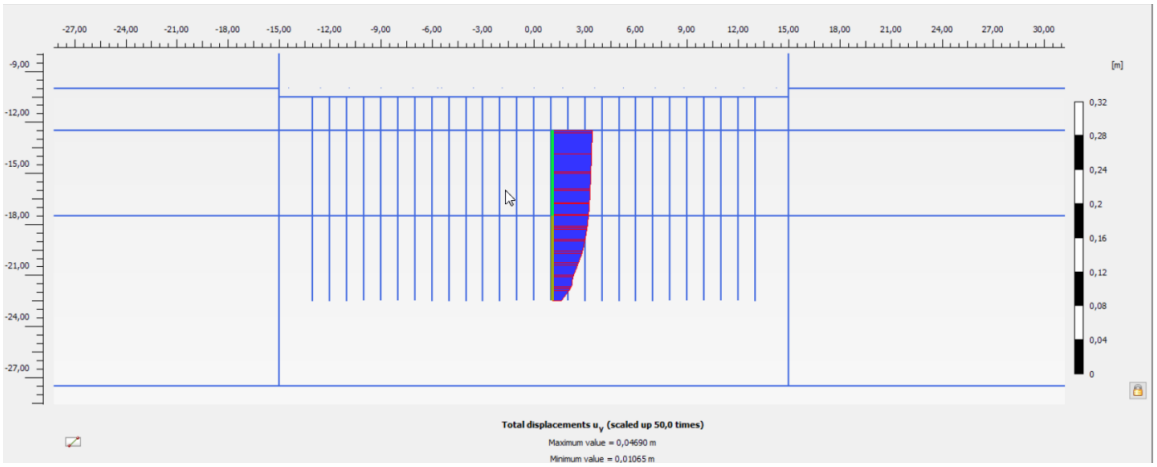

FIGURE 58: VERTICAL DISPLACEMENT OF SOIL CLOSE TO THE MIDDLE PILE FOR 5D PILE SPACING

The results of vertical displacement of the pile, soil and their differences are plotted in the next figure.

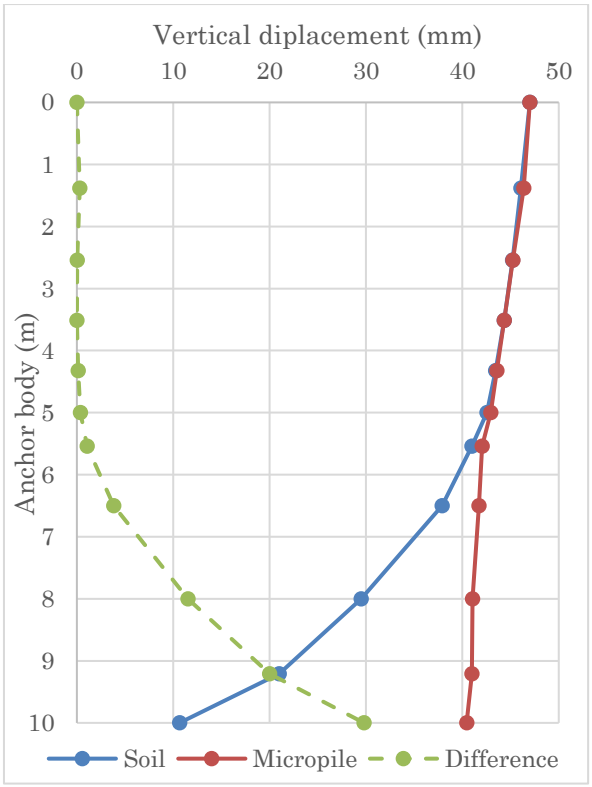

FIGURE 59: VERTICAL DISPLACEMENT OF PILE, SOIL AND THEIR DIFFERENCES FOR 5D

According to the figure one can conclude that pile moves together with the soil for 5.5 meter and after that, they have been separated and failure occurs which is due to soil plug pull-out. The total bearing capacity of the piles for this case is calculated as follow;

$$\sum M_{stage} \times F_{input} \times W \times L_s = 0.8130 \times 150 \times 30 \times 3 = \mathbf{10976\ kN} \quad \text{for a group of 27 piles} \tag{59}$$

$\sum M_{stage}$ is the proportion of the specified changes that has been applied and will range from 0 to 1. If the value is 1, it means that 100% of the pre-scribed load has been applied. In case the calculation finishes while $\sum M_{stage}$ is smaller than 1, most likely reason is that a failure mechanism has occurred.

b) 10D pile spacing

In this part the piles are installed with a center to center distance of 10D which is 2 m and is visualized in figure 60. According to figure 60 the maximum vertical displacement of the pile group model is 183.6 mm for this case. Again the shading contour and line contour of vertical displacement are showed in figure 61 and 62 respectively to have a better understanding about the failure mechanism.

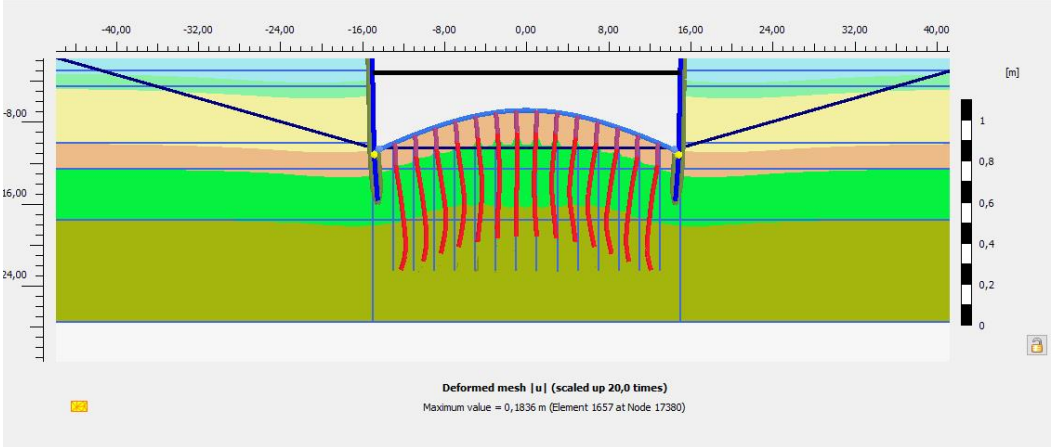

FIGURE 60: MAXIMUM VERTICAL DISPLACEMENT FOR 10D PILE SPACING

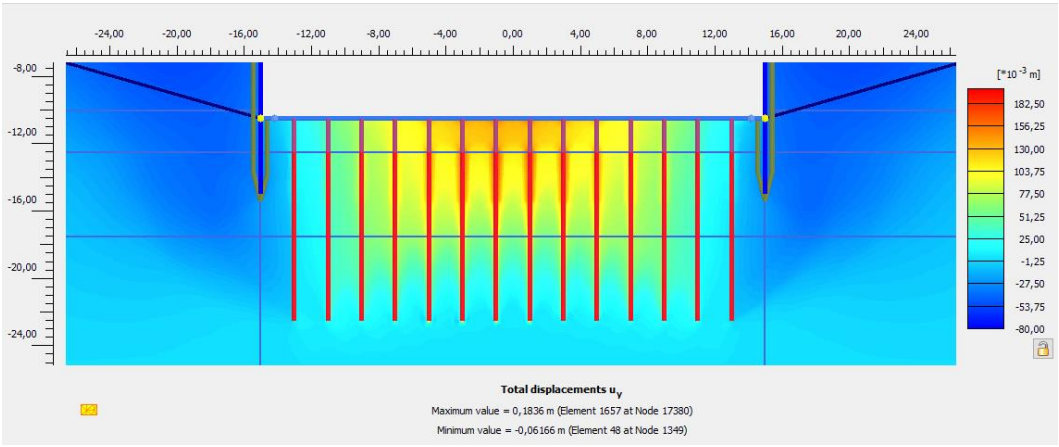

FIGURE 61: RESULT OF SHADING CONTOUR OF VERTICAL DISPLACEMENT FOR 10D PILE SPACING

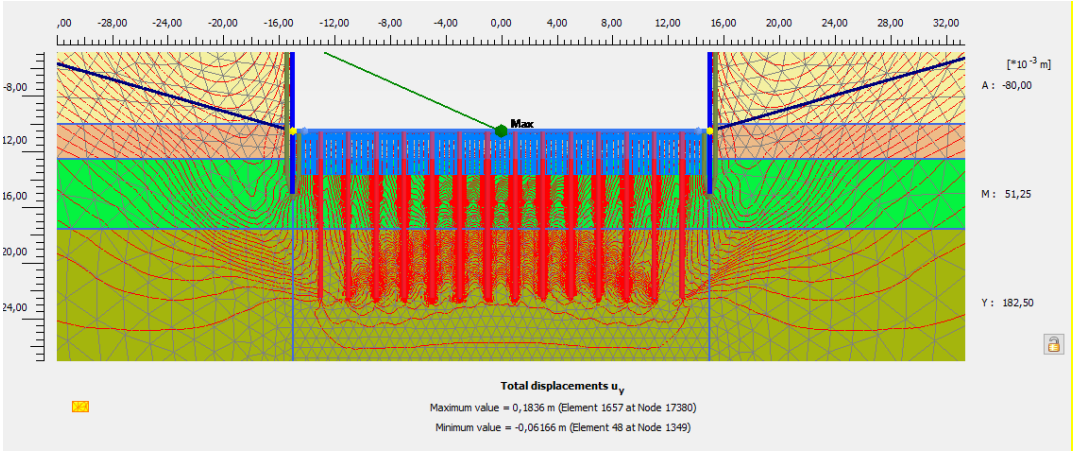

FIGURE 62: RESULT OF LINE CONTOUR OF VERTICAL DISPLACEMENT FOR 10D PILE SPACING

The same procedure of what has been done for 1 m pile spacing, is also here followed. A cross section of middle pile and soil close to that pile is viewed and the results including the difference in vertical displacements are plotted in the next figure 63.

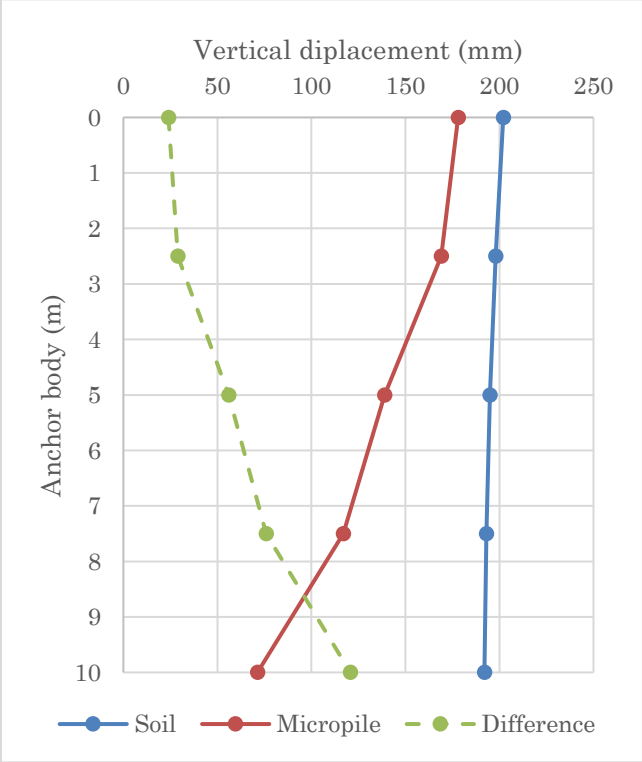

FIGURE 63: VERTICAL DISPLACEMENT OF PILE, SOIL AND THEIR DIFFERENCES FOR 10D

According to the graph it is not clear which kind of failure in this case occurs but by referring to the vertical displacement contour of figures 61 and 62, the failure is still mostly due to soil plug pull-out with some minor pile slip for this case. However it can be seen that the development of a smaller soil plug seems likely to occur due to smaller mobilized volume of soil compared to 5D pile spacing.

The total bearing capacity of the piles for this case is calculated as follow which is higher compared to 1m pile spacing case.

$$\sum M_{stage} \times F_{input} \times W \times L_s = 0.8225 \times 150 \times 30 \times 3 = \mathbf{11104\ kN} \quad \text{for a group of 14 piles} \qquad (60)$$

c) 15D pile spacing

The pile spacing is increased to 3 m center to center distances. The configuration of the pile group model can be found in next figure 64. It also shows the deformed piles at failure.

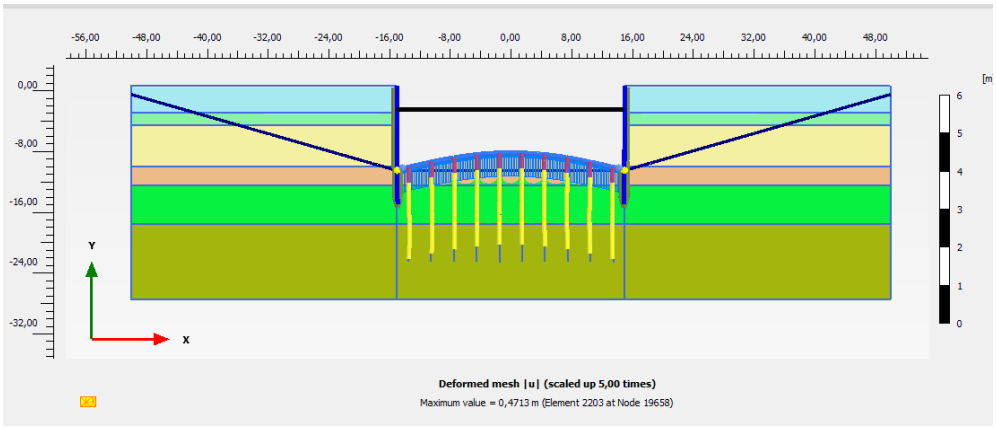

FIGURE 64: MAXIMUM VERTICAL DISPLACEMENT FOR 15D PILE SPACING

Next figure 65 shows the shading contour of total displacement in vertical direction of pile and the surrounding soil. Based on the contour lines it could be seen the movement of the pile is more than the soil mobilization cone. Figure 66 also illustrates the total vertical displacement in y-direction by help of line contours.

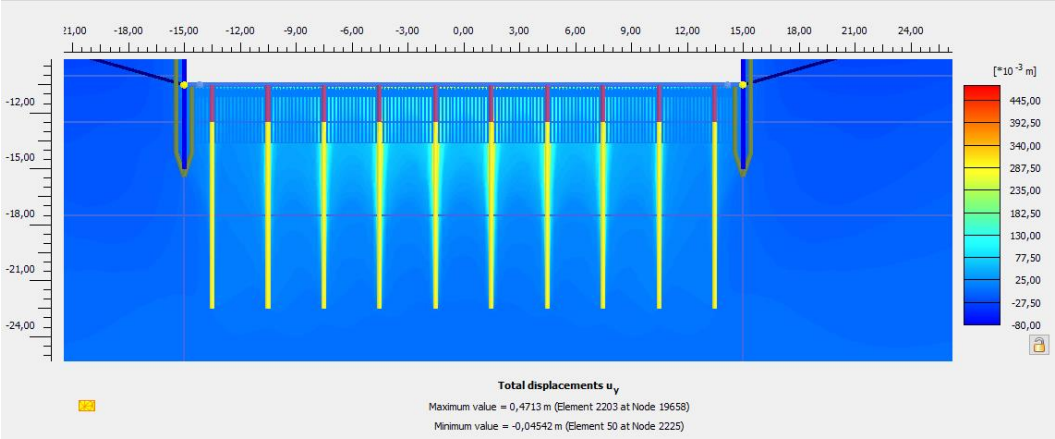

FIGURE 65: RESULT OF SHADING CONTOUR OF VERTICAL DISPLACEMENT FOR 15D PILE SPACING

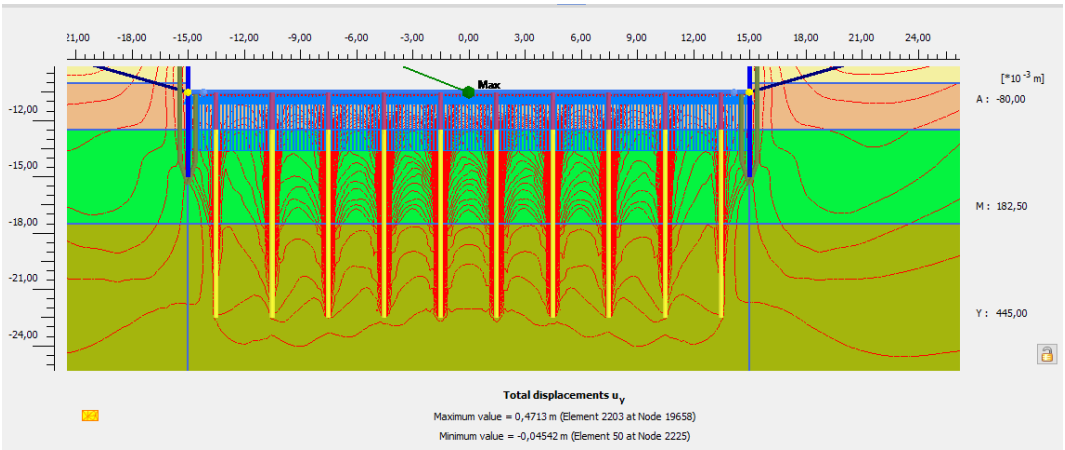

FIGURE 66: RESULT OF LINE CONTOUR OF VERTICAL DISPLACEMENT FOR 15D PILE SPACING

Next figures 67 and 68 demonstrate the total displacement of the cross sectional middle pile and the soil close to it respectively. It can be seen that again the soil mobilization is less significant compared to the pile.

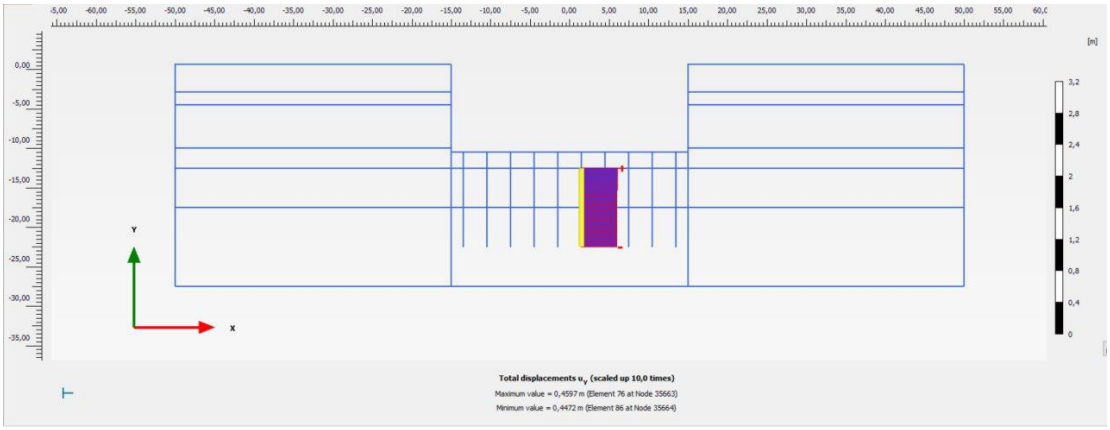

FIGURE 67: VERTICAL DISPLACEMENT OF CROSS SECTION FOR MIDDLE PILE FOR 15D PILE SPACING

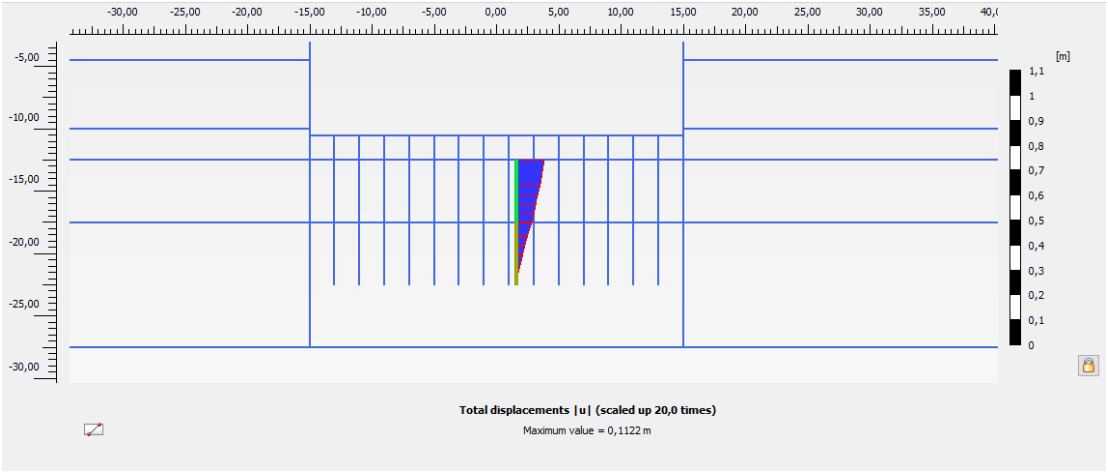

FIGURE 68: VERTICAL DISPLACEMENT OF SOIL CLOSE TO THE MIDDLE PILE FOR 15D PILE SPACING

The results of vertical displacements of the pile and soil including their differences for 3 m pile spacing are plotted in the next figure.

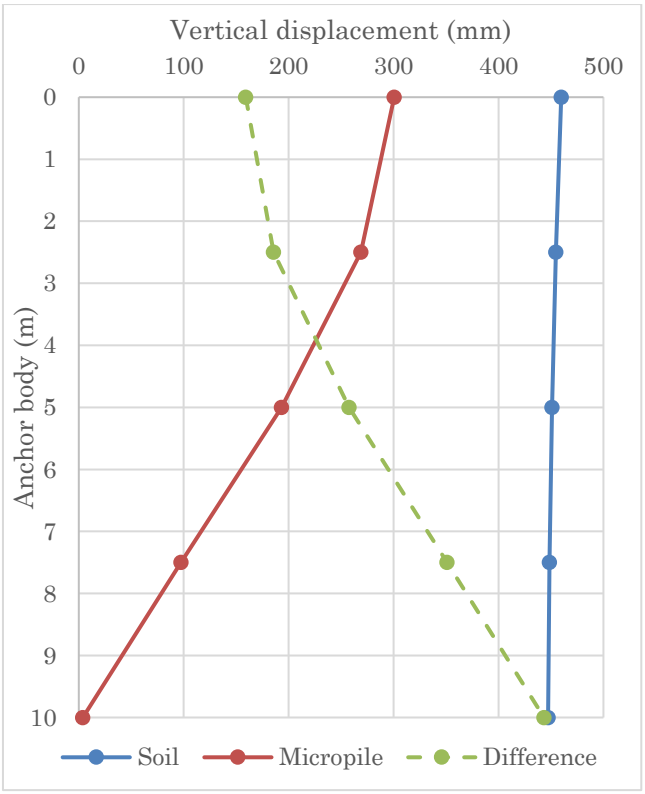

FIGURE 69: VERTICAL DISPLACEMENT OF PILE, SOIL AND THEIR DIFFERENCES FOR 15D

According to the results and the contour lines, it can be concluded the failure is based on the pile slip failure mechanism.

The total bearing capacity of the piles for this case is calculated as follow which has increased compared to previous cases. The reason is that there is a limited group effect presented in this case compared to other two cases and therefore piles have a higher bearing capacity.

$$\sum M_{stage} \times F_{input} \times W \times L_s = 0.90 \times 150 \times 30 \times 3 = \mathbf{12150\ kN} \quad \text{for a group of 10 piles} \tag{61}$$

CHAPTER 8: CLOSURE

8.1 DISCUSSION AND CONCLUSIONS

CUR 236 design procedure states that the bearing capacity of a pile in a pile group is less than the bearing capacity of that pile when it is loaded not in a group. To take this effect into account for the acceptance test, an additional load is added to the test load. It turned out at the Amsterdam car parking project that piles failed the acceptance tests due to this additional load which is required to apply according to CUR 236 design guide. This procedure is questionable because the pile is loaded into a much higher level than it will actually experience during its lifetime.

The primary goal of this thesis was to analyze Amsterdam case study test data provided by CRUX Company. The test data consisted of information of failure tests for 6 piles and the relevant CPT profiles. Since the calculations and designs were based on current Dutch standards, first it was needed to study and evaluate the Dutch design guide and second to focus to investigate the influence of group effects on micro pile behavior. Therefore the main research question was to improve the Dutch design standards for tension pile group based on the methods used in other countries and/or advanced numerical methods.

In this chapter the main research question including sub tasks/ questions are answered following with a conclusion for each one.

1. Comparison of international design standards to the Dutch design standards;

   The initial plan of approach to the main research question was to investigate the standards of other countries and compare them to Dutch standards for tension pile group which did not succeed. The reason was that the standards of other countries were all written in their national language and therefore it was not possible to study them. Seeking for the research on tension pile group behavior did not help so much because many researchers believe that including a realistic group effect in the design is not an easy task. There was only a general conclusion about the behavior of tension pile group which was due to interaction effects lower bearing capacity compared to the single tension pile. So they only used a factor of safety for the calculation of bearing capacity of the piles within a group rather than formulating new formulas for it.

   Also the international methods for calculating the skin resistance of the tension pile were mostly for driven piles in offshore application which differ to the pressurized grouted tension piles used in the Amsterdam car parking case study.

2. Evaluating Dutch design standards about design bearing capacity of single and group tension piles;

   Dutch CUR 236 design guide states that the limit values should be applied in the design for cone resistance, maximum mobilized shear stress and value for shaft friction coefficient. The limit values for the cone resistance is maximized on 20 MPa and for shaft friction coefficient (α_t) the maximum value is 0.025. Maximum mobilized shear stress is also limited to 2.5% of cone resistance limit.

   Results of α_t according to raw data and data proceeded by limit values of CUR 236, showed that the value of α_t is heightened by applying limit values and loses its physical meaning which could give a wrong image for the pile with high bearing capacity than it actually is.

3. What is an appropriate model for single tension pile in Finite Element Method?

In this research the single pile is modelled both in plane strain and axisymmetric conditions in Plaxis. It is modelled based on the sensitivity analysis so that the results of load-displacement diagram of model pile fits to the one obtained from field failure test.

In the plane strain approximation single pile is modelled in two ways. The first model was by using node to node anchor and embedded beam row with grout behavior and the second model was only based on embedded beam pile element for linear and layer dependent axial skin resistances. The results of both models were comparable to the field failure test data. In the layer dependent condition, the installation effect due to grouting is modelled by increasing the effective horizontal stress around the grout body. Effective horizontal stress has a direct relation with lateral earth pressure coefficient (K_0) since the effective vertical stress is constant. By defining an appropriate value for K_0, the installation effects could be simulated in the model.

In the axisymmetric volume element model the installation effect is modelled by increasing the radial stresses around the grout body. It is important to consider the installation effects in the model due to the existence of the pre-stressed zone around the grout body which leads to a higher effective horizontal stress in reality.

4. What is an appropriate model for the tensile pile groups in Finite Element Method?

The pile group is modelled in two ways and the results are studied. The model with a combination of node to node anchor and embedded beam row element with grout behavior is disregarded due to fact that by increasing the pile spacing, the capacity of the pile decreased.

The embedded beam row element with pile behavior for both un-bounded and bounded length of the micro pile had a good performance and this model is chosen as the final pile group model.

5. How the distances between the piles in the group are of importance? And could this parameter affect the mechanism of failure?

The capacity of the pile for different pile spacing is investigated based on the embedded beam pile model in Plaxis. The model is based on the validated single pile model and the construction phases are according to the data of Boerenwetering car parking project. According to the results, the bearing capacity of the pile increased with increasing the pile spacing due to existence of less group effect.

Also the capacity of the pile is calculated according to CUR 236 for soil plug pull-out and slip failure mechanisms. Since it is not clear that micro piles are soil displacing or non-displacing piles, the soil plug pull-out is calculated for two cases with a lower cone angle of 45^o and $2/3\phi$. The result of hand calculations and plane strain embedded beam row pile group model is presented in the next figure.

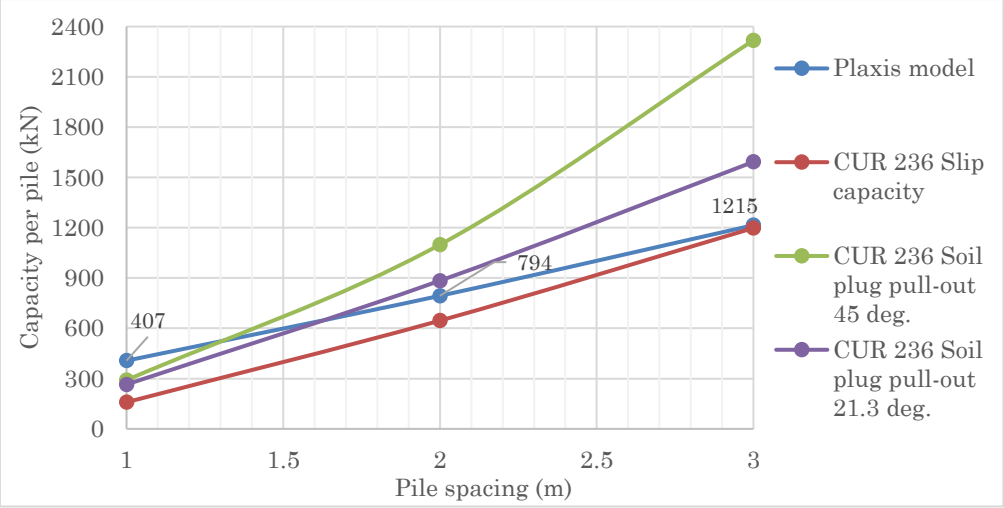

FIGURE 70: BEARING CAPACITY PER PILE BASED ON CUR 236 METHOD AND PLAXIS MODEL

Figure 70 shows a clear difference of pile bearing capacity based on the Plaxis model and the hand calculations according to the standards for 1 meter (5D) pile spacing. The standards are conservative for this pile spacing because this closely spaced piles in practice should not be applied. For 2 meter pile spacing (10D) the capacity of the model is in between slip failure mechanism and soil plug pull-out 21.3 deg. Therefore the failure mechanism is not clear as it has been already mentioned in section 7.4.5. However it can be seen that the failure is closer to soil plug pull-out failure. Finally the capacity of 3 m spaced (15D) model pile coincides the slip capacity of the pile according to CUR 236.

6. At what pile spacing the failure mechanism transition is likely to occur?

As it has been already explained in section 7.4.5 for each pile spacing, the vertical displacements of middle anchor pile and soil close to it including differences in vertical displacement are plotted. To increase the level of accuracy about the results, the vertical displacement differences for all piles are also determined which can be found in appendix H. By calculating the area under the graph of "differences in vertical displacement of pile and soil", the transition point to slip failure mechanism can be determined. Based on figure 71 it can be seen that the transition starts from pile spacing 2 m (10D).

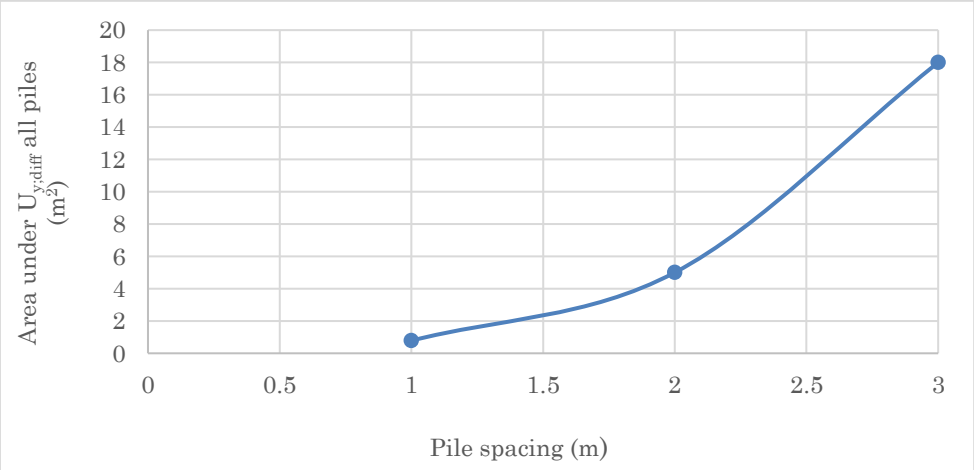

FIGURE 71: FAILURE MECHANISM TRANSITION POINT

7. How can the Dutch design guide be improved?

With the validation of the EBR pile group model, an improvement for the Dutch design guide could be proposed. According to the results, the space between the piles within a pile group can be designed as 10D where the slip failure is not reached and it is not a limiting state.

8.2 LIMITATIONS

During the modelling process, several limitations were encountered regarding the model which are listed below;

- For the modelling of bounded length of micro piles, it has been used from Embedded Beam Element. In combination with this element it is not possible to use interfaces to model interaction of pile and the surrounding soil. To simulate the effect of interaction, it has been used from skin resistance parameter (T_{skin}) and it is back-calculated according to the field failure test data.

- For the modelling of pile group, it has been used from data of single pile model and field failure test. The failure test is done on piles with 5 m grouting located either in first or second sand layer. However the grout length in pile groups is 10 m situated in both first and second sand layer. Due to the fact that no data was available for the failure test on piles with 10 m grout in first and second sand layer, it has been used from data with 5 m grouting and made a correlation to have a model with 10 m grout length.

- Since there are two layers of grout injection, defining two different grout body behaviors for first and second sand layer in layer dependent axial capacity was not possible. Therefore it has been used from multi-linear axial capacity in pile group model.

8.3 RECOMMENDATIONS

The pile group model can be validated based on full-scale failure test or small scale test by using geo-centrifuge models. By doing a full scale failure test the parameters of the pile group model can be calibrated and fitted to the load-displacement diagram similar to what has been done for single pile model.

With the Geo-centrifuge, a very controllable model could be made and the stress level in the model could be increased to simulate the installation effects. In this way it is possible to check how the installation affects the behavior of the piles within a group.

Also by monitoring of for example Boerenwetering car parking project, a real data base of the group behavior can be obtained. Comparing the monitoring data to the design values based on CUR 236 could give an idea how well the design guide is formulated.

BIBLIOGRAPHY

Addendum to CUR report 236 (2016). “Micro piles” - Axial spring stiffness. Technical report, Stichting SBRCURnet, Delft.

API RP 2A-WSD (2010). Planning, designing and constructing fixed offshore platforms-working stress design. 21st edition, December 2000.

CUR report 236 (2017). “Micro piles”. Technical report, second edition. ISBN: 978-90-5367-655-4, 2017.

CUR report 2001-4 (2003). “Design rules for tension piles”. Technical report, Stichting CUR, Gouda.

Dieteren, H. M. H. (2016). UO Funderingsadvies voor Parkeergarage Boerenwetering te Amsterdam, CRUX Engineering.

De Nicola, A. and Randolph, M. F. (1994). Tensile and compressive shaft capacity of piles in sand. Journal of Geo-technical Engineering.

Firoozfar, A., Rostami, A., Ghaderi, H., Zamani, H. and Rostamkhani, A. (2017). Assessing the effects of length, slope and distance between piles on the bearing capacity of a pile group under axial loading in granular soil. Engineering, technology and applied sciences research, pages 1894-1899, 2017.

Federal Highway Administration research and technology (March 2006). Analyses of the axial load test at the route 351 bridge report. Publication NO. FHWA-HRT-04-043.

Federal Highway Administration (2005). Micro pile design and construction guide line, reference manual. Publication No. FHWA NHI-05-039.

Houlsby, G. T. (1991). How the dilatancy of the soils affects their behavior. Pages 1192-1200.

Jardine, R. and Merrit, A. (March 2015). The ICP design method and application to a North Sea offshore wind farm. Geotechnical special publication.

Kyung, D. and Lee, J. (2017). Uplift load carrying capacity of single and group micro piles installed with inclined conditions. Journal of Geo-technical and Geo-environmental Engineering. ISSN 1090-0241.

Lehane, B. M., Schneider, J. and Xu, X. (October 2007). Development of the UWA-05 design method for open and closed ended driven piles in siliceous sand. Conference paper.

Lehane, B. M. (1993). Mechanisms of shaft friction in sand from instrumented pile tests. Journal of Geo-technical Engineering, 119(1):19-35.

Lehane, B. M. and Jardine, R. J. (1994). Shaft capacity of driven piles in sand. In conference on the behaviour of offshore structures, pages 25-40.

Molendijk, J. A. W. (2017). The influence of group effects on micro pile behavior. Master’s thesis, Delft University of Technology.

Meerdink, L. (2013). Performance of Micro piles under axial tensile loading. Master's thesis, Delft University of Technology.

Nederlands Normalisatie Institute (2016). NEN 9997-1 Geotechnical design of structures-part 1: General Rules, Delft.

Park, D., Park, D. and Lee, J. (2016). Analyzing load response and load sharing behavior of piled rafts installed with driven piles in sand. School of civil and environmental engineering,. URL: http://dx.doi.org/10.1016/j.compgeo.2016.05.008.

Plaxis 2D (2018). Tutorial manual. Technical report, Build 9462.

Plaxis 2D (2018). Reference manual. Technical report, Build 9462.

Plaxis 2D (2018). Material models manual. Technical report, Build 9462.

Sluis, J. J. M. (2012). Validation of Embedded Pile Row in PLAXIS 2D. Master's thesis, Delft University of Technology.

Slaghuis, J. (2016). Waterbodemonderzoek Hobbemakade te Amsterdam. Multuconsult report, Amsterdam.

Tomlinson, M. J. (1994). Pile design and construction practice. Fourth edition, ISBN 0419184503.

Tension piles design code, CT 5330. Foundation Engineering, Delft University of Technology.

Van Renswounde, A. (2017). An evaluation and improvement of the limit and design values stated in CUR 236- Micro piles. Master's thesis, Delft University of Technology.

Van den Berg, J. P. (2015). Evaluatie proefpalen voor Boerenwetering Parkeergarage project. Document number BWG-PGB-1.1.1.1-TM-ONO-7002.

APPENDICES

A CPT DATA OF PILE LOAD TEST

A.1 CPT DATA BEFORE EXCAVATION

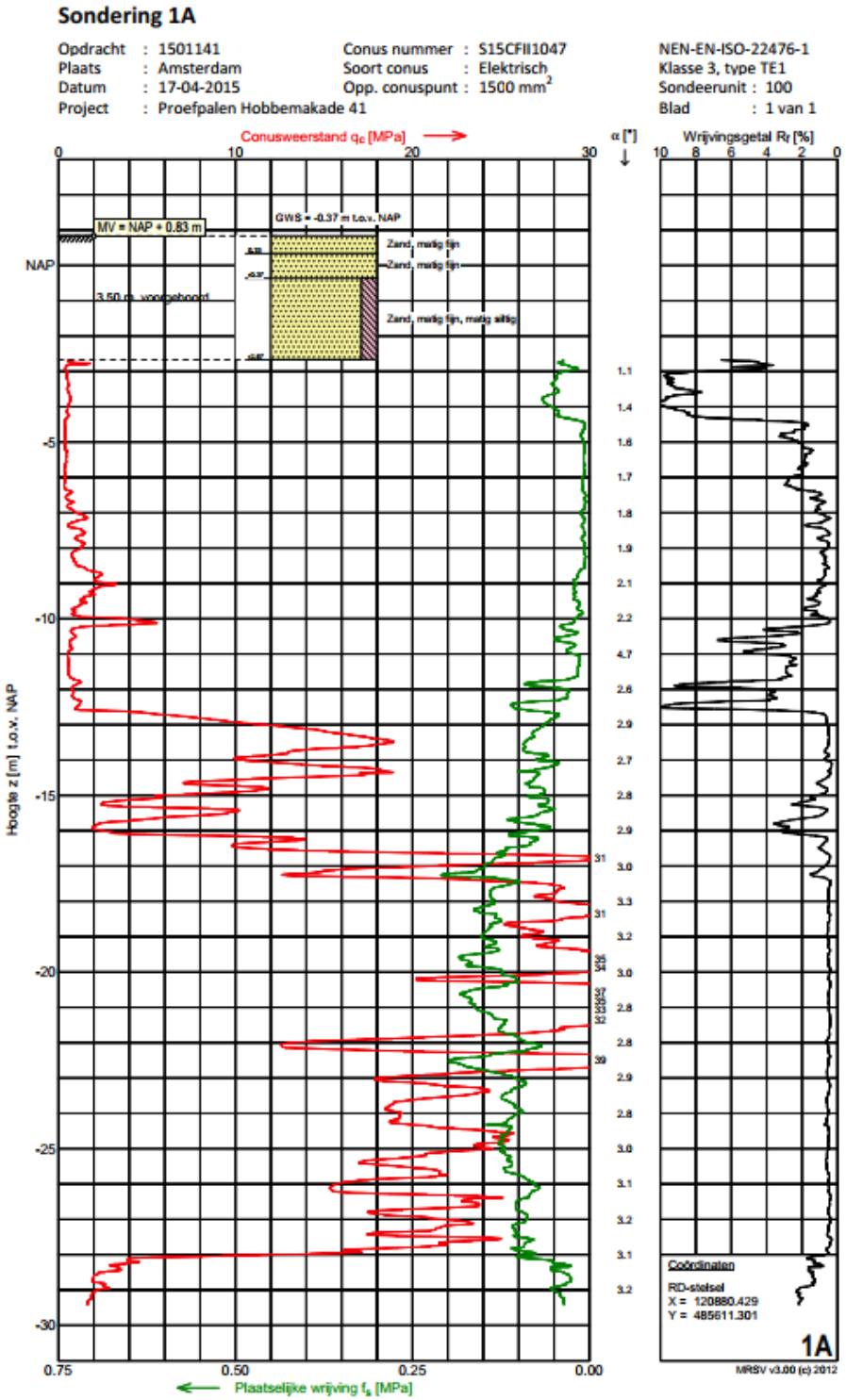

FIGURE 72: CPT 1 AT THE SITE OF THE PILE LOAD TESTS

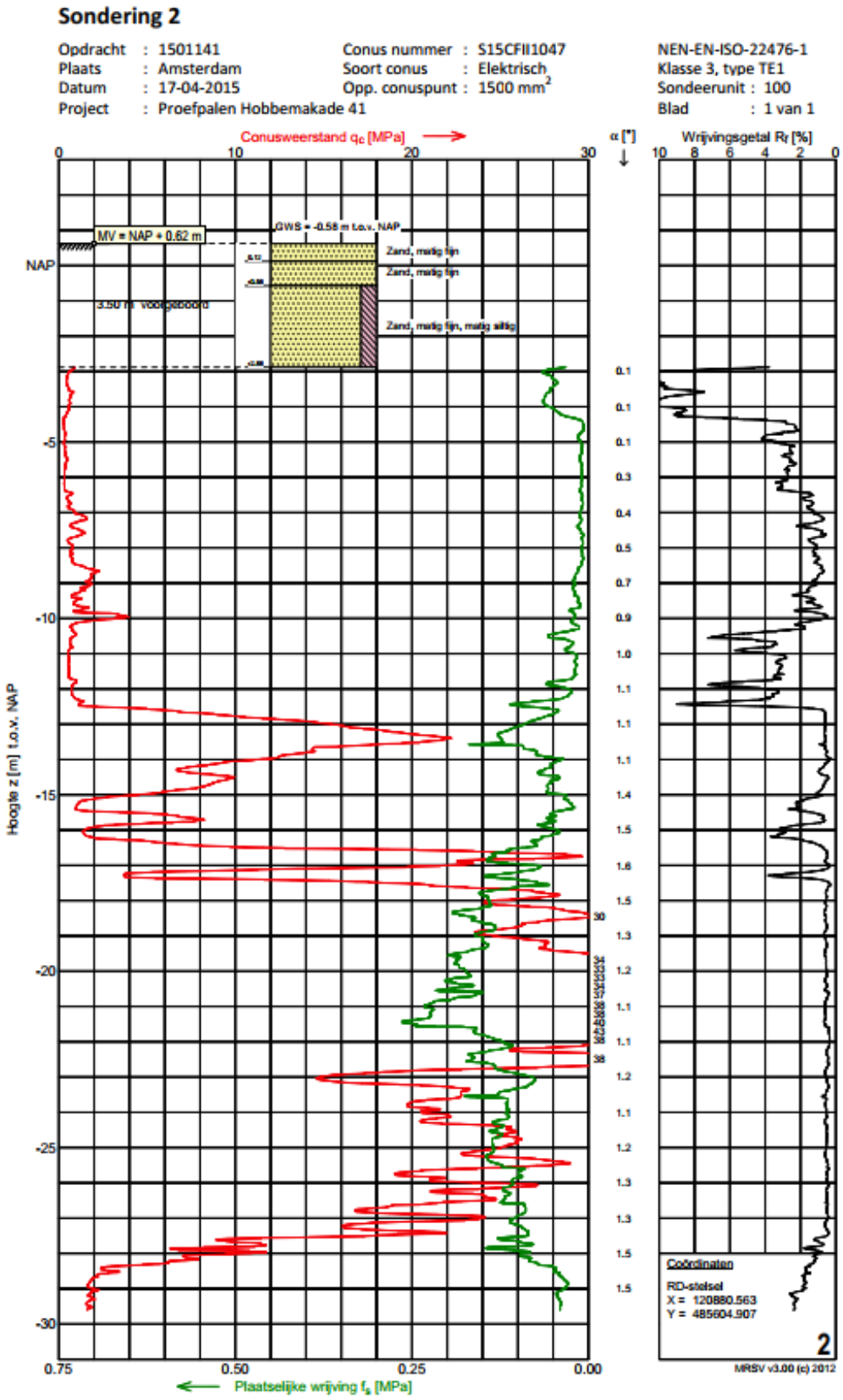

FIGURE 73: CPT 2 AT THE SITE OF THE PILE LOAD TESTS

A.2 CPT DATA AFTER EXCAVATION

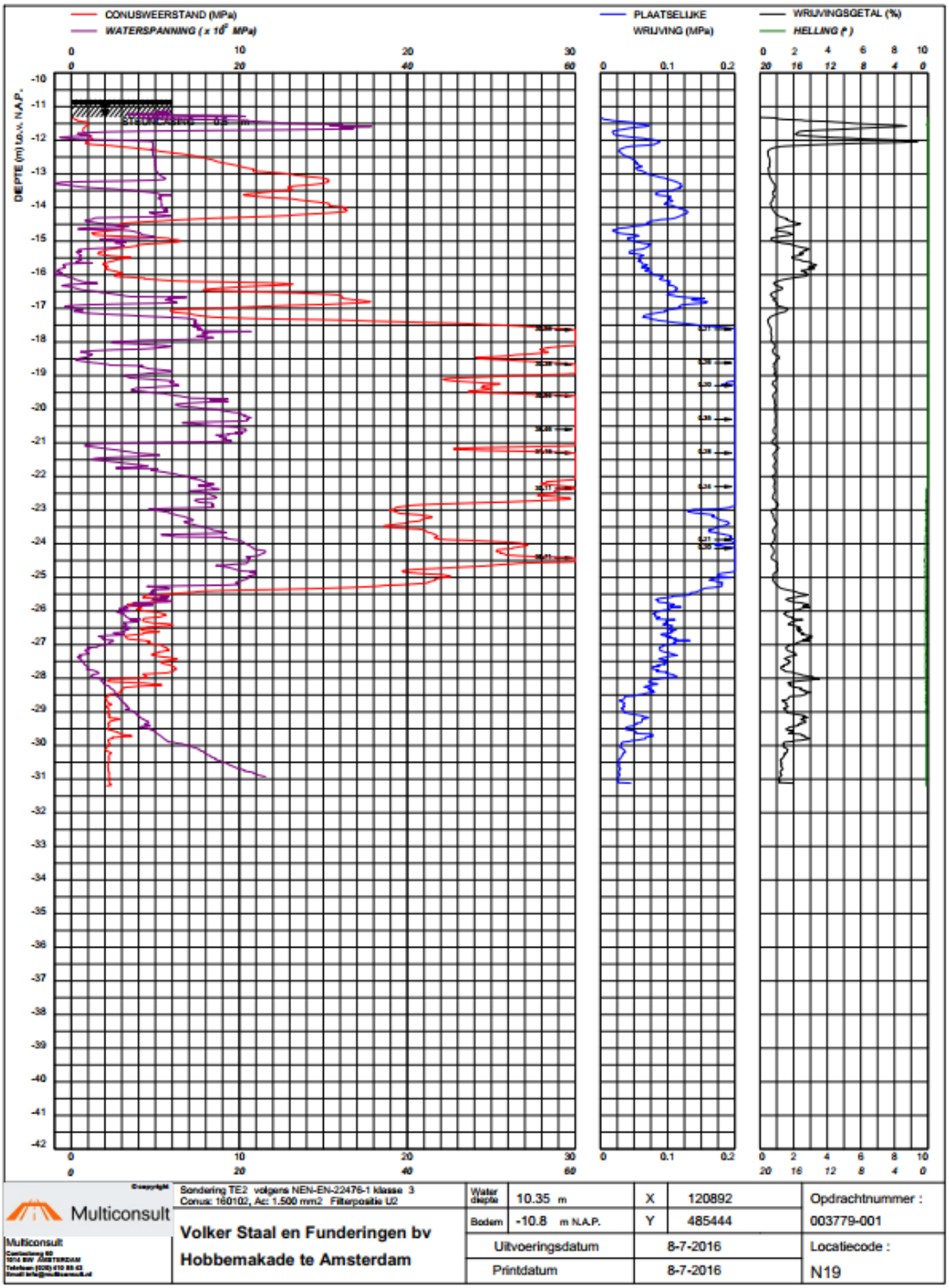

FIGURE 74: REPRESENTATIVE CPT FOR AFTER EXCAVATION

A.3 Location of CPT for Amsterdam case study

FIGURE 75: CPT LOCATION

B DERIVATION AND THEORY BEHIND OF DUTCH CALCULATION RULE

B.1 EFFECT OF INSTALLATION f_1

The effects of installation could be taken into account by factor f_1. Determination of f_1 is especially important in case of pile groups because for the single pile the effect is taken into account by shaft friction coefficient α_t. This coefficient is derived based on tension tests on single piles.

To find the effect of the densification and displacement, first the initial void ratio e_0 is determined. The relation between the cone resistance, the vertical effective stress and the relative density R_e according to Lunne and Christoffersen for normally consolidated from fine to medium fine sands has been chosen.

$$R_e = 0.34 \cdot \ln \frac{q_{c;z;0}}{61\left(\sigma'_{v;z;0}\right)^{0.71}} \tag{62}$$

Which R_e is the initial density, $q_{c;z;0}$ is the cone resistance and $\sigma'_{v;z;0}$ is the effective vertical stress before driving (either with or without a possible reduction for excavation). The initial void ratio e_0 can be found using R_e and estimated values for e_{max} and e_{min}. e_{max} and e_{min} are maximum and minimum void ratio of the soil. In the Netherlands the value for e_{max} and e_{min} is mostly chosen to be 0.8 and 0.4 respectively both for normally- and over consolidation soils. The influence of these parameters is limited so a global estimate is sufficient;

$$R_e = \frac{e_{max} - e_0}{e_{max} - e_{min}} \tag{63}$$

The densification influence due to installation on neighboring pile is calculated using a cylindrical area around the pile that is to be installed. It may be assumed that the decrease is linear from the edge of the pile to a distance of $6D_{eq}$ from the center of the pile. The influence for pile groups can be found by summating the influence of the single piles that are located within a center line distance of $6D_{eq}$ from the pile that is to be calculated.

The decrease of e_0 at a distance r from the pile is:

$$\sum_{1}^{n} \Delta e = -\frac{(r-6)}{5.5} \cdot \frac{(1+e_0)}{50} \tag{64}$$

In which:

Δe Decrease in void ratio of the soil after the installation of a neighboring pile within a distance of $6D_{eq}$;

n Number of piles within a distance of $6\,D_{eq}$;

r Distance to the neighboring pile expressed in D_{eq} ;

The derivation of above formula is as follows;

Before the installation of the pile:

$$V_{p0} = \frac{e_0}{1+e_0} \cdot \frac{\pi}{4} \cdot \left(12\,D_{eq}\right)^2 \tag{65}$$

In which V_{p0} is the pore volume within the area of influence before installation in [m³/m].

After the installation of the pile:

$$V_{p1} = \frac{e_{1;av}}{1+\ e_{1;av}} \cdot \frac{\pi}{4} \cdot \left(143 D_{eq}^2\right) \tag{66}$$

In which:

$e_{1;av}$ Average value of the void ratio within the area of influence after the pile has been installed; $e_{1;av}$ is approximately $\left(e_0 - 1/3\Delta e\right)$ for a linear course of Δe;

V_{p1} Volume of the pores after installation in [m³/m]

$$V_{p1} = \left(\frac{e_0 - 1/3\Delta e}{1+e_0 - 1/3\Delta e}\right) \cdot \frac{\pi}{4} \cdot 143 D_{eq}^2 \tag{67}$$

Also:

$$V_k + V_{p0} = V_k + V_{p1} + V_{pile} \tag{68}$$

In which:

V_k Grain volume in [m³/m];

V_{pile} Volume of the pile in [m³/m]

Therefore the following formula can be derived now;

$$e_0 = \frac{V_{p1}}{V_k} + \frac{V_{pile}}{V_k} \tag{69}$$

From (68) and (69):

$$V_{p0} - V_{pile} = \left(\frac{e_0 - 1/3\Delta \mathrm{e}}{1+e_0 - 1/3\Delta \mathrm{e}}\right) \cdot \frac{\pi}{4} \cdot 143\, D_{eq}^2 \tag{70}$$

$$V_{p0} = V_g \frac{e_0}{1+e_0} \tag{71}$$

$$V_g = 144 \cdot \frac{\pi}{4} \cdot D_{eq}^2 \tag{72}$$

In which V_g is the total volume of soil within the area of influence in [m³/m].

From (70), (71) and (72) the following can be derived:

$$\Delta e_{max} = \frac{1+e_0}{50} \tag{73}$$

The value of $e_{1;av}$ for the pile in question can be calculated by summating the densification effects and stressing effects Δe of the surrounding piles. Field piles, edge piles and corner piles can be distinguished. The void ratio after the piles have been installed can be found from:

$$e_{1;av} = e_0 - \sum_{1}^{n} \Delta e \tag{74}$$

The order of driving is not taken into account. This maximum densification next to the pile is translated into a densification at the location of the pile using (70).

The value of ΔR_e can be determined using:

$$\Delta R_e = \frac{\sum_{1}^{n} \Delta e}{\left(e_{max} - e_{min}\right)} \tag{75}$$

In which ΔR_e is the increase in relative density due to the installation of the pile according to (75).

The ratio of the cone resistance after ($q_{c;z;1}$) and before ($q_{c;z;0}$) installation is called f_1. The factor f_1 is determined from the extent of densification due to the installation of the pile group. This is expressed in an increase in the relative density R_e. The factor f_1 can be determined according to:

$$f_1 = \frac{q_{c;z;1}}{q_{c;z;0}} = e^{2.93 \cdot \Delta R_e} \tag{76}$$

In reality it is possible that the effect of densification does not occur therefore it should be checked by doing cone penetration test at the location or between the piles in a complete pile field. The densification must be checked for minimally 1 % of total piles, with a minimum of three CPT's.

B.2 EFFECT OF RELAXATION DUE TO TENSIONAL LOAD F_2

Due to tensional loading a relaxation or decrease in effective stress in the layers occur. This tensional strength decrease is taken into account by factor f_2 and could be determined according to cone resistance of before and after tensional loading.

$$f_2 = \frac{q_{c;z;2}}{q_{c;z;1}} \tag{77}$$

In which:

$q_{c;z;1}$ Design value of the cone resistance at a depth z after the installation of the pile and before the tensional load has been applied in [MPa];

$q_{c;z;2}$ Design value of the cone resistance at a depth z after the tensional load has been applied in [MPa].

The stress path due to different order of installation around the pile shaft are shown in figure 76.

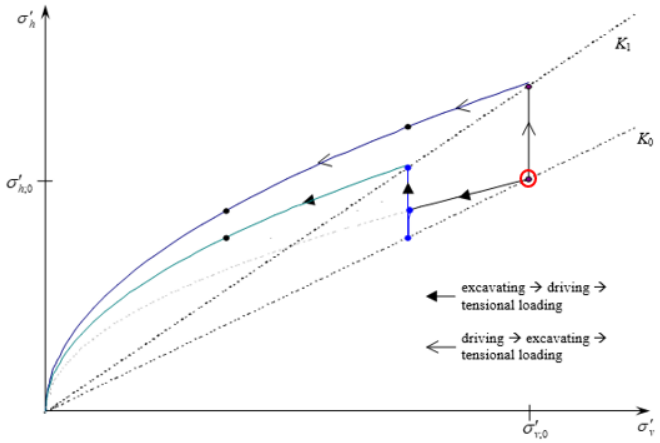

FIGURE 76: STRESS PATH DUE TO INSTALLATION OF THE PILE AND TENSILE LOADING

Next formula shows the calculation of shaft friction based on the vertical effective stress for one layer of the soil;

$$\sigma'_{v;d;2} = \sigma'_{v;d;0} - \frac{O_{p;z} \cdot f_1 \cdot f_2 \cdot \alpha_t \cdot q_{c;z;d} \cdot d_i}{A} \tag{78}$$

In which:

$\sigma'_{v;d;0}$ Design value of the vertical effective stress before loading the pile group in [kPa];

$\sigma'_{v;d;2}$ Design value of the vertical effective stress during the loading of the pile group in [kPa];

$O_{p;z}$ Circumference of the pile at a depth z in [m];

A The area of influence of a pile [m²];

d_i Thickness of the layer [m];

$q_{c;z;d}$ Design value of the cone resistance at depth z (including possible excavation reduction)

Next figure 77 shows an illustration of the above formula;

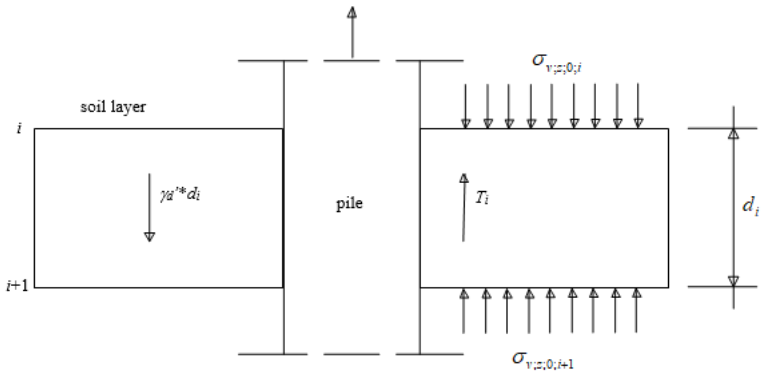

FIGURE 77: STRESSES IN THE SOIL NEXT TO A PILE

Due to tensional load, the effective stress decreases and this concept is similar to an over-consolidation situation with an OCR equal to;

$$OCR = \frac{\sigma'_{v;z;0}}{\sigma'_{v;z;2}} \tag{79}$$

For the relief, the following calculations are made using the soil pressure coefficient:

$$K_{0;unl} = K_{0;nc} \cdot \mathrm{OCR}^{\sin\varphi'} \tag{80}$$

Combining (79) and (80) by taking into account that $\sin\varphi' = 0.5$:

$$f_2 = \sqrt{\frac{\sigma'_{v;z;2}}{\sigma'_{v;z;0}}} \tag{81}$$

$$f_2 = \frac{q_{c;z;2}}{q_{c;z;1}} = \frac{K_{0;unl}}{K_{0;nc}} \cdot \frac{\sigma'_{v;z;2}}{\sigma'_{v;z;0}} \tag{82}$$

$$f_2 = \sqrt{OCR} \cdot \frac{\sigma'_{v;z;2}}{\sigma'_{v;z;0}} \tag{83}$$

In which:

$\sigma'_{v;d;0}$ Design value of the vertical effective stress before loading the pile group in [kPa];

$\sigma'_{v;d;2}$ Design value of the vertical effective stress during the loading of the pile group in [kPa];

$q_{c;z;1}$ Design value of the cone resistance at a depth z after the installation of the pile and before the tensional load has been applied in [MPa];

$q_{c;z;2}$ Design value of the cone resistance at a depth z after the tensional load has been applied in [MPa];

$K_{0;nc}$ Horizontal soil pressure coefficient for normal-consolidation soils;

$K_{0;unl}$ Horizontal soil pressure coefficient after the piles have been loaded in tension;

OCR Grade of over-consolidation

By combining (78), (81), (82) and (83) the following quadratic equation is formed, in which f_2 is the only unknown:

$$\left(\sigma'_{v;d;0}\right)\cdot f_2^{\,2}+\left(\frac{O_{p;z}\cdot f_1\cdot\alpha_t\cdot q_{c;z;d}\cdot d_i}{A}\right)\cdot f_2-\sigma'_{v;d;0}=0 \tag{84}$$

Application of soil with multiple layers:

In reality we are dealing with multiple layer soil system. Therefore the above formula should be adjusted for multiple layer case system. An additional term should be used in the above formula because the vertical effective stress in layer i should be decreased by the shaft friction that is mobilized up to the layer $i-1$. This term takes into account the reduction of effective stress due to shaft friction acting at a higher level.

$$\sigma'_{v;d;i;2}=\sigma'_{v;d;i;0}-\frac{O_p\cdot\alpha_t\cdot d_i\left(f_{1;i}\cdot f_{2;i}\cdot q_{c;d;i}+\sum_{n=0}^{i-1}f_{1;n}\cdot f_{2;n}\cdot q_{c;d;n}\right)}{A} \tag{85}$$

In which:

Layer i layer for which the shaft friction is calculated;

Layer i-1 layer located above layer i

This requires a method which the calculation process is started from the highest layer, and no shaft friction is still mobilized.

The system of equations given above can be solved by iteration, but it is easier to use the following formula:

$$f_{2;i}=\frac{-M_i+\sqrt{M_i^{\,2}+4\cdot\sigma'_{v;d;i;0}\left(\sigma'_{v;d;i;0}-\sum_{n=0}^{i-1}T_{d;n}\right)}}{2\sigma'_{v;d;i;0}} \tag{86}$$

In which:

$$M_i = \frac{f_{1;i} \cdot O_p \cdot \alpha_t \cdot q_{c;d;i} \cdot d_i}{A} \tag{87}$$

$$T_i = M_i \cdot f_{2;i} \tag{88}$$

The shaft friction in layer i is calculated using:

$$p_{r;d;i} = f_{1;i} \cdot f_{2;i} \cdot \alpha_t \cdot q_{c;d;i} \tag{89}$$

The area over which the stress spreads out around a pile within a pile group is limited to the area covering half of the distance between center lines to the next piles. The following formula is used for this concept; (see figure 78):

$$A = \left(\tfrac{1}{2} Y_2 + \tfrac{1}{2} Y_1\right) \cdot X - A_{pile} \tag{90}$$

In which:

A Spreading area around the pile in [m²];

Y_1 Distance between center lines to the first neighboring row of piles in [m];

Y_2 Distance between center lines in the direction normal to the row of piles in [m];

A_{pile} Area of the cross section of the pile in [m²];

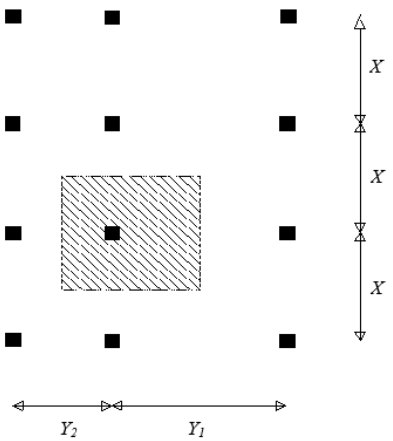

FIGURE 78: AREA OF INFLUENCE OF A PILE

The calculation can take place in this manner under the condition that the distances X and Y are such that the ratio between X and Y may not be greater than 2, otherwise the formula for a random pile pattern should be used;

For a regular pile pattern:

$$A = \left(\text{spacing}\right)^2 - A_{pile} \tag{91}$$

For a random pile pattern (see next figures 79 and 80):

$$A_\beta = \pi \cdot R_\beta^2 - A_{pile} \tag{92}$$

$$R_\beta = \sqrt{\frac{A_{segment} \cdot 360/\alpha}{\pi}} \tag{93}$$

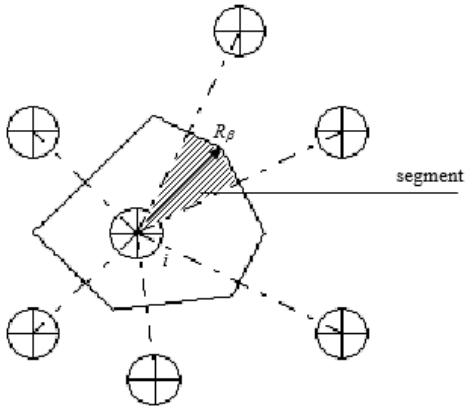

FIGURE 79: DETERMINATION AREA OF INFLUENCE OF PILE IN RANDOM ARRANGEMENT

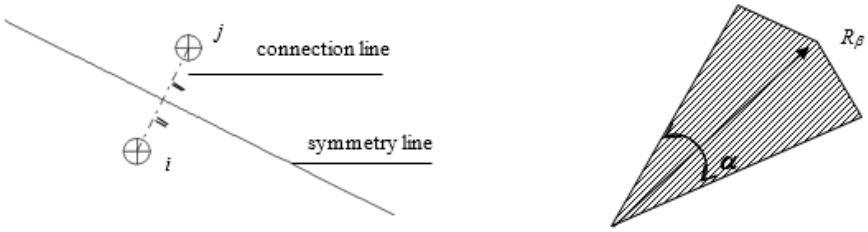

FIGURE 80: CONSTRUCTION OF SYMMETRY LINE AND SEGMENT FOR RANDOM PILE

B.3 CONCLUSIONS

Single pile:

Based on CUR report 2001-4; the used method to calculate the bearing capacity of micro-piles is divided into two different types considering a single pile and group of piles. The method is in general for pile groups but by ignoring set of factors will result in procedure calculation for single pile. Considering a single micro-pile, its capacity for tensional loads is equal to integration of perimeter of the pile multiplied with shaft friction in tension at depth z.

For this calculation the perimeter of the micro-pile is taken into account which is an important factor. Frictional tension of micro-pile body is related to design value of CPT diagram which is corrected for some factors. Also to compute frictional tension a coefficient of α is taken into account which considers the installation method. Wide range of values for this coefficient is a powerful meaning to consider densification or loosening of soil due to performed installation method. It should be noted that effect of α will be much more when constructing piles in clay. So the difference between CPT results is not the only difference and therefore soil type should be also considered.

Pile in pile group:

For a pile in a pile group two additional factors are added to consider the effect of being in a group. These factors are used to calculate bearing capacity under tensional loads (a reduction) and densification effect of adjacent pile installation (an increase). These factors are only valid for sand layers. When the soil is over-consolidated, only the over-consolidation ratio is used to correct the cone resistance but when there is an excavation, based on the degree of its effect on strength of soil, cone resistance is reduced.

Next step is determination of a design value for cone resistance. Its first part is considering the effect of redistribution capacity of related structure. Flexibility or rigidity of structure will determine how forces transfer from a weak to strong foundation element. Also more CPT provides more knowledge about the soil and leads to a better estimation. There are two other factors; one accounting for pile material and the other one for load variations. The effect of pile material is straight forward but load variations and its different effects should be addressed clearly. Dynamic or cyclic types of loading and occurrence of stress reversal and its effect on strength characteristics of soil specimen is much more complicated than determining a simple factor. Uplift caused by liquefaction as result of dynamic or cyclic loads is of great concern which should be also considered.

After determination of design value for cone resistance, effect of installation on densification is considered using a factor called f_1. This factor is an exponential function of relative density increase. Increase in relative density is dependent on limit values of void ratio (min and max), initial value of void ratio and distance of adjacent micro-piles. For loose specimen the effect will be considerable and also when the adjacent piles are near the calculated pile the coefficient will increase. Cone resistance and soil stress are effective in calculation of f_1. The important point is that only the distance and the number of piles are considered while the geometry and dimension could have significant importance on stress redistribution and densification in three dimensions which is not considered in this calculation.

Next step is to calculate f_2. f_2 is calculated based on f_1 and also after applying tensional load which reduces the bearing capacity of micro-piles due to effect of tensile loading. Magnitude of factor f_2 is used to determine the value of decrease in capacity by doing a recurring relationship in which this factor for each layer is dependent on previous layer.

After calculation of all parameters a simple equation is used to calculate the overall amount of bearing capacity.

In the last step of this study the geometry of mechanisms is effectively considered only to calculate the weight of soil which is an ultimate value for capacity of mechanism because if the pull out resistance is enough, the shaft will fail totally and therefore it requires the mass of soil to be displaced. So the volume of soil and its weight is calculated to assure that the capacity is not overestimated.

Below, a limited summation is given of the aspects which are not sufficiently investigated in the present calculation rule:

- The factor α_t is determined based on test loads; it appears that a number of properly documented test loads, especially per pile type is limited, and that a distinction is often not made between single piles and piles in a pile group, which makes it unclear if densification caused by the installation of surrounding piles has taken place;

- By using the factor f_1, the effect of densification due to the installation of soil displacement piles is taken into account. The effect of increasing the stresses in the soil is not taken into account separately.

- The factor α_t for tensional piles in cohesive soil types should be determined by carrying out test loads.

C INTERNATIONAL DESIGN BEARING CAPACITY OF SINGLE PILE

C.1 API (2010)

First sand layer

Beta	0.37	
f(max)	81	kN/m2

Second sand layer

Beta	0.46	
f(max)	96	kN/m2
A(shaft)	0.314	m^2

TABLE 42: DESIGN BEARING CAPACITY FOR PILE IN FIRST SAND LAYER ACCORDING TO API (2010)

P'_0 [kPa]	f_s =< 81 [kN/m²]	Shaft capacity [kN]
82	30.34	10
87	32.19	20
92	34.04	30
97	35.89	42
102	37.74	53
107	39.59	66
112	41.44	79
117	43.29	93
122	45.14	107
127	46.99	121
132	48.84	137

TABLE 43: DESIGN BEARING CAPACITY OF PILE IN SECOND SAND LAYER ACCORDING TO API (2010)

P'_0 [kPa]	f_s=< 96 [kN/m²]	Shaft capacity [kN]
128.1	58.93	19
133.1	61.23	38
138.1	63.53	58
143.1	65.83	78
148.1	68.13	100
153.1	70.43	122
158.1	72.73	145
163.1	75.03	168
168.1	77.33	193
173.1	79.63	218
178.1	81.93	243

C.2 UWA (05)

Assuming close ended pile		
D_i	0	
$A_{r;eff}$	1	
f_t/f_c	0.75	Tension
f_t/f_c	1	Compression
Diameter	0.2	m
Radius	0.1	m
P_a	100	kPa
Delta y (dilation)	0.00002	m
Delta sigma'(rd)	(4G/D). Delta y	
tan(X)	0.42	
X= Interface friction angle	23	deg

TABLE 44: DESIGN BEARING CAPACITY OF PILE IN FIRST SAND LAYER ACCORDING TO UWA (05)

Depth [m+NAP]	q_{cz} [Mpa]	h [m]	$\sigma'_{v;d,j,0}$ [Mpa]	$q_{c,in}$ [-]	G/q_c [-]	G [MPa]	Delta sigma'(rd) [kPa]	q_s [kN/m²]	Shaft capacity [kN]
-12.5	1.5	5	82	16.6	23	34	13.5	7	2
-13	12	4.5	87	128.7	5	58	23.2	32	12
-13.5	19	4	92	198.1	4	67	26.6	49	28
-14	10	3.5	97	101.5	6	58	23.1	30	37
14.5	16	32	102	158.4	4	66	26.5	21	44
-15	9	2.5	107	87.0	6	58	23.4	32	53
-15.5	9	2	112	85.0	7	59	23.8	35	64
-16	3	1.5	117	27.7	15	46	18.4	16	70
-16.5	22	1	122	199.2	3	77	30.7	104	102
-17	22	0.5	127	195.2	4	78	31.2	143	147
-17.5	26	0	132	226.3	3	82	33.0	186	205

TABLE 45: DESIGN BEARING CAPACITY OF PILE IN SECOND SAND LAYER ACCORDING TO UWA (05)

Depth [m+NAP]	q_{cz} [Mpa]	h [m]	$\sigma'_{v;d,j,0}$ [Mpa]	$q_{c,in}$ [-]	G/q_c [-]	G [MPa]	Delta sigma'(rd) [kPa]	q_s [kN/m²]	Shaft capacity [kN]
-17.5	26	5	128.1	229.7	3	82	32.6	60	19
-18	29	4.5	133.1	251.3	3	85	34.0	69	41
-18.5	31	4	138.1	263.7	3	88	35.0	77	65
-19	26	3.5	143.1	217.3	3	85	34.0	70	87
-19.5	35	3	148.1	287.6	3	93	37.1	98	118
-20	34	2.5	153.1	274.7	3	93	37.3	104	150
-20.5	35	2	158.1	278.3	3	95	38.0	118	187
-21	33	1.5	163.1	258.4	3	95	37.9	127	227
-21.5	30	1	168.1	231.3	3	94	37.4	140	271
-22	17	0.5	173.1	129.2	5	82	32.8	113	307
-22.5	39	0	178.1	292.2	3	102	40.8	276	394

C.3 ICP (05)

a	1	
b	0.8	
P_{ref}	100	kPa
R_i	0	close ended piles
R*	0.1	m
Delta sigma' (rd)	same as UWA (05)	(4G/D). Delta y
tan X	0.42	
X= Interface friction angle	22	deg

TABLE 46: DESIGN BEARING CAPACITY FOR THE PILE IN FIRST SAND LAYER ACCORDING TO ICP (05)

Depth [m+NAP]	q_{cz} [Mpa]	$\sigma'_{v;d,j,0}$ [Mpa]	h [m]	Delta sigma'(rd) [kPa]	q_s [kN/m²]	Shaft capacity [kN]
-12.5	1.5	82	5	13.5	9	3
-13	12	87	4.5	23.2	37	14
-13.5	19	92	4	26.6	56	32
-14	10	97	3.5	23.1	35	43
14.5	16	102	32	26.5	29	52
-15	9	107	2.5	23.4	36	63
-15.5	9	112	2	23.8	38	75
-16	3	117	1.5	18.4	18	81
-16.5	22	122	1	30.7	105	114
-17	22	127	0.5	31.2	113	150
-17.5	26	132	0	33.0	133	191

TABLE 47: DESIGN BEARING CAPACITY FOR THE PILE IN SECOND SAND LAYER ACCORDING TO ICP (05)

Depth [m+NAP]	q_{cz} [Mpa]	$\sigma'_{v;d,j,0}$ [Mpa]	h [m]	Delta sigma'(rd) [kPa]	q_s [kN/m²]	Shaft capacity [kN]
-17.5	26	128.1	5	32.6	73	23
-18	29	133.1	4.5	34.0	83	49
-18.5	31	138.1	4	35.0	92	78
-19	26	143.1	3.5	34.0	83	104
-19.5	35	148.1	3	37.1	114	140
-20	34	153.1	2.5	37.3	119	177
-20.5	35	158.1	2	38.0	132	219
-21	33	163.1	1.5	37.9	138	262
-21.5	30	168.1	1	37.4	146	308
-22	17	173.1	0.5	32.8	95	338
-22.5	39	178.1	0	40.8	203	402

C.4 FHWA

Type B

Alfa, 1st sand	90	kN/m2
Alfa, 2nd sand	340	kN/m2
Diameter	0.2	m
Length of grout	5	m
Factor of safety	1	Single pile
Factor of safety	2	Pile groups

$$P_{G-allowable} = \frac{\alpha_{bond}}{FS} \times \pi \times D_b \times L_b \tag{94}$$

TABLE 48: DESIGN CAPACITY FOR PILE IN FIRST AND SECOND SAND LAYER ACCORDING TO FHWA

	$P_{(G,allowable)}$ [kN]	Ratio to field test [%]
First sand layer	283	75
Second sand layer	1068	76

D DETAILED ANALYTICAL CALCULATION

Below the used parameter and values for the calculation of design bearing capacity of the single pile is presented. The calculations are done according to CUR 236, by using Microsoft Excel and are based on CPT data of Amsterdam case study.

- Pile type — Type A, Bored GEWI micro-pile
- Diameter of the pile — 200 mm with steel anchor of 63.5 mm
- Circumference — 0.628 m
- Pile length — Two types: 18m in first sand layer and 23m in second sand layer
- load — Static tensional load , $\gamma_{m,var}$= 1
- Ground level — NAP +0.5 m
- Excavation height — 10.8 m; effective weight of the excavated soil 78.5 kPa
- α -value — see the used values in each section
- Material factors — $\gamma_{s,t}$ = 1.25, $\gamma_{m;g}$ = 1.1, $\xi_{m,n,single}$= 1.39 (flexible) and $\xi_{m,n,group}$= 0.92 (rigid)
- $\gamma_{sat,sand}$ — 20 kN/m^3 and
- γ_{water} — 10 kN/m^3
- First sand layer: top of bearing sand layer NAP -12.5 m; original effective vertical stress at this level 82 kPa.
- Second sand layer: top of bearing sand layer NAP -17.5 m; original effective vertical stress at this level 128 kPa.

D.1 SINGLE PILE

The results of the calculation are shown in table 49 for the first sand layer and table 50 for the second sand layer. The calculations are done by applying different values of α_t and considering initially an average cone resistance without limit and later a cone resistance limited according to CUR 236.

TABLE 49: DESIGN VALUE OF BEARING CAPACITY OF A SINGLE PILE, FIRST SAND LAYER

Depth	$q_{c;z;avg;i}$	$q_{c;z;CUR}$	$F_{r;t;d}$ $\alpha_{t,\ raw}= 0.0117$	$F_{r;t;d\ CUR}$ $\alpha_{t,\ design}= 0.0122$	$F_{r;t;d,\ CUR}$ $\alpha_{t,\ lower\ bound}= 0.011$	$F_{r;t;d\ CUR}$ $\alpha_{t,\ expected}= 0.017$	$F_{r;t;d\ CUR}$ $\alpha_{t,\ fit}= 0.0167$	$F_{r;t;d}$ $\alpha_{t,\ fit}= 0.0162$
[m + N.A.P.]	[MPa]	[MPa]	[kN]	[kN]	[kN]	[kN]	[kN]	[kN]
-12.5	1.5	1.5	3	3	3	5	5	4
-13	13	13	31	32	29	45	44	42
-13.5	20	20	73	76	69	106	104	101
-14	11.5	11.5	97	101	91	141	139	135
14.5	13	13	125	130	117	181	178	173
-15	6	6	137	143	129	200	196	190
-15.5	7	7	152	159	143	221	217	211
-16	2.4	2.4	157	164	148	228	224	218
-16.5	10	10	178	186	168	259	255	247
-17	22	20	225	230	207	321	315	311
-17.5	22	20	271	274	247	382	377	377

TABLE 50: DESIGN VALUE OF BEARING CAPACITY OF A SINGLE PILE, SECOND SAND LAYER

Depth	$q_{c;z;avg;i}$	$q_{c;z;CUR}$	$F_{r;t;d}$ $\alpha_{t,\ raw}= 0.0144$	$F_{r;t;d\ CUR}$ $\alpha_{t,\ design}= 0.0230$	$F_{r;t;d,\ CUR}$ $\alpha_{t,\ lower\ bound}= 0.011$	$F_{r;t;d\ CUR}$ $\alpha_{t,\ expected}= 0.017$	$F_{r;t;d\ CUR}$ $\alpha_{t,\ fit}= 0.0356$	$F_{r;t;d}$ $\alpha_{t,\ fit}= 0.0227$
[m + N.A.P.]	[MPa]	[MPa]	[kN]	[kN]	[kN]	[kN]	[kN]	[kN]
-17.5	22	20	57	83	40	61	129	90
-18	26.5	20	126	166	80	123	257	199
-18.5	30.5	20	206	249	119	184	386	324
-19	25.5	20	272	333	159	246	515	429
19.5	34.5	20	362	416	199	307	643	570
-20	33.5	20	449	499	239	369	772	708
-20.5	35.5	20	541	582	278	430	901	853
-21	35.5	20	634	665	318	492	1029	999
-21.5	36	20	727	748	358	553	1158	1147
-22	26	20	795	831	398	614	1287	1253
-22.5	38.5	20	895	914	437	676	1414	1414

D.2 PILE GROUP

D.2.1 DESIGN BEARING CAPACITY OF THE PILE WITHIN GROUP

The distance center to center of the piles are varied by 1m, 2m and 3m.

- Center to center = 1 m
- A = 0.96 m^2
- $\alpha_t = 0.0230$
- $f_1 = 1$

TABLE 51: DETERMINATION OF DESIGN BEARING CAPACITY FOR 1 M PILE SPACING

Depth [m + N.A.P]	$q_{c;z;exc}$ [MPa]	$q_{c;z;CUR}$ [MPa]	$q_{c;d}$ [MPa]	γ'_d [kN/m^3]	M_i [kPa]	$\sigma'_{v;d,j,0}$ [kPa]	$f_{2;i}$ [-]	T_{i-1} [kPa]	ΣT_{i-1} [kPa]	$F_{r;tension;d}$ [kN]
-12.5	7.5	7.5	6.52	8.2	49.06	82	-	-	-	-
-13	13	13	11.30	8.2	85.04	86.1	0.628	53.4	53.4	51
-13.5	13	13	11.30	8.2	85.04	90.2	0.335	28.5	81.9	79
-14	16	16	13.91	8.2	104.67	94.3	0.124	13.0	94.9	91
14.5	3	3	2.61	8.2	19.63	98.4	0.157	3.1	98	94
-15	6.5	6.5	5.65	8.2	42.52	102.5	0.120	5.1	103.1	99
-15.5	3.5	3.5	3.04	8.2	22.90	106.6	0.145	3.3	106.4	102
-16	2.5	2.5	2.17	8.2	16.35	110.7	0.176	2.9	109.3	105
-16.5	8.5	8.5	7.39	8.2	55.60	114.8	0.111	6.2	115.4	111
-17	9	9	7.83	8.2	58.88	118.9	0.081	4.7	120.2	115
-17.5	25	20	17.39	8.2	130.83	123	0.036	4.7	124.9	120
-18	30.5	20	17.39	8.2	130.83	127.1	0.032	4.1	129.0	124
-18.5	25	20	17.39	8.2	130.83	131.2	0.031	4.1	133.1	128
-19	28	20	17.39	8.2	130.83	135.3	0.031	4.1	137.2	132
-19.5	23.5	20	17.39	8.2	130.83	139.4	0.031	4.1	141.3	136
-20	30.9	20	17.39	8.2	130.83	143.5	0.031	4.1	145.4	140
-20.5	36.4	20	17.39	8.2	130.83	147.6	0.031	4.1	149.5	144
-21	36.4	20	17.39	8.2	130.83	151.7	0.031	4.1	153.6	147
-21.5	31.1	20	17.39	8.2	130.83	155.8	0.031	4.1	157.7	151
-22	31.1	20	17.39	8.2	130.83	159.9	0.031	4.1	161.8	155
-22.5	28.5	20	17.39	8.2	130.83	164	0.031	4.1	165.9	159

- Center to center = 2 m
- A = 3.96 m^2
- $\alpha_t = 0.0230$
- $f_l = 1$

TABLE 52: DETERMINATION OF DESIGN BEARING CAPACITY FOR 2 M PILE SPACING

Depth [m + N.A.P]	$q_{c;z;exc}$ [MPa]	$q_{c;z;CUR}$ [MPa]	$q_{c;d}$ [MPa]	γ'_d [kN/m3]	M_i [kPa]	$\sigma'_{v;d,j,0}$ [kPa]	$f_{2;i}$ [-]	T_{i-1} [kPa]	ΣT_{i-1} [kPa]	$F_{r;tension;d}$ [kN]
-12.5	7.5	7.5	6.52	8.2	11.9	82	-	-	-	-
-13	13	13	11.30	8.2	20.6	86.1	0.890	18.3	18.3	73
-13.5	13	13	11.30	8.2	20.6	90.2	0.790	16.3	34.6	137
-14	16	16	13.91	8.2	25.4	94.3	0.679	17.2	51.9	205
-14.5	3	3	2.61	8.2	4.8	98.4	0.672	3.2	55.1	218
-15	6.5	6.5	5.65	8.2	10.3	102.5	0.640	6.6	61.7	244
-15.5	3.5	3.5	3.04	8.2	5.6	106.6	0.632	3.5	65.2	258
-16	2.5	2.5	2.17	8.2	4.0	110.7	0.632	2.5	67.7	268
-16.5	8.5	8.5	7.39	8.2	13.5	114.8	0.593	8.0	75.7	300
-17	9	9	7.83	8.2	14.3	118.9	0.556	7.9	83.6	331
-17.5	25	20	17.39	8.2	31.7	123	0.463	14.7	98.3	389
-18	30.5	20	17.39	8.2	31.7	127.1	0.381	12.1	110.4	437
-18.5	25	20	17.39	8.2	31.7	131.2	0.312	9.9	120.3	476
-19	28	20	17.39	8.2	31.7	135.3	0.256	8.1	128.4	508
-19.5	23.5	20	17.39	8.2	31.7	139.4	0.212	6.7	135.1	535
-20	30.9	20	17.39	8.2	31.7	143.5	0.180	5.7	140.8	558
-20.5	36.4	20	17.39	8.2	31.7	147.6	0.159	5.0	145.9	578
-21	36.4	20	17.39	8.2	31.7	151.7	0.146	4.6	150.5	596
-21.5	31.1	20	17.39	8.2	31.7	155.8	0.138	4.4	154.9	613
-22	31.1	20	17.39	8.2	31.7	159.9	0.133	4.2	159.1	630
-22.5	28.5	20	17.39	8.2	31.7	164	0.131	4.1	163.2	646

- Center to center = 3 m
- A = 8.96 m^2
- α_t= 0.0230
- f_1= 1

TABLE 53: DETERMINATION OF DESIGN BEARING CAPACITY FOR 3 M PILE SPACING

Depth [m + N.A.P]	$q_{c;z;exc}$ [MPa]	$q_{c;z;CUR}$ [MPa]	$q_{c;d}$ [MPa]	γ'_d [kN/m3]	M_i [kPa]	$\sigma'_{v;d,j,0}$ [kPa]	$f_{2;i}$ [-]	T_{i-1} [kPa]	ΣT_{i-1} [kPa]	$F_{r;tension;d}$ [kN]
-12.5	7.5	7.5	6.52	8.2	5.3	82	-	-	-	-
-13	13	13	11.30	8.2	9.1	86.1	0.950	8.7	8.7	78
-13.5	13	13	11.30	8.2	9.1	90.2	0.904	8.2	16.9	151
-14	16	16	13.91	8.2	11.2	94.3	0.852	9.6	26.4	237
-14.5	3	3	2.61	8.2	2.1	98.4	0.848	1.8	28.2	253
-15	6.5	6.5	5.65	8.2	4.6	102.5	0.833	3.8	32.0	287
-15.5	3.5	3.5	3.04	8.2	2.5	106.6	0.829	2.0	34.1	305
-16	2.5	2.5	2.17	8.2	1.8	110.7	0.828	1.5	35.5	318
-16.5	8.5	8.5	7.39	8.2	6.0	114.8	0.809	4.8	40.3	361
-17	9	9	7.83	8.2	6.3	118.9	0.791	5.0	45.3	406
-17.5	25	20	17.39	8.2	14.0	123	0.744	10.4	55.7	499
-18	30.5	20	17.39	8.2	14.0	127.1	0.702	9.8	65.6	588
-18.5	25	20	17.39	8.2	14.0	131.2	0.662	9.3	74.9	671
-19	28	20	17.39	8.2	14.0	135.3	0.625	8.8	83.6	749
-19.5	23.5	20	17.39	8.2	14.0	139.4	0.592	8.3	91.9	824
-20	30.9	20	17.39	8.2	14.0	143.5	0.561	7.9	99.8	894
-20.5	36.4	20	17.39	8.2	14.0	147.6	0.532	7.5	107.2	961
-21	36.4	20	17.39	8.2	14.0	151.7	0.506	7.1	114.3	1025
-21.5	31.1	20	17.39	8.2	14.0	155.8	0.482	6.8	121.1	1085
-22	31.1	20	17.39	8.2	14.0	159.9	0.461	6.5	127.6	1143
-22.5	28.5	20	17.39	8.2	14.0	164	0.441	6.2	133.7	1198

D.2.2 SOIL PLUG PULL-OUT FORCE, $F_{R;T;D,MAX}$

			1 m	2 m	3 m
Case 1	Angle: 45 (deg)	Cone height (m)	1	2	3
Case 2	Angle:21.3 (deg)	Cone height (m)	2.56	5.13	7.69

Note: The total length of all piles are 12 m and the angle of internal friction is 32 deg.

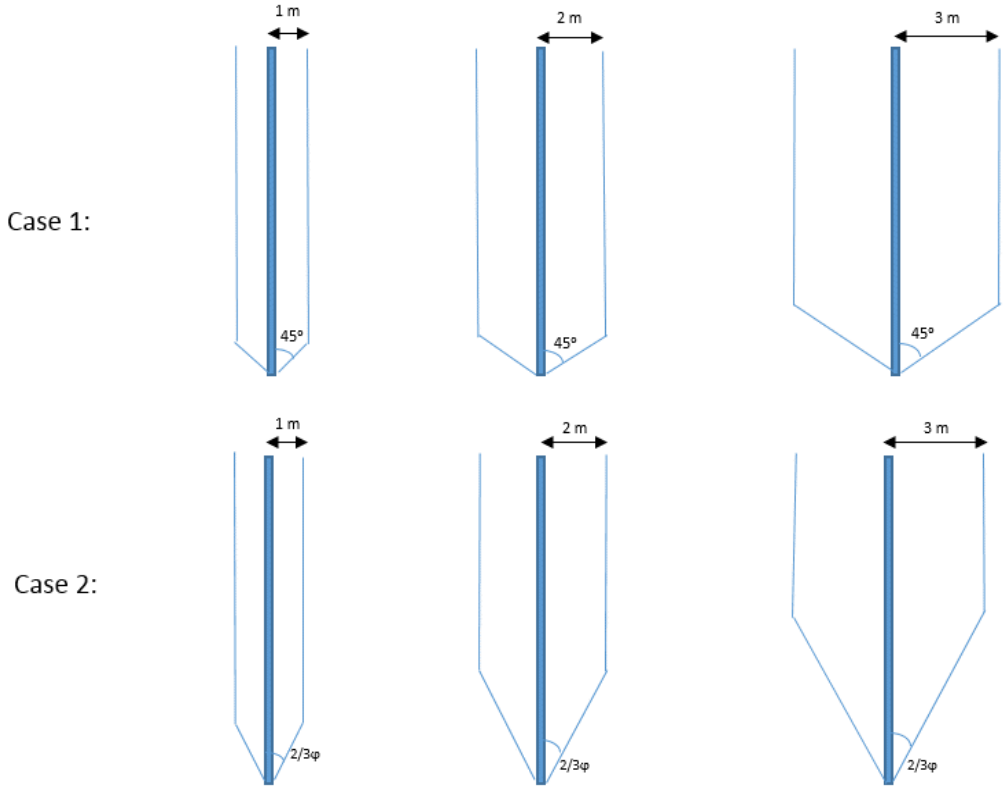

FIGURE 81: LAY-OUT OF THE PILES WITH DIFFERENT PILE SPACING FOR TWO MENTIONED CASES

1 m:

TABLE 54: SOIL PLUG PULL-OUT FORCE FOR TWO CASES AND 1 M PILE SPACING

Case number	Cone height [m]	Cylinder height [m]	V_cone [m^3]	V_cylinder [m^3]	γ'_d [kN/m^3]	$F_{r;t;d,max}$ [kN]
1	1	11	1.047	34.55	8.2	291
2	2.56	9.44	2.68	29.65	8.2	265

2 m:

TABLE 55: SOIL PLUG PULL-OUT FORCE FOR TWO CASES AND 2 M PILE SPACING

Case number	Cone height [m]	Cylinder height [m]	V_cone [m^3]	V_cylinder [m^3]	γ'_d [kN/m^3]	$F_{r;t;d,max}$ [kN]
1	2	10	8.37	125.66	8.2	1099
2	5.13	6.87	21.48	86.33	8.2	884

3 m:

TABLE 56: SOIL PLUG PULL-OUT FORCE FOR TWO CASES AND 3 M PILE SPACING

Case number	Cone height [m]	Cylinder height [m]	V_cone [m^3]	V_cylinder [m^3]	γ'_d [kN/m^3]	$F_{r;t;d,max}$ [kN]
1	3	9	28.27	254.46	8.2	2318
2	7.69	4.31	72.47	121.86	8.2	1593

E AXISYMMETRIC APPROXIMATION

Axisymmetric analysis represents a circular pile scenario in which the pile is modelled as a cluster of volume elements for the bounded part and from Node to Node anchor element for the un-bounded length of the pile. Soil is modelled around and below of the pile and the boundary conditions are chosen in the way that it does not affect the final results. The horizontal domain is 30 meters. Pile and soil are modelled based on 15-noded triangular elements. An advantage of using an axisymmetric approximation is that the installation effect could be also included which considered to be an important section regarding the modeling of the pile.

E.1 SOIL PROFILE AND PROPERTIES

The soil profile and properties including the used parameters for the model pile analysis in Plaxis are shown in table 57. For the modeling soil behavior, it is used from Hardening soil with small stiffness (HSs) in which the values and properties are already described in section 7.3.1 in the main part of the report.

TABLE 57: SOIL PROFILE AND PROPERTIES FOR MODEL PILE

Layer Number	Soil type	Top Level Layer (m NAP)	$\gamma_{dry}(\frac{kN}{m^3})$	$\gamma_{sat}(\frac{kN}{m^3})$	φ (deg)
L1	Sandy fill	+0.6	17	19	28
L2	Dutch Peat	-2.9	10.5	10.5	17
L3	Clay deposits	-4.5	16.5	16.5	25
L4	Base Peat	-10.0	12	12	18
L5	1st Sand Layer	-12.5	18	20	32
L6	Clayey/Silty Sand	-15.0	18.5	18.5	28
L7	2nd Sand Layer	-17.5	18	20	32

E.2 BOUNDARY CONDITIONS

Boundary conditions of the model is according to next figure 82. It can be seen from the figure that $u_x = u_y = 0$ for the bottom of the model and for the sides, only u_x is assigned to 0.

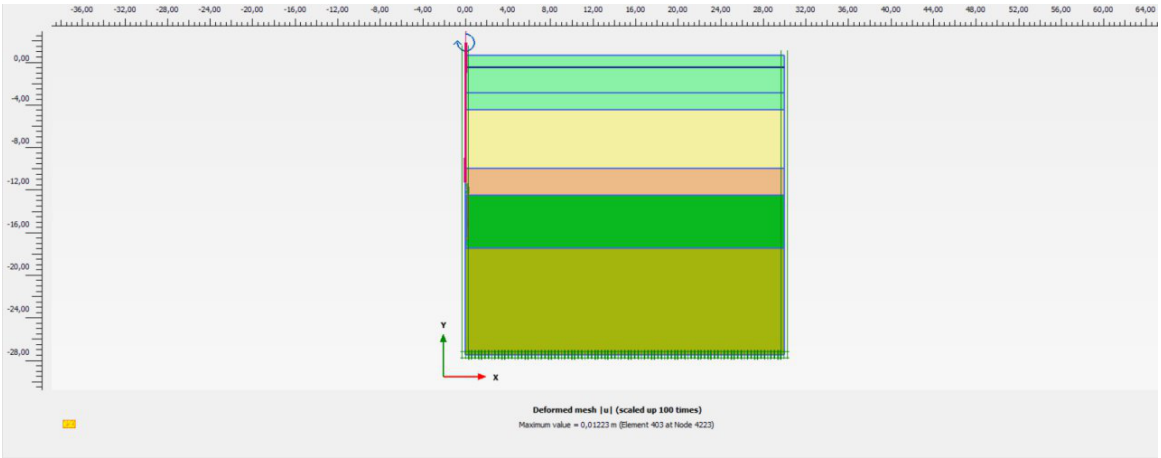

FIGURE 82: MODEL BOUNDARY CONDITIONS

E.3 PILE PROPERTIES

The axial stiffness of the pile which is the resistance against elongation, is formed by EA of the anchor. The resistance of the grout body (concrete) against tension loading and elongation is limited and upon loading of the anchor, tensile cracks will occur over the whole length of the grout. For the axial stiffness of the anchor body the value of the steel stiffness is used and for the grout area the stiffnesses are calculated based on sensitivity analysis which can be found in table 58.

For axisymmetric approximation, grout part of the pile is modelled as a cluster of volume elements (linear elastic non-porous concrete) which provides a possibility to consider the effects of installation due to grout pressurizing and the free length of the pile is modelled by using node to node anchor element.

Next table 58 shows the used values for the pile model and figure 83 illustrates the pile model for first sand layer in Plaxis.

TABLE 58: MODEL PILE PROPERTIES

Layer type	Total length [m]	Radius from x-axis [m]	Stiffness [kPa]
First sand	5	0.1	21.0e6
Second sand	5	0.1	21.0e6
Un-bounded length (steel)	13/ 18	0.001	210.0e6

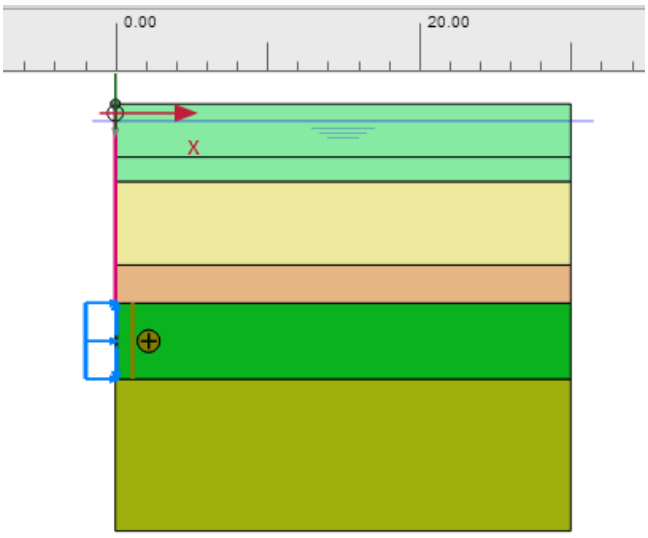

FIGURE 83: AXISYMMETRIC PILE MODEL FOR FIRST SAND LAYER IN PLAXIS

Interface:

For the modeling of the pile in axisymmetric condition, it has been used from interface elements to model the interaction between the volume element (pile) and soil body. Since only the grout area has zone of interaction with surrounding soil, only this part is activated with interface elements (see figure 83).

The roughness of the interaction is modelled by choosing a suitable value for the strength reduction factor R_{inter}. Each interface has assigned to it a "virtual thickness" which is an imaginary dimension used to define the material properties of the interface. The higher the virtual thickness is, the more elastic deformations are generated. (Plaxis 2D manual).

For free length of the pile R_{inter} is assigned to 0.1 and for the grout part which is 5 meter, it is chosen to be rigid (R_{inter} =1). Rigid means that there is no reduction of strength and stiffness and pile is assumed to be stiff in this part.

E.4 GENERATION OF MESH

For the generation of mesh in Plaxis it could be used from the mesh sizes of very fine to very coarse dependent on the needed accuracy. Here it has been used from fine mesh size to evaluate the results.

E.5 MODELLING PHASES AND DESCRIPTION

The model pile is made based on the previous explained properties and elements. For including the installation effect due to pressurizing for the grout part, it has been chosen for increasing the radial stresses by applying line loads in this part.

The calculation is done in 3 phases.

Phase 1: Initial condition

In this part the generation of the initial stresses is defined. For initial stress it is used from the procedure of K_0. K_0 is the lateral earth pressure coefficient at rest.

$$\sigma'_{h0} = K_0 . \sigma'_{v0} \quad \text{with} \quad K_0 = K_{0;NC} \, . OCR^{0.5} \qquad \text{(95) and (96)}$$

For NC soils:
$$K_0^{NC} = 1 - Sin\varphi \qquad (97)$$

For OC soils:
$$K_0 = K_0^{NC} \times OCR - \frac{\nu ur}{1-\nu ur}(OCR - 1) + \frac{K_0^{NC} \times POP - \frac{\nu ur}{1-\nu ur} \times POP}{\sigma'^0_{yy}} \qquad (98)$$

Which;

OCR= Over consolidation ratio, POP= pre-overburden ratio, V_{ur} = Poisson ratio for unloading-reloading and σ'^0_{yy}= in-situ vertical effective stress.

Phase 2: Inclusion of installation effect due to grouting

Here it has been tried to consider the installation effects and including them in the model because Plaxis does not consider this effect and it should be modelled properly to obtain optimal results. Due to grouting the radial stresses increases which leads to a higher anchor capacity. The installation effect is modelled based on the following steps;

- Surface load which has the same magnitude as grout pressure is activated but de-activate the volume cluster to avoid tension failure detected by Plaxis

- Activate the volume cluster while the surface loads remain activate too (this causes new equilibrium with the displaced soil around the grout part)

- De-activate the surface load and reset the displacements

Since the machine applies a pressure of around 10 bar to the soil, it is not known how much pressure is actually around the bottom 5 meter of the pile. There should be some loss due to soil resistance and therefore a lower value should be considered. Based on the performed sensitivity analysis, it has been calculated that for the first sand layer the pressure around the grout part is about 2.7 bar while this pressure is about 10 bar for the second sand layer.

Phase 3: Apply tensile load

By applying the tensile load in Plaxis, the calculation of the model pile can be started and the results will be analyzed. The load is applied by using pre-defined displacement option.

E.6 RESULTS

The final results of the model can be found in the next figures.

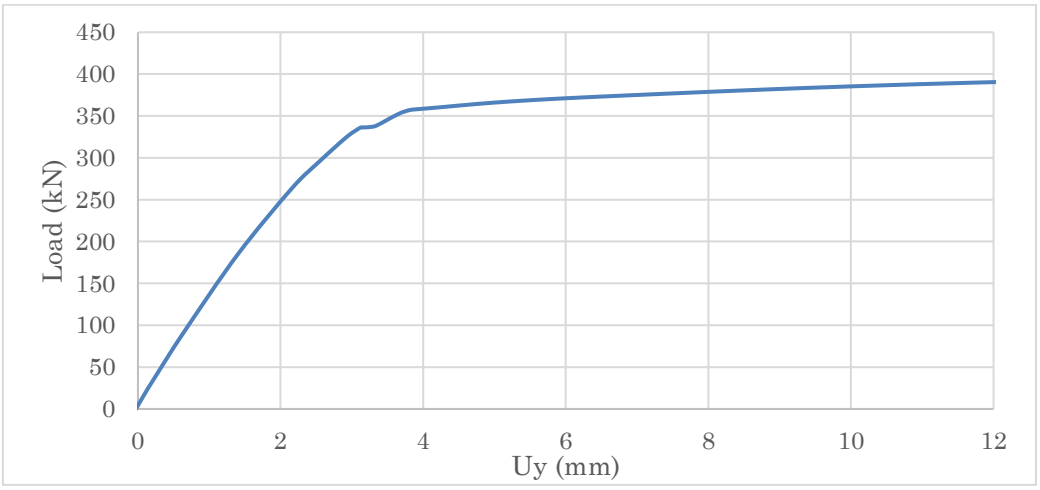

FIGURE 84: LOAD VS. DISPLACEMENT FOR PILE MODEL 18 M, AXISYMMETRIC

The final value for the tensile failure load differs only 13 kN compared to the reached value from failure test for first sand layer.

Figure 85 shows the result of load versus displacement for the pile with length of 23 m. The total tensile failure load is 1430 kN which has difference of about 1% compared to the failure value from field test for second sand layer.

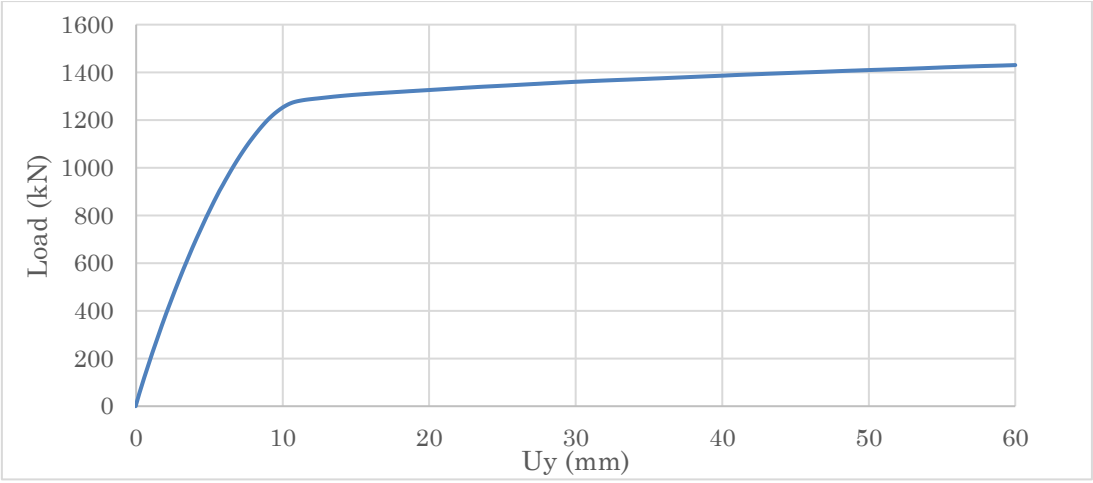

FIGURE 85: LOAD VS. DISPLACEMENT FOR PILE MODEL 23 M, AXISYMMETRIC

F FLOW CHART FOR THE DETERMINATION OF K_0

F.1 DETERMINATION OF K_0 BASED ON $K_{0,MIN}$

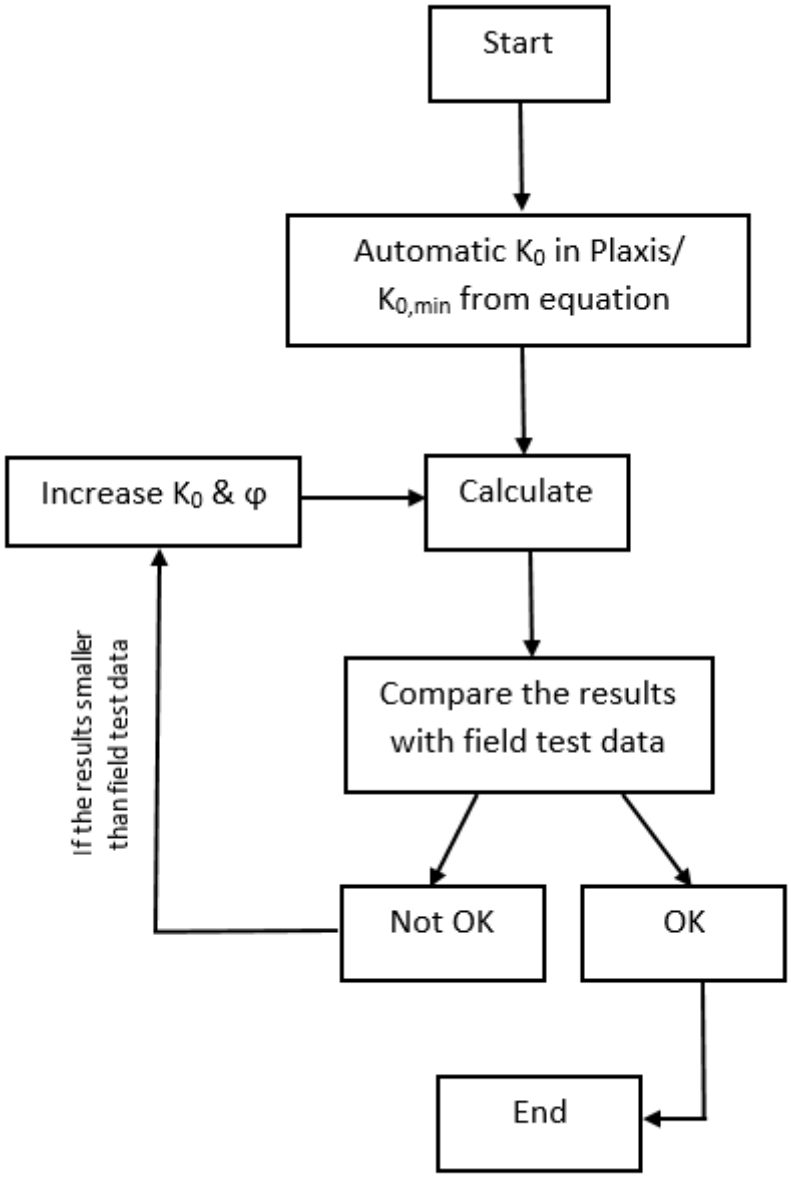

F.2 DETERMINATION OF K_0 BASED ON $K_{0,MAX}$

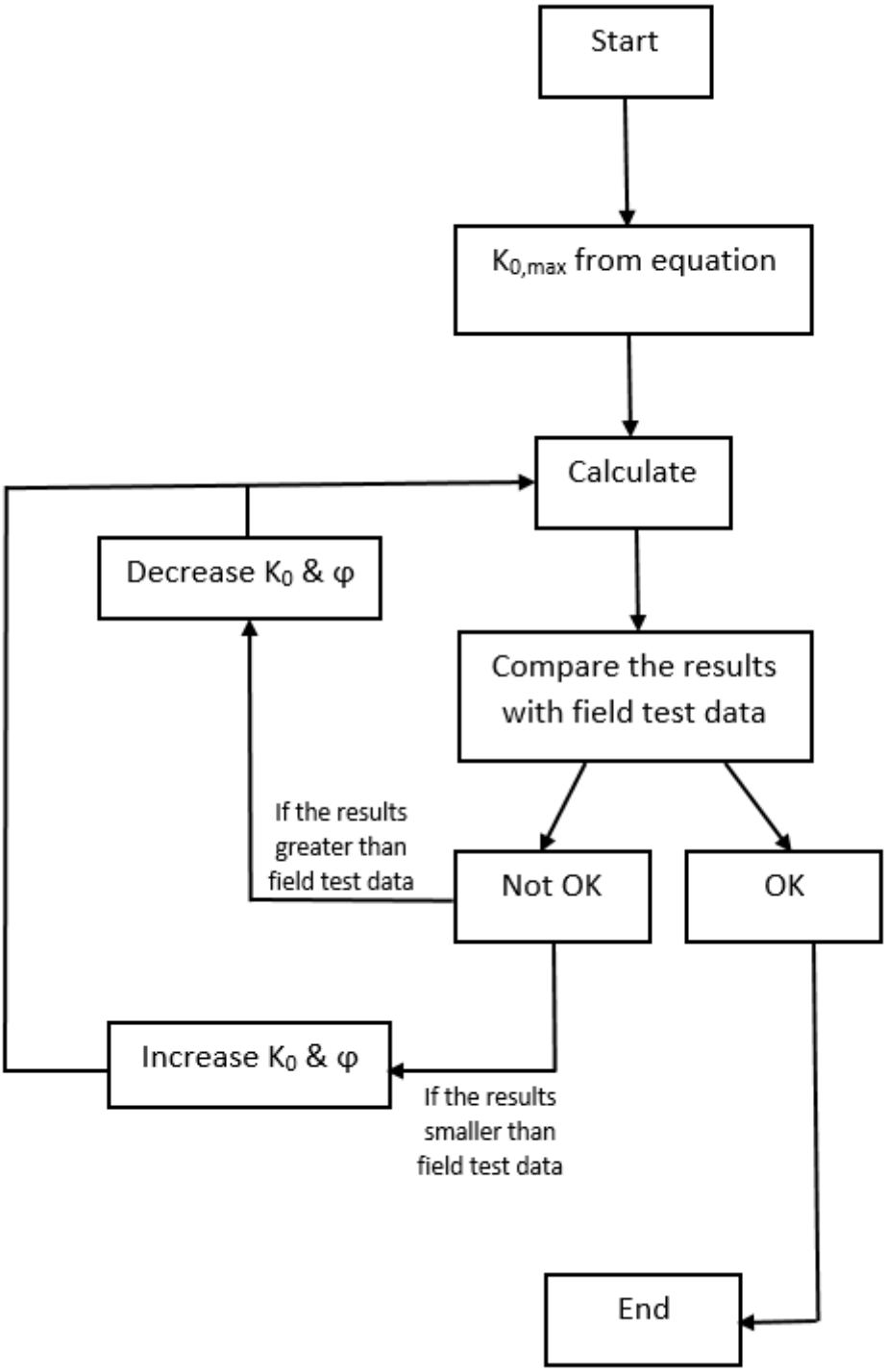

G NTN AND EBR WITH GROUT BEHAVIOR, PILE GROUP MODEL

G.1 PILE STRUCTURE AND PROPERTIES

This is the first option which is used for the modeling of the pile group. For the free length of the micro pile node to node anchor (NTN) element is used since it has a friction-less behavior and for the bounded length of the pile it is selected for embedded beam row (EBR) element with grout behavior. The used parameters and properties of the pile group model are the same as single pile model which has been already explained in section 7.3.3.1.

In single pile model, the axial resistance of the pile for two different sand layers is defined based on the parametric study. The results of the axial resistance will be further in this part used for modeling the pile as group.

Since the axial resistance of the first sand layer and the second sand layer differs, a distinction should be made. Therefore multi-linear option is chosen. Figure 86 shows the soil layering and the structure of the pile as group in Plaxis.

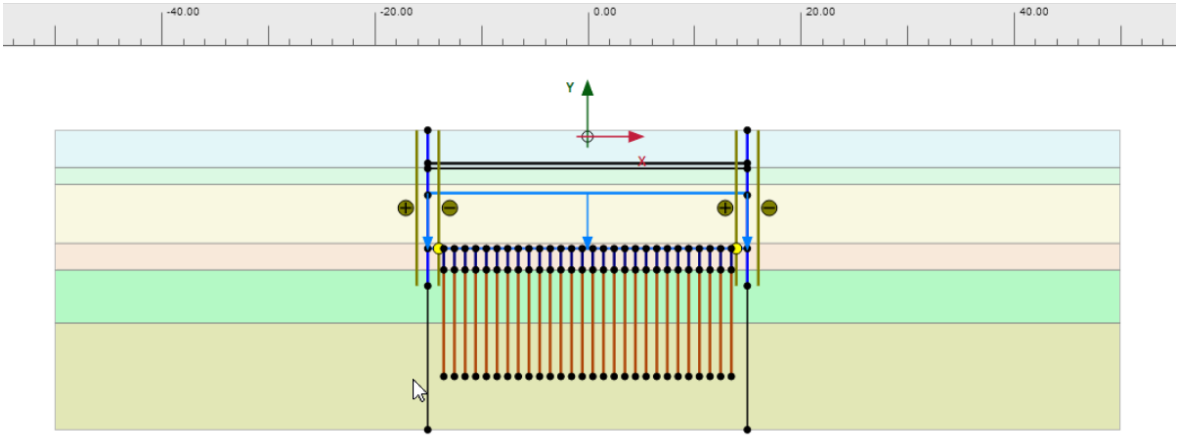

FIGURE 86: SOIL LAYERING AND THE STRUCTURE OF THE PILE AS GROUP IN EBR (OPTION 1)

For pile group model, the total length of the piles are 12 m and the grout body is 10 m long which starts from first sand layer (NAP -12.5 m) and continues until NAP -22.5 m in second sand layer. The width of the excavation is 30 m. The boundary from the center of excavation is assumed to be 50 m, far enough from model at each side to make sure that it does not influence the results. Next figure 87 shows the used mesh size for the model pile group.

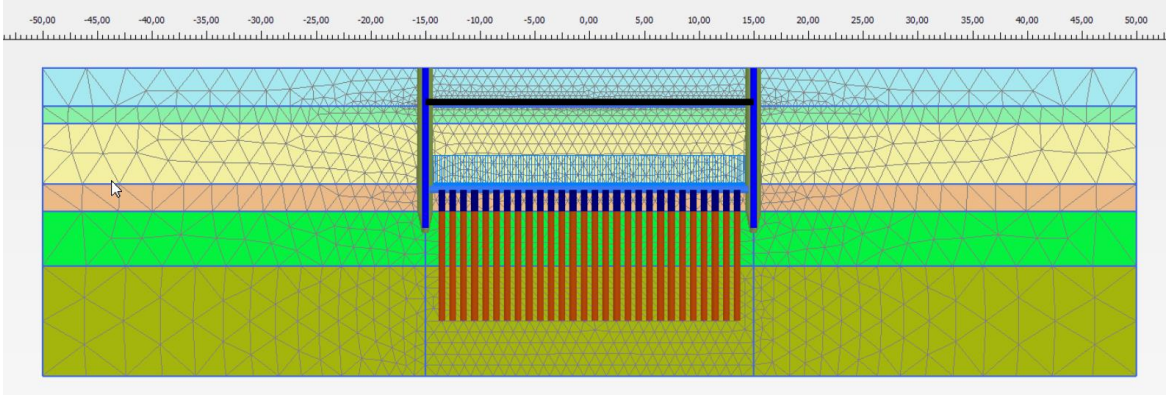

FIGURE 87: USED MESH SIZE FOR THE MODEL PILE GROUP IN EBR (OPTION 1)

G.2 CALCULATION PHASES AND DESCRIPTION

The numerical analysis is divided into 6 main phases. The phases and descriptions are the same as section 7.4.4 in the main part of report.

Figures 88 until 94 illustrate the modeling phases and constructions in EBR with grout behavior.

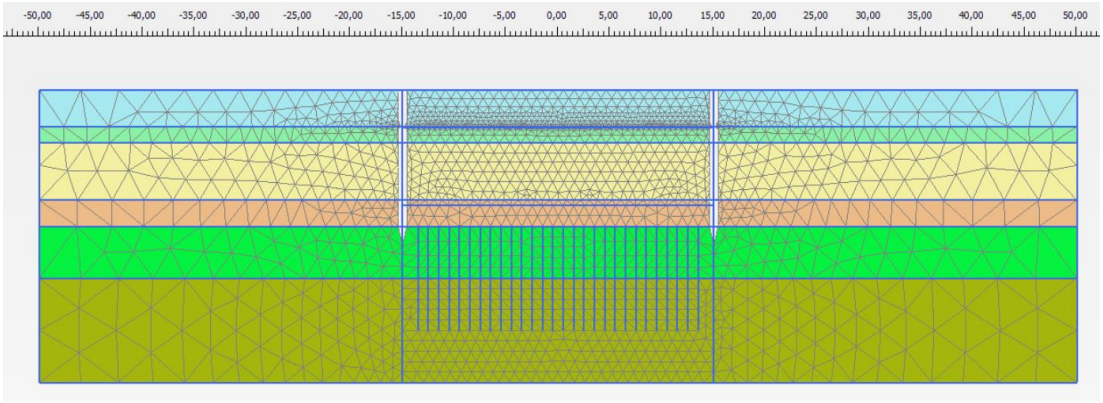

FIGURE 88: INITIAL PHASE (OPTION 1)

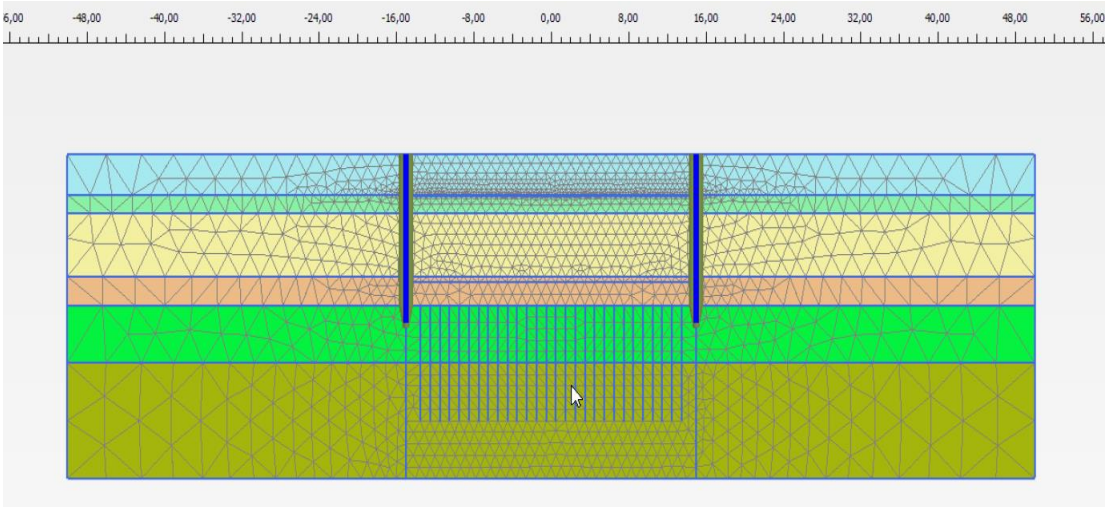

FIGURE 89: ACTIVE SHEET PILES AND INTERFACES (OPTION 1)

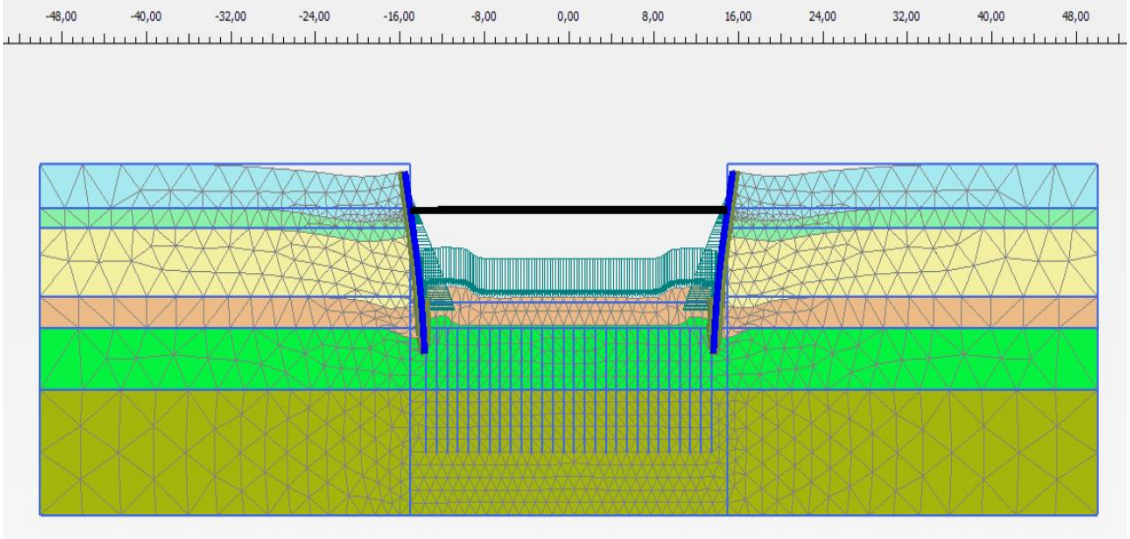

FIGURE 90: EXCAVATION AND ACTIVE STRUT (OPTION 1)

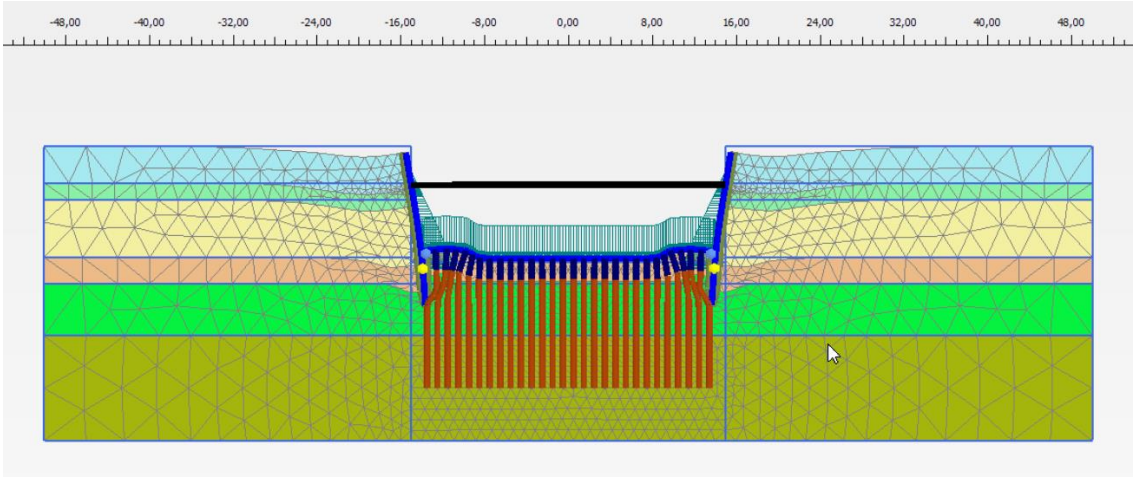

FIGURE 91: ACTIVE GROUND ANCHOR AND FOUNDATION FLOOR (OPTION 1)

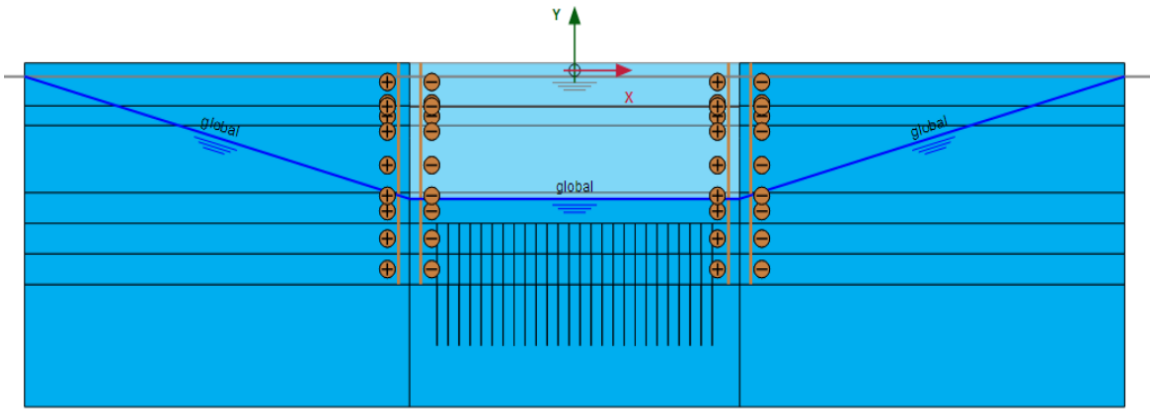

FIGURE 92: DE-WATERING (OPTION 1)

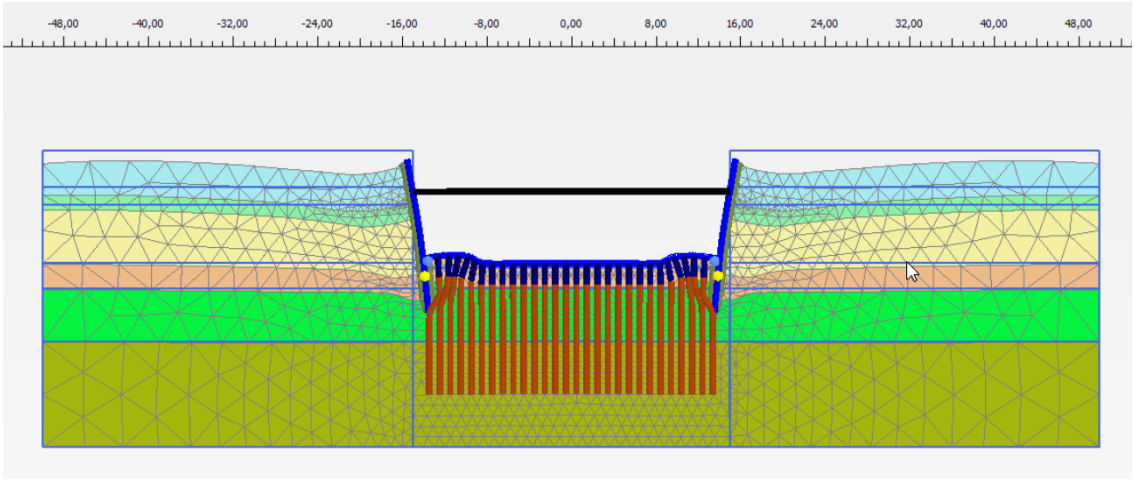

FIGURE 93: PILE GROUP MODEL AFTER DE-WATERING (OPTION 1)

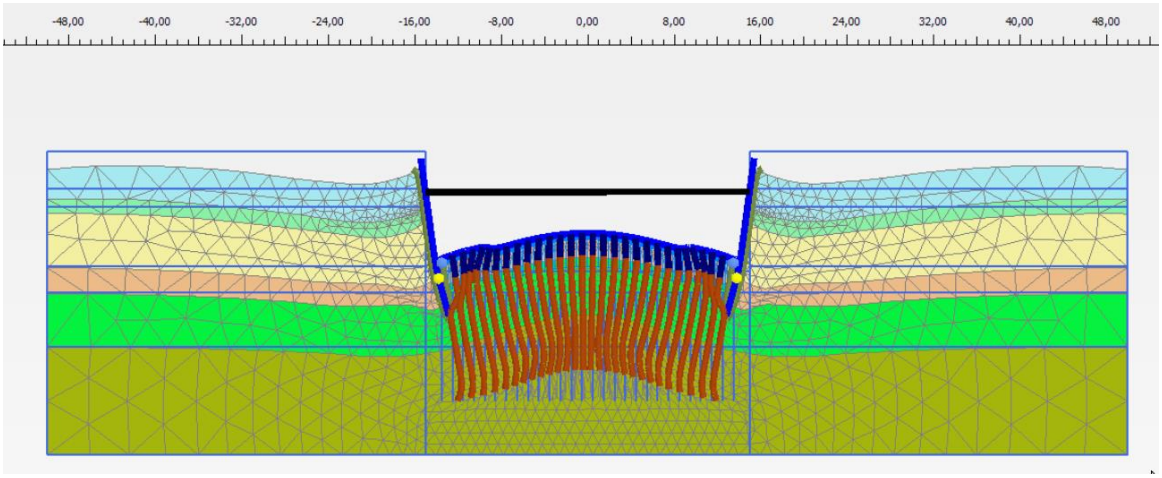

FIGURE 94: APPLYING TENSILE LOAD (OPTION 1)

In the last phase the pile group is pulled out with a tensile load of 150 kN/m^2. The load is high enough so that the failure occurs.

The piles are modelled for different pile spacing and the significance of this parameter in the group effect is evaluated. There are two failure mechanisms which can happen;

1. Pull-out of soil plug
2. Slip capacity of each individual micro pile is reached

The aim of this evaluation is to determine at what pile spacing, the above mentioned failure mechanisms take place.

G.3 RESULTS OF THE MODEL ANALYSIS

In this research the pile spacing is varied to investigate the significance of this parameter in the group effect behavior. There are three different configurations of micro pile evaluated which are 5D, 10D and 15D pile spacing installed in a construction pit with a width of 30 m.

The micro piles have a constant $L_{spacing}$ of 3 m in out-of-plane direction and only the pile spacing in x-direction varies.

a) 5D pile spacing

In this model the pile spacing is 5D which is equal to 1 m. The total vertical displacement is calculated 70.56 mm. Figure 95 shows the result of mesh change for this pile spacing. For a better visualization of the result, the shading contour and line contour of vertical displacement are provided in figure 96 and 97 respectively.

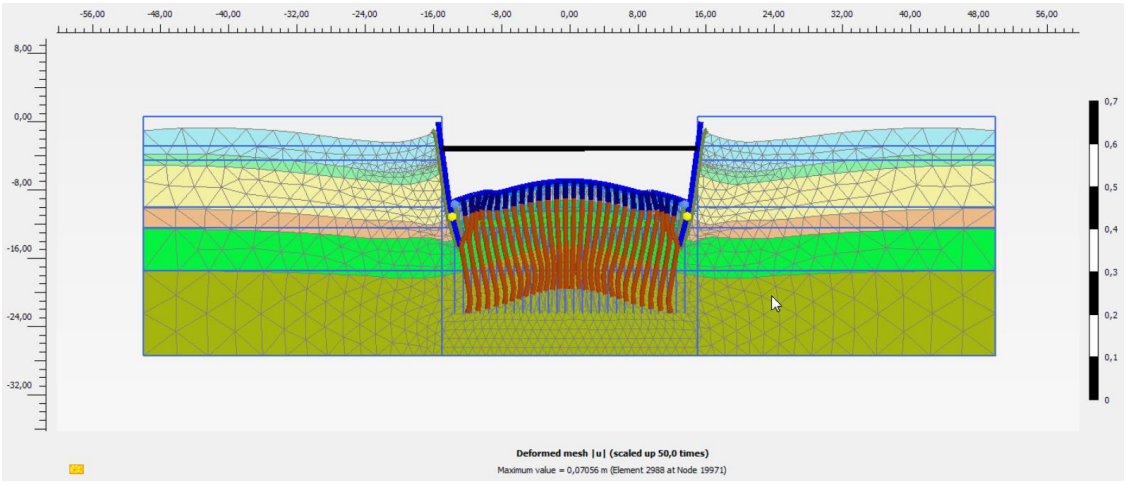

FIGURE 95: MESH CHANGE FOR 5D PILE SPACING (OPTION 1)

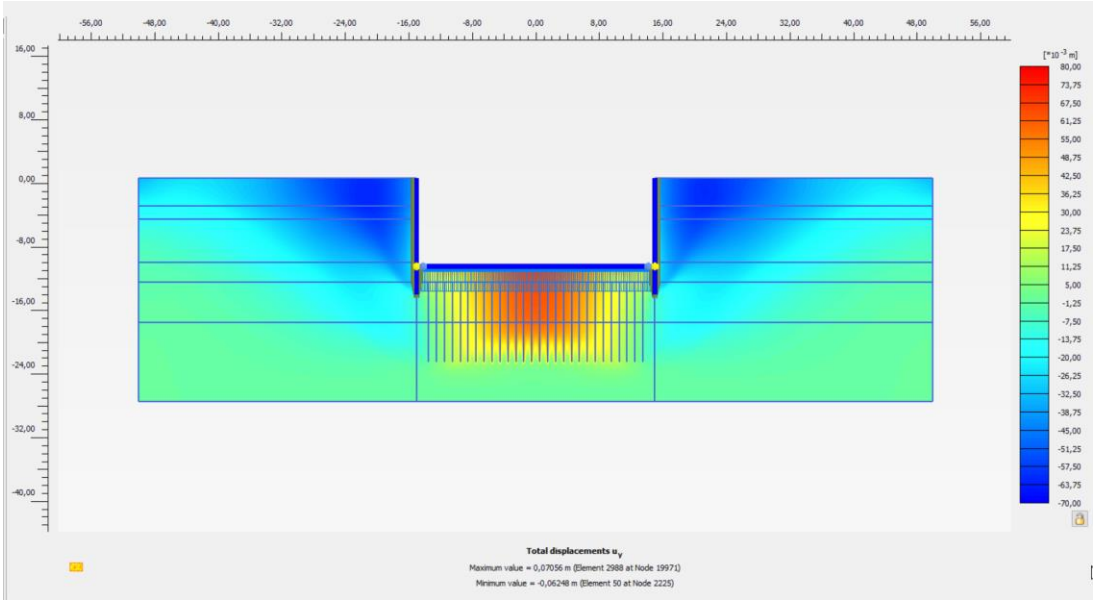

FIGURE 96: SHADING CONTOUR OF VERTICAL DISPLACEMENT FOR 5D PILE SPACING (OPTION 1)

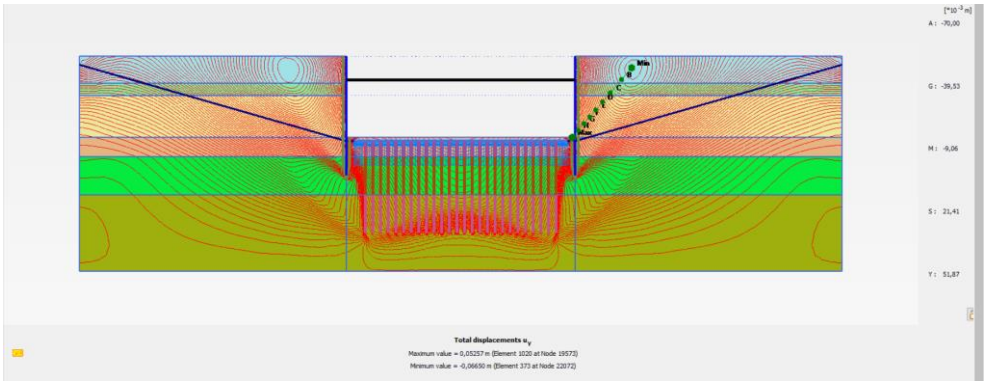

FIGURE 97: LINE CONTOUR OF VERTICAL DISPLACEMENT FOR 5D PILE SPACING (OPTION 1)

According to the results, it can be concluded that the failure mechanism for 1 m pile spacing is based on the pull-out of soil plug.

In order to make sure that the failure mechanism is based on soil plug pull-out, a cross section of the middle pile in the pile group model and a cross section of soil close to that pile is selected to investigate the pile and soil vertical displacements. Figure 98 shows the result of the cross section for middle pile and figure 99 illustrates the cross section result of the soil close to that pile. The results are scaled up to 50 times and the maximum calculated vertical displacement for pile and soil is 69.5 mm and 64.8 mm respectively.

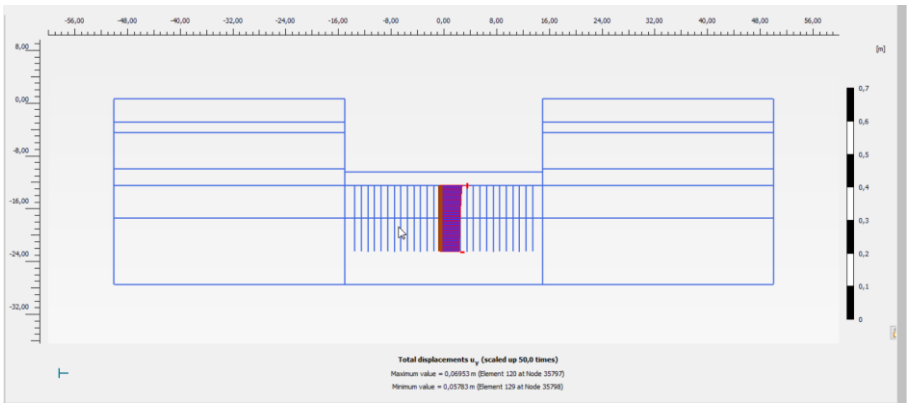

FIGURE 98: VERTICAL DISPLACEMENT OF MIDDLE PILE FOR 5D PILE SPACING (OPTION 1)

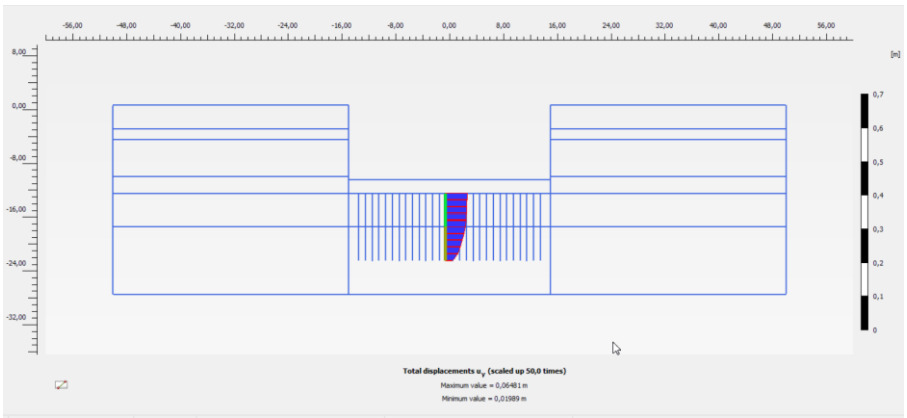

FIGURE 99: VERTICAL DISPLACEMENT OF SOIL FOR 5D PILE SPACING (OPTION 1)

The results of vertical displacement of the pile, soil and their differences are plotted in the next figure.

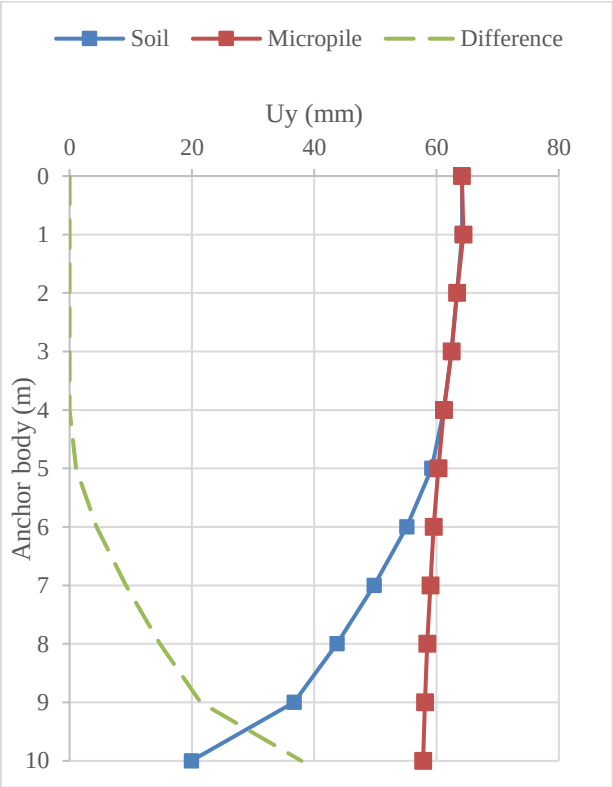

FIGURE 100: VERTICAL DISPLACEMENT OF PILE, SOIL AND THEIR DIFFERENCES FOR 5D (OPTION 1)

According to the figure one can conclude that pile moves together with the soil for 5 meter and after that they are separated and failure occurs which is due to soil plug pull-out. The total bearing capacity of the piles for this case is calculated as follow;

$$\sum M_{stage} \times F = 0.8130 \times 150 = 121.95\ kN/m^2 \tag{99}$$

b) 10D pile spacing

In this part the piles are installed with a center to center distance of 10 D which is 2 m and is visualized in figure 101. According to figure 101 the maximum vertical displacement of the pile group model is 118 mm. Again the shading contour and line contour of vertical displacements are showed in figure 102 and 103 respectively to have a better understanding about the failure mechanism.

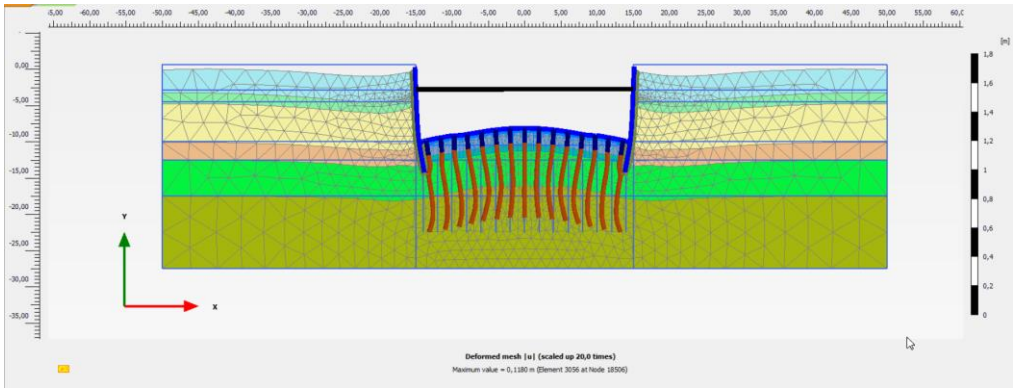

FIGURE 101: DEFORMED MESH AND MAXIMUM VERTICAL DISPLACEMENT FOR 10D (OPTION 1)

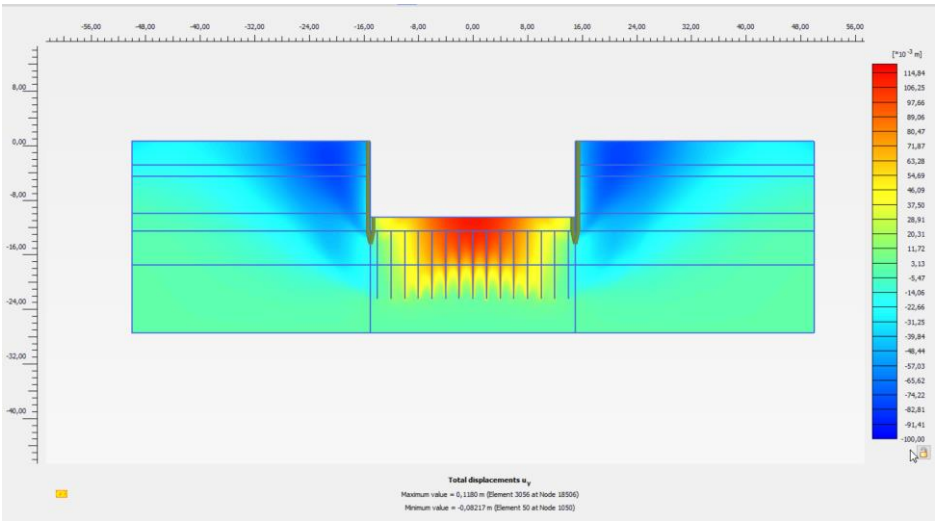

FIGURE 102: SHADING CONTOUR OF VERTICAL DISPLACEMENT FOR 10D PILE SPACING (OPTION 1)

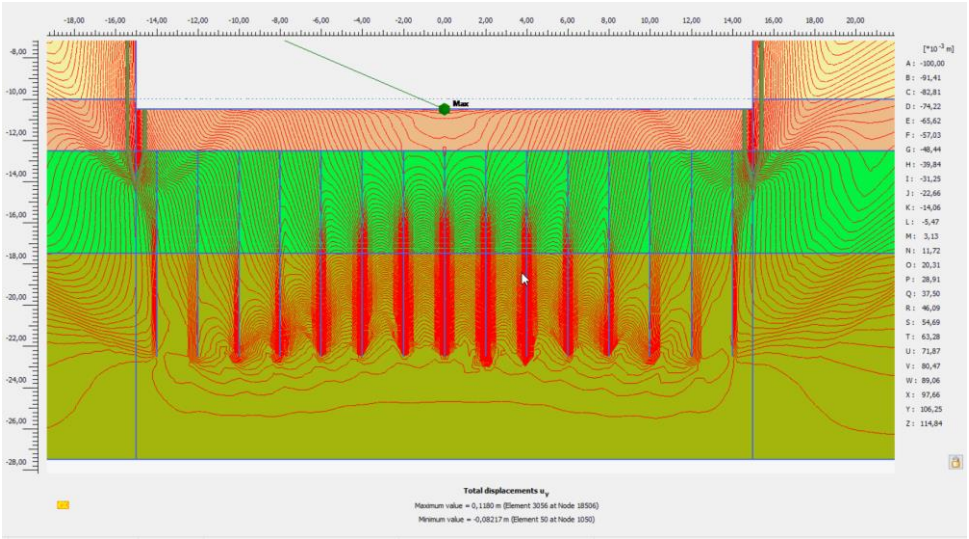

FIGURE 103: LINE CONTOUR OF VERTICAL DISPLACEMENT FOR 10D PILE SPACING (OPTION 1)

The same procedure of what has been done for 1 m pile spacing, is also here followed. Vertical displacement of middle pile and soil close to that pile including their differences are plotted in the next figure 104.

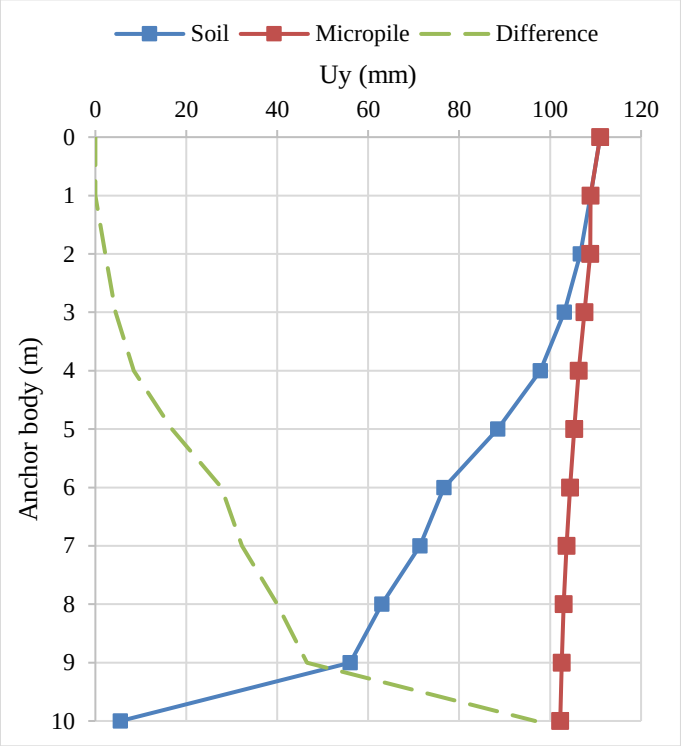

FIGURE 104: VERTICAL DISPLACEMENT OF PILE, SOIL AND THEIR DIFFERENCES FOR 10D (OPTION 1)

Based on the above graph, it can be seen that pile moves together with the soil for about first 2 meters and after that they become separated. It is doubtful which kind of failure in this case occurs but referring to the contour lines of figures 102 and 103, the failure is mostly due to soil plug pull-out with some minor pile slip for this case. However it can be seen that the development of a smaller soil plug seems likely to occur due to smaller mobilized volume of soil compared to 5D pile spacing.

The total bearing capacity of the piles for this case is calculated as follow which is higher compared to 1m pile spacing case.

$$\sum M_{stage} \times F = 0.8284 \times 150 = 124.26\ kN/m^2 \qquad (100)$$

c) 15D pile spacing

The pile spacing is increased to 3 m center to center distances. The configuration of this pile group model can be found in next figure 105. It also shows the deformed mesh of the group model.

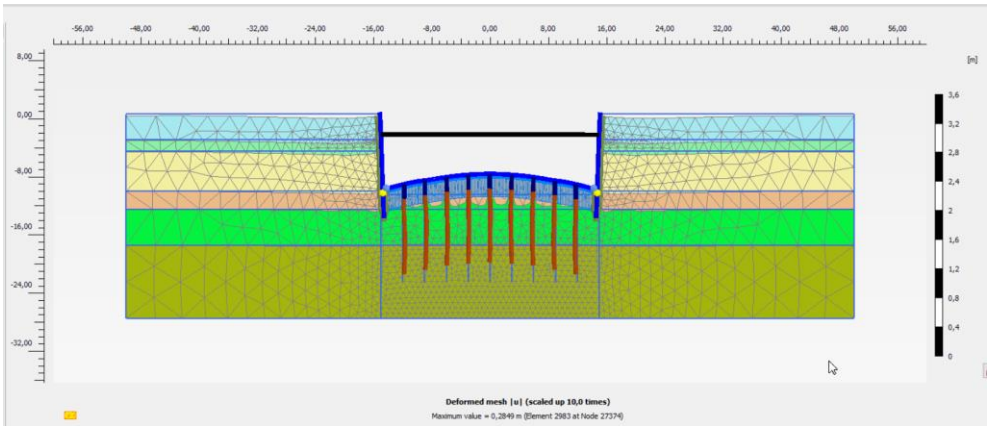

FIGURE 105: DEFORMED MESH AND MAXIMUM VERTICAL DISPLACEMENT FOR 15D (OPTION 1)

Next figure 106 shows the shading contour of total displacement in vertical direction of pile and the surrounding soil. Based on the contour lines it could be seen the movement of the pile is more than the soil mobilization cone. Figure 107 illustrates the total vertical displacement in y-direction by help of line contours.

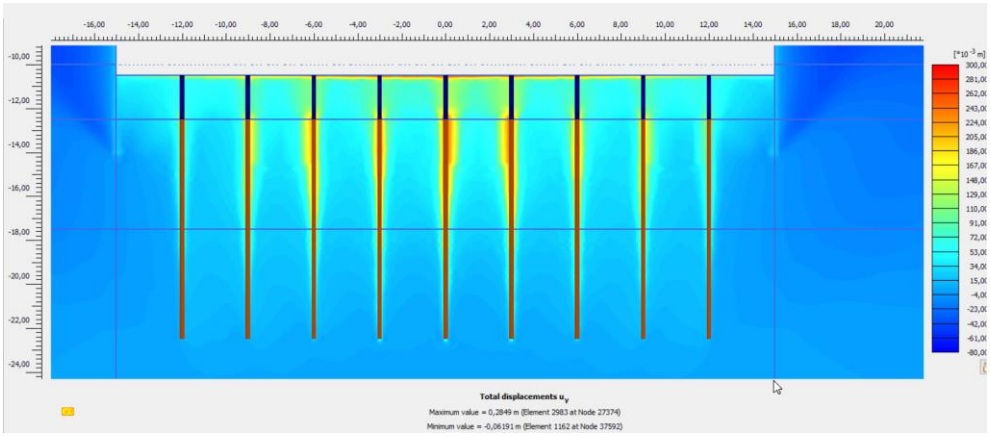

FIGURE 106: SHADING CONTOUR OF VERTICAL DISPLACEMENT FOR 15D PILE SPACING (OPTION 1)

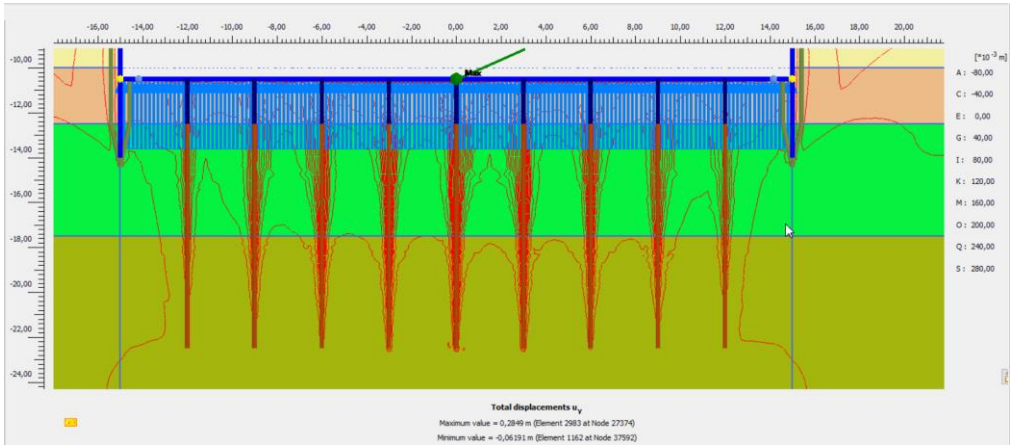

FIGURE 107: LINE CONTOUR OF VERTICAL DISPLACEMENT FOR 15D PILE SPACING (OPTION 1)

Next figures 108 and 109 demonstrate the total displacement of the cross sectional middle pile and the soil close to it respectively. It can be seen again that the soil mobilization is less significant compared to the pile.

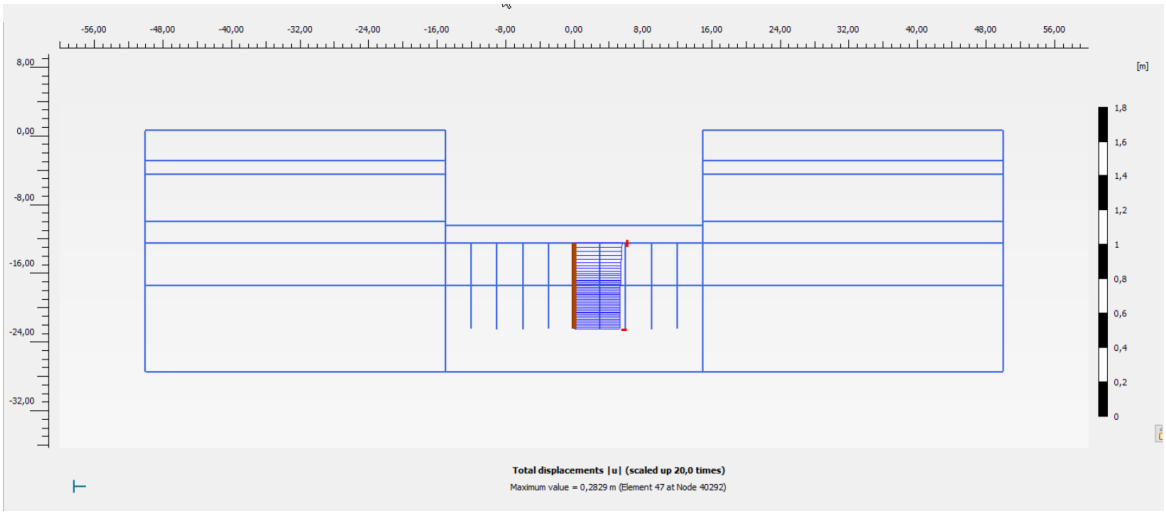

FIGURE 108: VERTICAL DISPLACEMENT OF MIDDLE PILE FOR 15D PILE SPACING (OPTION 1)

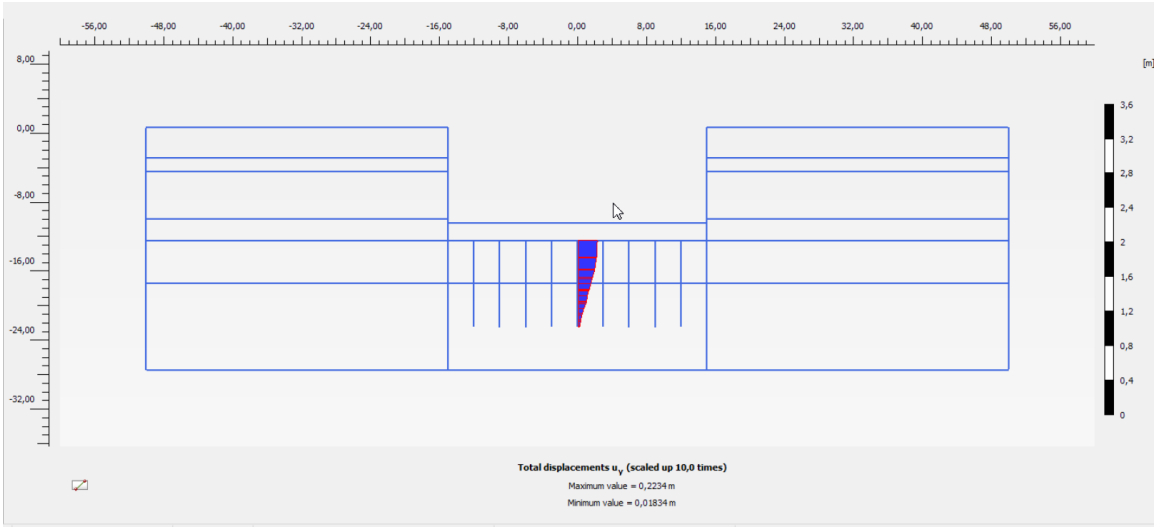

FIGURE 109: VERTICAL DISPLACEMENT OF SOIL FOR 15D PILE SPACING (OPTION 1)

The results of vertical displacement of the pile, soil and their differences for 3 m pile spacing are plotted in the next figure.

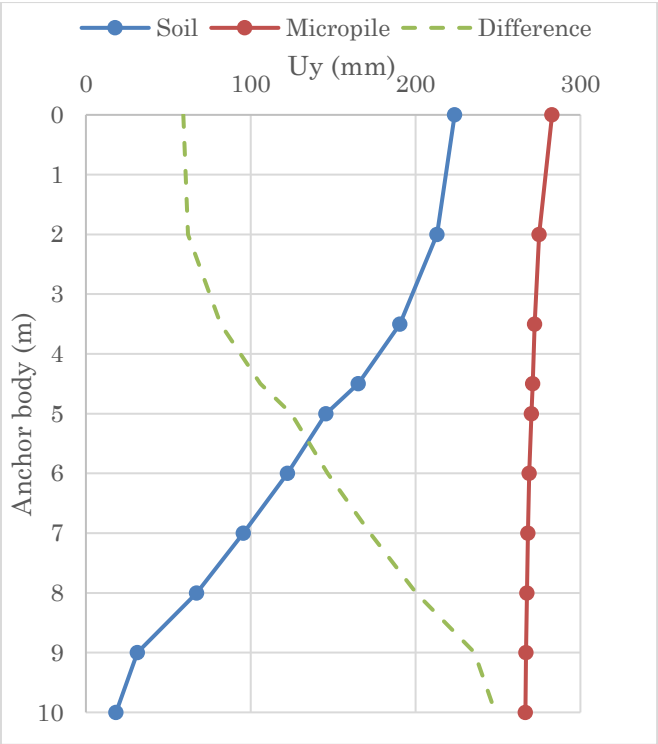

FIGURE 110: VERTICAL DISPLACEMENT OF PILE, SOIL AND THEIR DIFFERENCES FOR 15D (OPTION 1)

Based on the above graph, it can be seen that from initial state pile and soil are separated from each other. Together with the contour line figures and the obtained graph of vertical displacement of the pile and soil, it can be concluded the failure mechanism is according to the pile slip failure.

The total bearing capacity of the piles for this case is calculated as follow which decreased compared to the previous cases.

$$\sum M_{stage} \times F = 0.7004 \times 150 = 105.06\ kN/m^2 \quad (101)$$

An extra evaluation between 10D and 15D pile spacing will be further done to analyze at what minimum pile spacing the slip failure mechanism happens. Therefore 12.5D pile spacing has been chosen to carry out this extra analysis.

d) 12.5D pile spacing

The lay-out of the pile group model with 2.5 m pile spacing is presented in the next figure. Also this figure shows the pile vertical displacement after that the tensile load is applied. The total vertical displacement is calculated 137.5 mm.

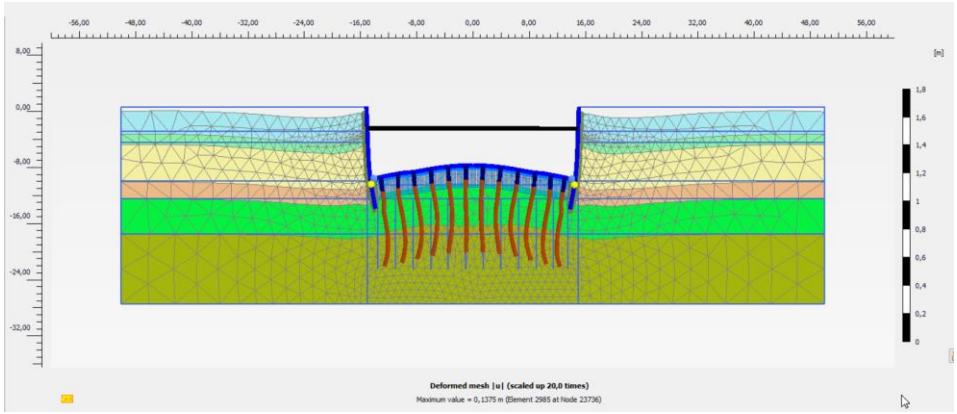

FIGURE 111: DEFORMED MESH AND MAXIMUM VERTICAL DISPLACEMENT FOR 12.5D (OPTION 1)

Figures 112 and 113 show the shading and line contours of vertical displacement in y-direction.

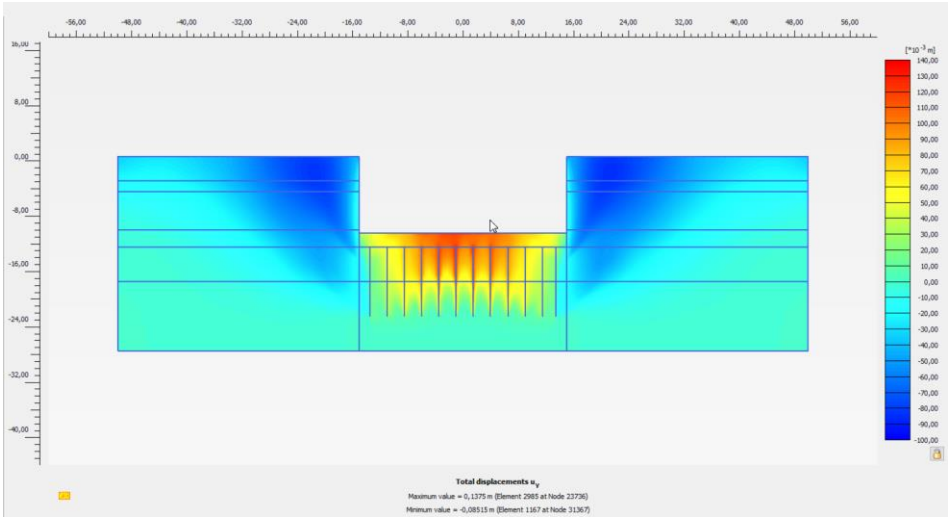

FIGURE 112: SHADING CONTOUR OF VERTICAL DISPLACEMENT FOR 12.5D PILE SPACING (OPTION 1)

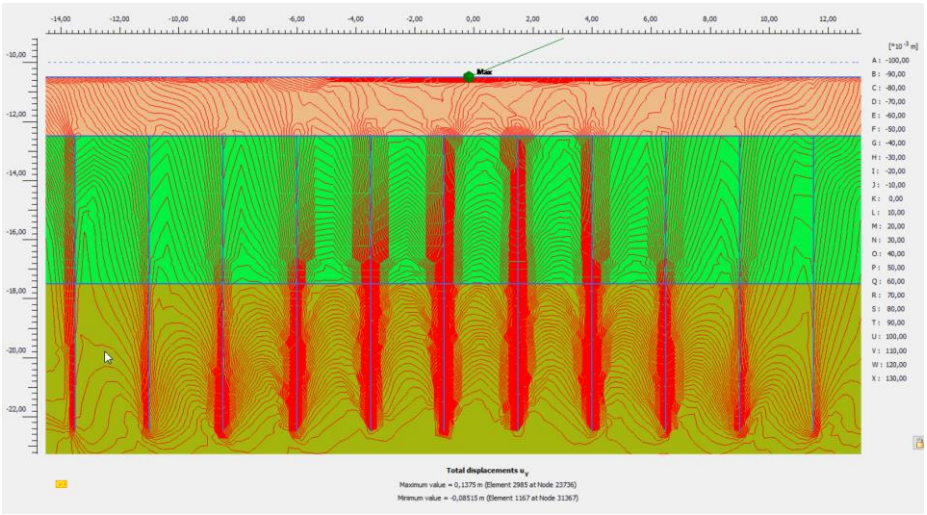

FIGURE 113: LINE CONTOUR OF VERTICAL DISPLACEMENT FOR 12.5D PILE SPACING (OPTION 1)

To have a better view of what exactly happening, the vertical displacement for the middle pile and soil close to it including their differences are plotted in the next figure.

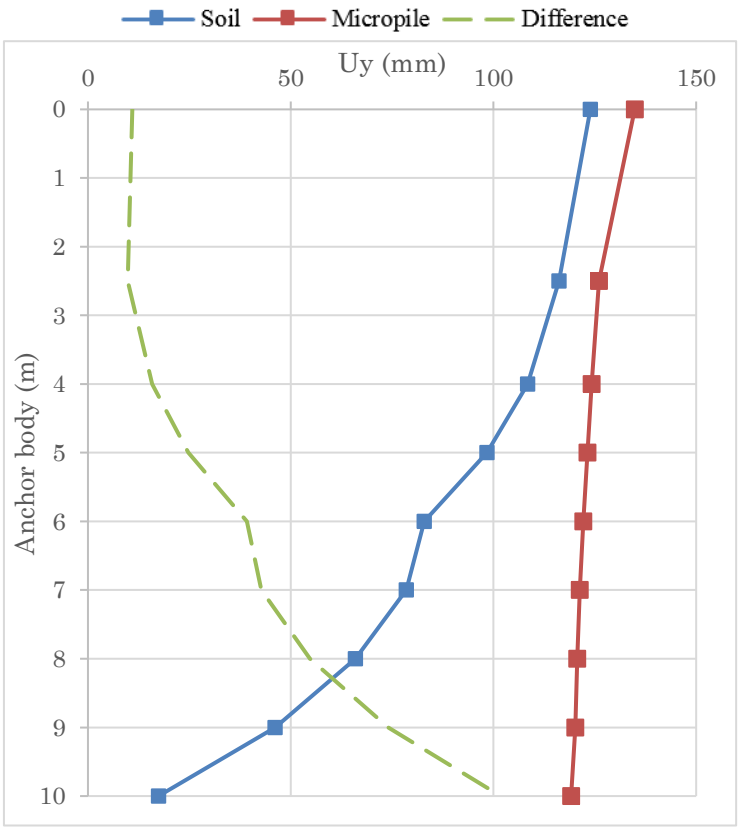

FIGURE 114: VERTICAL DISPLACEMENT OF PILE, SOIL AND THEIR DIFFERENCES FOR 12.5D (OPTION 1)

According to the above graph, pile and soil displacements are separated from each other at initial state. Figure 112 shading contour demonstrates that the soil mobilization mostly happens from top of the anchor body until somewhere in the middle of it. Therefore the development of a smaller soil plug seems likely to occur due to smaller mobilized volume of soil compared to 10D pile spacing. The failure mechanism is mostly based on slip failure of the pile with some minor soil plug pull-out in this case.

The total bearing capacity of the piles for this case is calculated as follow;

$$\sum M_{stage} \times F = 0.8197 \times 150 = 123 \ \ kN/m^2 \qquad (102)$$

This value is higher than the bearing capacity of the piles with 5D pile spacing and it is lower compared to 10D case. According to the results the bearing capacity of the pile in 10D case is the highest and after that by increasing the pile spacing, it decreases.

G.4 EXTRA INFORMATION ABOUT PLAXIS PILE GROUP MODEL

TABLE 59: PROPERTIES OF SHEET PILE, UWC FLOOR AND STRUT

Sheet pile wall (plate)		
Material	Value	Unit
EA	6.0E6	kN/m
EI	1.27E6	kNm^2/m
d	1.5	m
v	0.2	-
UWC floor (plate)		
Material	Value	Unit
EA	16.0E6	kN/m
EI	860.0E3	kNm^2/m
d	0.8	m
Strut (NTN)		
Material	Value	Unit
EA	665.0E3	kN/m
$L_{spacing}$	3	m

H DIFFERENCES OF U(Y) IN PILE AND SOIL

- Pile spacing 5D:

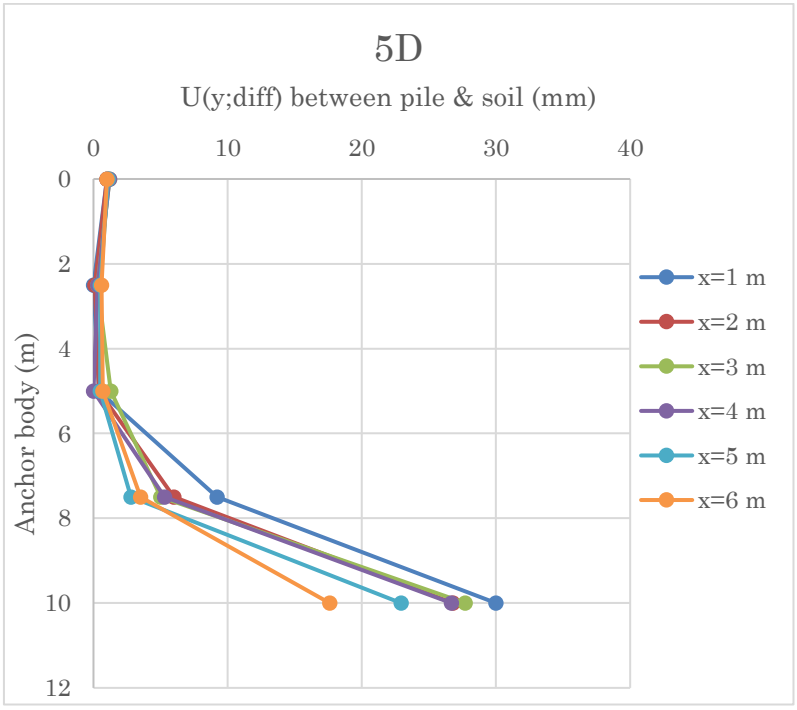

FIGURE 115: DIFFERENCES OF U(Y) IN PILE AND SOIL FOR 5D PILE SPACING

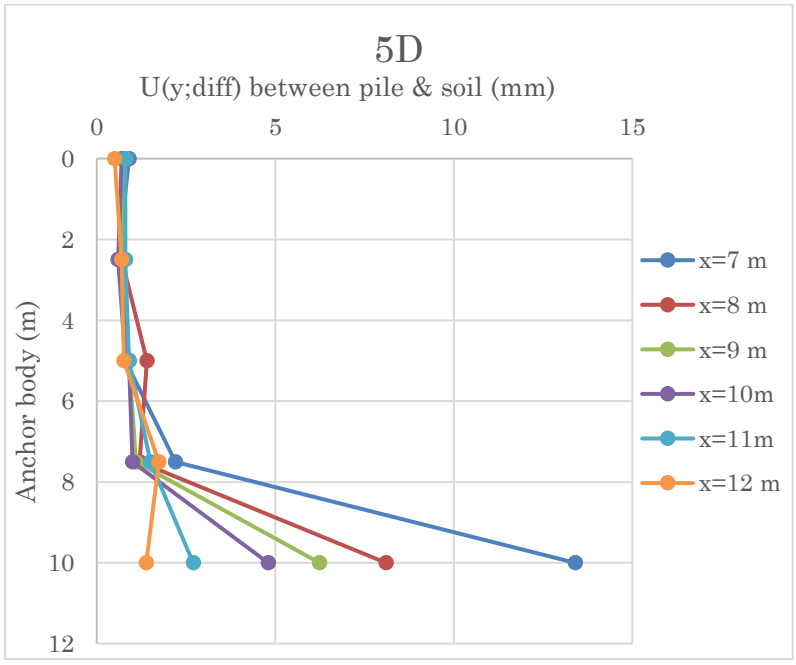

FIGURE 116: DIFFERENCES OF U(Y) IN PILE AND SOIL FOR 5D PILE SPACING

- Pile spacing 10D:

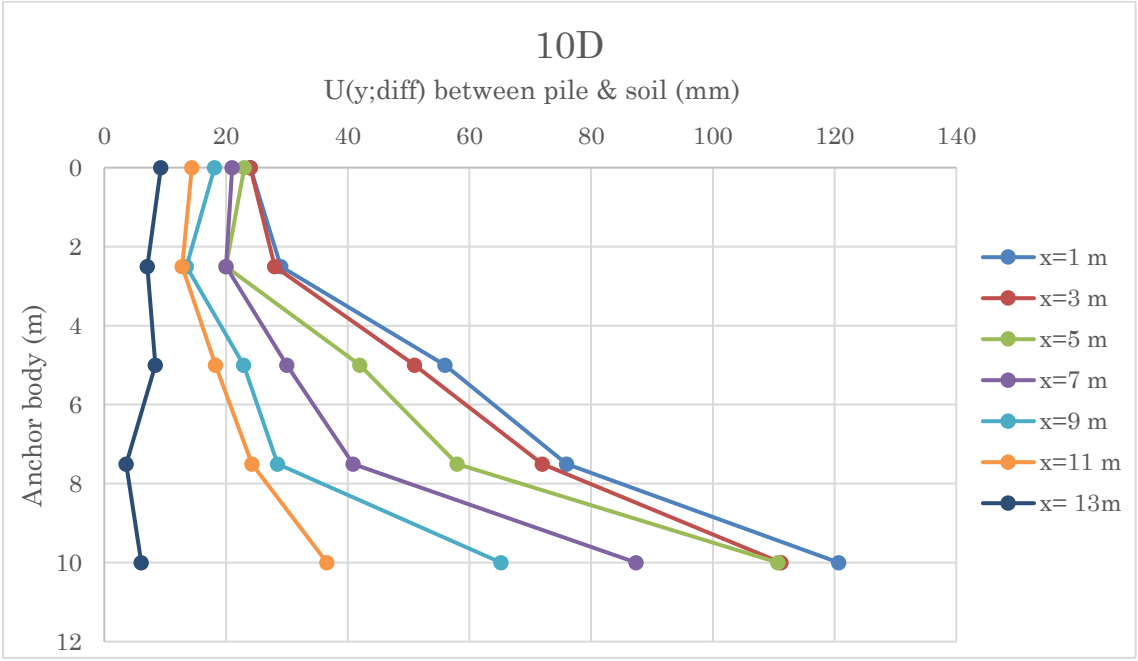

FIGURE 117: DIFFERENCES OF U(Y) IN PILE AND SOIL FOR 10D PILE SPACING

- Pile spacing 15D:

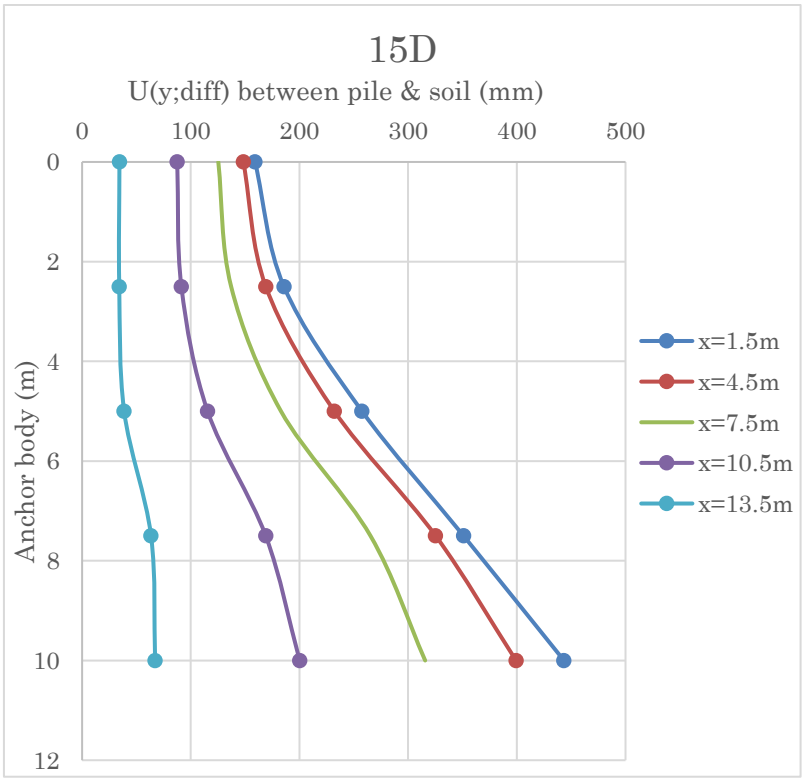

FIGURE 118: DIFFERENCES OF U(Y) IN PILE AND SOIL FOR 15D PILE SPACING